



DEVELOPMENT OF MEMBRANE CONTAINING PROPRANOLOL-  
SELECTIVE IMPRINTED POLYMER BEADS

By

Winita Chaijaroenluk

A Thesis Submitted in Partial Fulfillment of the Requirements for the Degree

MASTER OF PHARMACY

Program of PHARMACEUTICAL SCIENCES

Graduate School

SILPAKORN UNIVERSITY

2011

DEVELOPMENT OF MEMBRANE CONTAINING PROPRANOLOL-  
SELECTIVE IMPRINTED POLYMER BEADS

By

Winita Chaijaroenluk

A Thesis Submitted in Partial Fulfillment of the Requirements for the Degree

MASTER OF PHARMACY

Program of PHARMACEUTICAL SCIENCES

Graduate School

SILPAKORN UNIVERSITY

2011

การพัฒนาแผ่นเมมเบรนที่มีเม็ดพอลิเมอร์รอยพิมพ์ประทับ โมเลกุลซึ่งจำเพาะต่อโพรพราโนลอล

โดย

นางสาววินิตา ชัยเจริญลักษณ์

วิทยานิพนธ์นี้เป็นส่วนหนึ่งของการศึกษาตามหลักสูตรปริญญาเภสัชศาสตรมหาบัณฑิต

สาขาวิชา วิทยาการทางเภสัชศาสตร์

บัณฑิตวิทยาลัย มหาวิทยาลัยศิลปากร

ปีการศึกษา 2554

ลิขสิทธิ์ของบัณฑิตวิทยาลัย มหาวิทยาลัยศิลปากร

The Graduate School, Silpakorn University has approved and accredited the thesis title of “Development of Membrane Containing Propranolol-Selective Imprinted Polymer Beads” submitted by MissWinita Chaijaroenluk as a partial fulfillment of the requirements for the degree of Master of Pharmacy in Pharmaceutical Sciences.

.....  
(Assistant Professor Panjai Tantatsanawong, Ph.D.)  
Dean of Graduate School  
...../...../.....

The Thesis Advisors

1. Associate Professor Praneet Opanasopit, Ph.D.
2. Associate Professor Theerasak Rojanarata, Ph.D.
3. Associate Professor Prasert Akkaramongkolporn, Ph.D.

The Thesis Examination Committee

..... Chairman  
(Associate Professor Tanasait Ngawhirunpat, Ph.D.)  
...../...../.....

..... Member  
(Assistant Professor Warisada Sila-on, Ph.D.)  
...../...../.....

..... Member  
(Associate Professor Praneet Opanasopit, Ph.D.)  
...../...../.....

..... Member  
(Associate Professor Theerasak Rojanarata, Ph.D.)  
...../...../.....

..... Member  
(Associate Professor Prasert Akkaramongkolporn, Ph.D.)  
...../...../.....

52353204 : MAJOR : PHARMACEUTICAL SCIENCES

KEY WORDS : MOLECULARLY IMPRINTED / SELECTIVE MOLECULAR IMPRINTING  
/PROPRANOLOL / ELECTROSPUN

WINITA CHAIJAROENLUK : DEVELOPMENT OF MEMBRANE  
CONTAINING PROPRANOLOL-SELECTIVE IMPRINTED POLYMER BEADS. THESIS  
ADVISORS : ASSOC. PROF. PRANEET OPANASOPIT, Ph.D, ASSOC. PROF  
THEERASAK ROJANARATA, Ph.D, AND ASSOC. PROF PRASERT  
AKKARAMONGKOLPORN, Ph.D. 97 pp.

The aim of this study was to synthesize the MIP beads capable of selective binding to propranolol (PPL) via oil in water (o/w) polymerization using methyl methacrylate (MMA) monomer and divinylbenzene (DVB) crosslinker. PPL was added during polymerization as an imprinted template molecule. Non molecularly imprinted polymer (NIP) beads were prepared by the same way as MIP except the addition of a template during polymerization which was used as a control in order to determine the selectivity of the resultant MIP beads. The selectivity for PPL of MIP beads or milled MIP beads incorporated with Eudragit fiber membranes prepared by electrospinning technique was investigated by comparing the binding ability to other  $\beta$ -blockers (atenolol, metoprolol and timolol). The morphology and particle size of MIP and NIP were investigated by scanning electron microscopic (SEM). The results revealed that particle size and percentage yield of NIP and MIP beads depended on amounts of DVB and PPL. Both MIP and NIP had a spherical shape with the micron-size about 50-100  $\mu$ m. Therefore, NIP2 (MMA:DVB; 75:2.5) and MIP8 (PPL:MMA:DVB; 0.8:75:2.5) were chosen for further characterization and binding experiments. The percentage reloading of PPL was increased by an increasing the ratio of PPL to polymer beads. Comparing the binding ability to other  $\beta$ -blockers, PPL showed the highest percentage reloading in MIP8 (> 80%). The reloading of other  $\beta$ -blockers in MIP8 was similar to NIP2, which was about 40-60%. 40% w/v Eudragit-RS100 in DMF/EtOH (33/67) was chosen for the preparation of fiber membrane containing 10-50% NIP2 or MIP8. PPL could be bound with higher extent and rate to the 50 % MIP8 composite Eudragit-RS100 fiber than NIP2 composite Eudragit-RS100 fiber. Moreover, PPL had higher affinity to the MIP8 than the other  $\beta$ -blockers. This result indicated that MIP8 composite Eudragit-RS100 fiber had higher selectivity to PPL than the other  $\beta$ -blockers. In conclusion, the PPL imprinted microspheres were successfully prepared and this MIP8 composite Eudragit-RS100 membrane can be further developed for various applications in pharmaceutical and other affinity separation fields.

---

Program of Pharmaceutical Sciences Graduate School, Silpakorn University Academic year 2011

Student's signature .....

Thesis Advisors' signature 1..... 2..... 3.....



## ACKNOWLEDGEMENTS

I would like to express my sincere gratitude and appreciation to my thesis advisor, Associate Professor Dr. Praneet Opanasopit, for her invaluable advices, guidance, attention and encouragement throughout my study.

To my co-advisors, Associate Professor Dr. Theerasak Rojanarata and Associate Professor Dr. Prasert akkaramongkolporn. I would like to thank for his guidance and meaningful advice, and for his help in making all contacts possible and successful. For Assistant Professor Dr. Warisada Sila-on, I would like to thank for her criticism on my thesis manuscript.

I would like to acknowledge the Graduate School, Silpakorn University for the financial support (Annual Government Budget Expenditures for the fiscal year 2011)

I would like to sincere thanks to all teachers, follow graduate students, researchers and the staff in Faculty of Pharmacy, Silpakorn University, for giving me the place, equipments, knowledge and friendship.

To my laboratory brother, sisters and friends, thanks for their assistance and kindness, and to my friends, I would like to thank for their assisting and entertaining me through the years.

This thesis is partially supported by Faculty of Pharmacy, Silpakorn University.

Finally, I would like to express my most thankfulness to my beloved family for constant supportive and encouragement. I would like to thanks for their kind understanding, warmth and wonderful job as both financial and emotional backing. Moreover, thanks for taking care of me physically and encouraging me though all the obstacles.

## CONTENTS

	Page
English Abstract .....	d
Thai Abstract.....	e
Acknowledgements .....	f
List of Tables .....	h
List of Figures .....	l
Chapter	
1    Introduction .....	1
2    Literature Reviews .....	3
3    Materials and Methods.....	33
4    Results and Discussion.....	41
5    Conclusions.....	63
Bibliography.....	65
Appendix .....	69
Biography.....	97

## LIST OF TABLES

Table		Page
1	Functional monomer for use in covalent molecular imprinting.....	7
2	Important print molecules used for generating MIPs applied in separation techniques .....	10
3	Commonly used functional monomers for non-covalent imprinting.....	12
4	Methacrylate-based copolymers with a variety of functional properties....	24
5	Use of poly(meth) acrylates in the pharmaceutical industry.....	25
6	Formulations of PPL-imprinted and non-PPL imprinted polymer beads ...	37
7	Percentage yield of PPL-imprinted and non-PPL imprinted polymer beads formulations .....	42
8	SEM images of polymer beads obtaining PPL as a template, MMA as a functional monomer, DVB as crosslinker and BP as an initiator (at magnification of 100X) .....	44
9	The polymer concentration and solvents used to prepare of fibers .....	53
10	SEM images at magnification of 1500X and diameter of methacrylate-based copolymers (E- L100) fiber mats obtained from 20 and 25% E-L100 solutions in DMA/EtOH (80/20) and DMF/EtOH (33/67) ....	54
11	SEM images at magnification of 1500X and diameter of methacrylate-based copolymers (E-S100) fiber mats obtained from 20% and 25% E-S100 solution in DMA/EtOH (80/20) and DMF/EtOH (33/67).....	54
12	SEM images at magnification of 1500X and diameter of methacrylate-based copolymers (E-EPO) fiber mats obtained from 25, 30 and 35% EPO solutions in EtOH, DMA/EtOH (80/20) and DMF/EtOH (33/67).....	55
13	SEM images at magnification of 1500X and diameter of methacrylate-based copolymers (E-RLPO) fiber mats obtained from 25, 30, 35% RLPO solutions in EtOH, DMA/EtOH (80/20) and DMF/EtOH (33/67).....	56

Table	Page
14 SEM images at magnification of 1500X and diameter of methacrylate-based copolymers (E-RL100) fiber mats obtained from 30, 35, 40% RL100 solutions in DMF/EtOH (33/67).....	56
15 SEM images at magnification of 1500X and diameter of methacrylate-based copolymers (E-RS100) fiber mats obtained from 30, 40, 50 and 60% E-RS100 solution in DMA/EtOH (80/20) and DMF/EtOH (33/67).....	57
16 The bead content after electrospinning process of an initially added 10-50% w/w of MIP8 beads in 40% w/v E-RS100 solutions .....	58
17 Conductivity and viscosity of 20 and 25 % w/v Eudragit®L100 and S100 solution in DMA/EtOH and DMF/EtOH.....	71
18 Conductivity and viscosity of 25 and 30 % w/v Eudragit®EPO solution in EtOH, DMA/EtOH and DMF/EtOH.....	71
19 Conductivity and viscosity of 25-40 % w/v Eudragit®RLPO and RL100 solution in EtOH, DMA/EtOH and DMF/EtOH.....	71
20 Conductivity and viscosity of 30-60% w/v Eudragit®RS100 solution in DMA/EtOH and DMF/EtOH.....	72
21 The percentage PPL reloading in NIP3 at the drug to polymer bead ratio of 1:0.5 .....	78
22 The percentage PPL reloading in MIP9 at the drug to polymer bead ratio of 1:0.5 .....	78
23 The percentage PPL reloading in NIP3 at the drug to polymer bead ratio of 1:1 .....	79
24 The percentage PPL reloading in MIP9 at the drug to polymer bead ratio of 1:1 .....	79
25 The percentage PPL reloading in NIP3 at the drug to polymer bead ratio of 1:2.....	80
26 The percentage PPL reloading in MIP9 at the drug to polymer bead ratio of 1:2.....	80
27 The percentage PPL reloading in polymer beads at the drug to polymer bead ratio of (1:1) at various amount of PPL: NIP3 (PPL0 g).....	81

Table	Page
28	The percentage PPL reloading in polymer beads at the drug to polymer bead ratio of (1:1) at various amount of PPL: MIP3 (PPL0.4 g) ..... 81
29	The percentage PPL reloading in polymer beads at the drug to polymer bead ratio of (1:1) at various amount of PPL: MIP6 (PPL0.6 g) ..... 82
30	The percentage PPL reloading in polymer beads at the drug to polymer bead ratio of (1:1) at various amount of PPL: MIP9 (PPL0.8 g) ..... 82
31	The percentage PPL reloading in NIP; NIP1 (DVB 2 g) at the drug to polymer bead ratio of 1:1 ..... 83
32	The percentage PPL reloading in NIP; NIP2 (DVB 2.5 g) at the drug to polymer bead ratio of 1:1 ..... 83
33	The percentage PPL reloading in NIP; NIP3 (DVB 3 g) at the drug to polymer bead ratio of 1:1 ..... 84
34	The percentage PPL reloading in MIP; MIP7 (DVB 2 g) at the drug to polymer bead ratio of 1:1 ..... 84
35	The percentage PPL reloading in MIP; MIP8 (DVB 2.5 g) at the drug to polymer bead ratio of 1:1 ..... 85
36	The percentage PPL reloading in MIP; MIP9 (DVB 3 g) at the drug to polymer bead ratio of 1:1 ..... 85
37	The percentage reloading of $\beta$ -blocker at ratio of drug to polymer beads (1:1) NIPs, ATE ..... 86
38	The percentage reloading of $\beta$ -blocker at ratio of drug to polymer beads (1:1) NIPs, MET ..... 86
39	The percentage reloading of $\beta$ -blocker at ratio of drug to polymer beads (1:1) NIPs, TIM..... 87
40	The percentage reloading of $\beta$ -blocker at ratio of drug to polymer beads (1:1) NIPs, PPL ..... 87
41	The percentage reloading of $\beta$ -blocker at ratio of drug to polymer beads (1:1) MIPs, ATE ..... 88
42	The percentage reloading of $\beta$ -blocker at ratio of drug to polymer beads (1:1) MIPs, MET ..... 88

Table	Page	
43	The percentage reloading of $\beta$ -blocker at ratio of drug to polymer beads (1:1) MIPs, TIM ..... 89	89
44	The percentage reloading of $\beta$ -blocker at ratio of drug to polymer beads (1:1) MIPs, PPL ..... 89	89
45	The percentage reloading of $\beta$ -blocker at ratio of drug to polymer beads (1:1) NIPs composite E-RS100 fiber, ATE ..... 90	90
46	The percentage reloading of $\beta$ -blocker at ratio of drug to polymer beads (1:1) NIPs composite E-RS100 fiber, MET ..... 90	90
47	The percentage reloading of $\beta$ -blocker at ratio of drug to polymer beads (1:1) NIPs composite E-RS100 fiber, TIM ..... 91	91
48	The percentage reloading of $\beta$ -blocker at ratio of drug to polymer beads (1:1) NIPs composite E-RS100 fiber, PPL ..... 91	91
49	The percentage reloading of $\beta$ -blocker at ratio of drug to polymer beads (1:1) MIPs composite E-RS100 fiber, ATE ..... 92	92
50	The percentage reloading of $\beta$ -blocker at ratio of drug to polymer beads (1:1) MIPs composite E-RS100 fiber, MET ..... 92	92
51	The percentage reloading of $\beta$ -blocker at ratio of drug to polymer beads (1:1) MIPs composite E-RS100 fiber, TIM ..... 93	93
52	The percentage reloading of $\beta$ -blocker at ratio of drug to polymer beads (1:1) MIPs composite E-RS100 fiber, PPL ..... 93	93
53	List of abbreviations ..... 95	95

## LIST OF FIGURES

Figure		Page
1	Principle of molecular imprinting .....	5
2	Covalent molecular imprinting .....	7
3	Non-covalent molecular imprinting .....	9
4	Functional monomers commonly used in non-covalent molecular imprinting procedures .....	14
5	Chemical structure of common crosslinkers used in non-covalent molecular imprinting .....	16
6	The applications envisaged for MIPs .....	20
7	Schematic diagram of the electrospinning process .....	23
8	Poly(methacrylic acid-co-methyl methacrylate) (Eudragit L100; Mw 135,000 Da).....	26
9	Poly-(butyl methacrylate-co-(2-dimethylaminoethyl) methacrylate-co-methyl methacrylate) (Eudragit EPO; Mw 150,000 Da) .....	26
10	Poly(ethyl acrylate-co-methyl methacrylate-co-trimethyl-ammonioethyl methacrylate chloride) (Eudragit RLPO; Mw 150,000 Da).....	27
11	Structure of Propranolol Hydrochloride .....	28
12	Structure of Atenolol.....	30
13	Structure of Metoprolol Tartrate .....	31
14	Structure of Timolol Maleate .....	32
15	FT-IR spectra of (a) NIP2 and (b) MIP8 beads.....	45
16	FT-IR spectra of (a) non hydrolyzed and (b) hydrolyzed MIP8 beads .....	46
17	The percentage PPL reloading in (a) NIP3 and (b) MIP9 at the drug to polymer bead ratio of 1:0.5, 1:1 and 1:2 .....	48
18	The percentage PPL reloading in polymer beads at the drug to polymer bead ratio of (1:1) at various amount of PPL: NIP3 (PPL0 g), MIP3 (PPL0.4 g), MIP6 (PPL0.6 g), and MIP9 (PPL0.8 g).....	49

Figure		Page
19	The percentage PPL reloading in (a) NIP; NIP1 (DVB 2 g), NIP2 (DVB 2.5 g), NIP3 (DVB 3 g) and (b) MIP; MIP7 (DVB 2 g), MIP8 (DVB 2.5 g), MIP9 (DVB 3 g) at the drug to polymer bead ratio of 1:1.....	50
20	The percentage reloading of $\beta$ -blocker at ratio of drug to polymer beads (1:1) (a) NIPs and (b) MIPs, ATE, MET, TIM, PPL.....	51
21	SEM images of the MIP8 after reduced the particle size by ball mill and sieving through the 400 mesh (a) at magnification of 100X and (b) at magnification of 350X. ....	59
22	SEM images of the (a, b) E-RS100 fibers; (c, d) E-RS100 fibers containing 50 % MIP8 (a, c at magnification of 100X and b, d at magnification of 350X). ....	60
23	The percentage reloading of $\beta$ -blocker at ratio of drug to polymer beads (1:1) (a) NIPs composite E-RS100 fiber and (b) MIPs composite E-RS100 fiber, ATE, MET, TIM and PPL .....	61
24	The calibration curve of PPL for percentage drug reloading assay .....	70
25	The calibration curve of ATE for percentage drug reloading assay .....	70
26	The calibration curve of MET for percentage drug reloading assay.....	71
27	The calibration curve of TIM for percentage drug reloading assay.....	71
28	The calibration curve of PPL for percentage drug reloading assay .....	72
29	The calibration curve of ATE for percentage drug reloading assay .....	72
30	The calibration curve of MET for percentage drug reloading assay.....	73
31	The calibration curve of TIM for percentage drug reloading assay.....	73

## CHAPTER 1

### INTRODUCTION

#### **1. Statement and significance of the research problem**

To enhance the selectivity in the filtration process, affinity membranes have been developed to separate the molecules rather than in molecular size. Ligand molecules were introduced into the inner surfaces of affinity membrane in order to specifically capture target molecules while letting other molecules to pass through. Combining both the high productivity associated with membranes and the outstanding selectivity of the chromatography resins, affinity membrane chromatography is now an attractive and competitive method for purifying proteins or other biomolecules from biological fluids. (Ma et al. 2006: 179–187).

Molecularly imprinted polymers (MIPs) are the synthetic polymers which contain the specific molecular cavities that are complementary in shape and functional groups with imprinted template molecule. Briefly, the MIPs are prepared by establishing the covalent bonds or non-covalent interactions between the template molecule and functional monomers. After that the imprinted template molecule is washed out, leaving hollow spaces in a sponge like polymeric network. MIPs possess several advantages over their biological counterparts including low cost, ease of preparation, storage stability, repeated operations without loss of activity, high mechanical strength, durability to heat and pressure, and applicability in harsh chemical media. The binding affinity can be moderate or high, depending on the application that is aimed for. Thus this technique has become an interesting in many fields of chemistry and biology, particularly as an affinity material for sensors, binding assays, artificial antibodies, adsorbents for solid phase extraction, and chromatographic stationary phases (Yan et al. 2006: 155-178).

Electrospinning is a polymer solution processing technique that provides a simple and versatile way to prepare ultrafine polymeric fibers with diameters ranging from a few nanometers to several micrometers. Having been discovered more than a

half century ago, electrospinning is not a new technique but has received an extensively renewed research interest in recent years. A rich variety of electrospun polymeric fibers with diameters ranging from several tens to several microns are now being fabricated and studied for applications in such diverse fields as tissue engineering scaffold, drug deliver carrier, biosensor/chemosensor, protective cloth and air filtration, electronic and semi-conductive materials and reinforced nanocomposite (Chronakis 2005: 283, Huang 2003: 2223–2253).

Previous studies have demonstrated that the other technology of incorporate preformed MIP particles with or into membranes such as encapsulation of MIP nanoparticles into a composite nanofiber membrane with a simple electrospinning method (Yoshimatsu et al.: 2008), MIP nanoparticle on microspheres composite cellulose membranes (Jantararat et al.: 2008). Therefore, the objective of this work is to develop a novel material for affinity membrane separation by using the electrospun fiber containing propranolol (PPL)-selective MIP.

## **2. Objective of this research**

2.1 To study factors affecting the preparation of PPL-selective MIP.

2.2 To study factors affecting the preparation and drug reloading of Eudragit fiber membranes by electrospinning.

2.3 To evaluate the ability of MIP beads and electrospun fibers containing MIP beads for the  $\beta$ -blocker affinity separation.

## **3. The research hypothesis**

3.1 The functional monomer to cross-linking monomer ratio and the amount of propranolol affect the morphology, particle size and % yield of PPL-selective MIP.

3.2 Polymer solution parameters affect the morphology, size of fiber and MIPs reloading.

3.3 The PPL-selective MIP beads are selective to PPL.

## **CHAPTER 2**

### **LITERATURE REVIEWS**

#### **1. Introduction to Molecularly imprinted polymers (MIPs)**

##### **1.1 Molecular imprinting technology**

Molecular imprinting is not a new science. The history of molecular imprinting is usually traced back to the experiments of Dickey in the 1940s and 1950s, who was inspired to create affinity for dry molecules in silica gel. Dickey's silicas can be considered to be the first imprinted materials (Mayes and Whitcombe 2005: 1744). Molecular imprinting in synthetic organic polymers was reported for the first time in 1972 by Wulff and Sarhan. They used a covalent approach to prepare an organic molecularly imprinted polymer capable of discriminating between the enantiomers of glyceric acid. In the early 1980s, a most important development was the introduction of a general non-covalent approach by the group of Masbach (Andersson and Nicholls 2000: 1-17, Sellergren and Allender 2005: 1733-1735). Therefore, the initial idea was to obtain the polymer having highly specific binding clefts with a predetermined size, shape and three-dimensional arrangement of functional groups that match to the separated molecule as require.

MIPs have been demonstrated to possess excellent properties for separation of many compounds, ranging from small molecules to macromolecules (Yan and Row 2006: 160). Moreover MIPs have showed high affinity and specificity comparable to biological antibodies (Ramstrom, Ye and Mosbach 1996: 471-477). Due to their favorable molecular recognition capability and stability, potential applications of MIPs have been investigated in broad areas, such as ligand binding assays, liquid chromatography, solid-phase extraction, artificial receptor for drug assays, synthetic receptors for peptides and biological molecule, drug delivery and enzyme mimetics (Yoshimatsu and Ye, et al. 2008: 1208-1209, Nostrum 2005: 119-124, Bruggemann 2003: 134-135, Sellergren and Allender 2005: 1733-1741).

## **1.2 The advantages of molecular imprinting (Yan and Row 2006: 156).**

### 1.2.1 Stability

1.2.1.1 Towards extremes of heat and pH

1.2.1.2 Storage for years without any loss of activity

1.2.1.3 Reused multiple times

### 1.2.2 Higher binding capacity

### 1.2.3 Synthesis is straightforward and inexpensive

1.2.3.1 Can be accomplished in short time in non-specialized laboratories with non-specialized equipment.

1.2.3.2 No animal experiments

## **1.3 The principle of molecular imprinting**

Molecular imprinting is a technique to generate polymeric mimics of biological receptors, for example antibodies or enzymes. In a first step a template (the antigen or substrate) is associated with functional monomers, for example molecules containing both a point of interaction (covalent or non-covalent bond) and a polymerizable group (usually a double bond). In a second step the polymerization is initiated in the presence of high amounts of crosslinker molecules containing at least two polymerizable groups. These crosslinkers are necessary to establish a rigid polymer network, which maintains imprints with high specificity. After an extraction step to remove the template, the produced “Molecularly imprinted polymer” (MIP) are able to recognize specifically the template due to selective interaction of this molecule with the cavities created in the polymer network (Bruggemann 2003: 134-142). The process by which MIPs are prepared is shown in Figure 1.

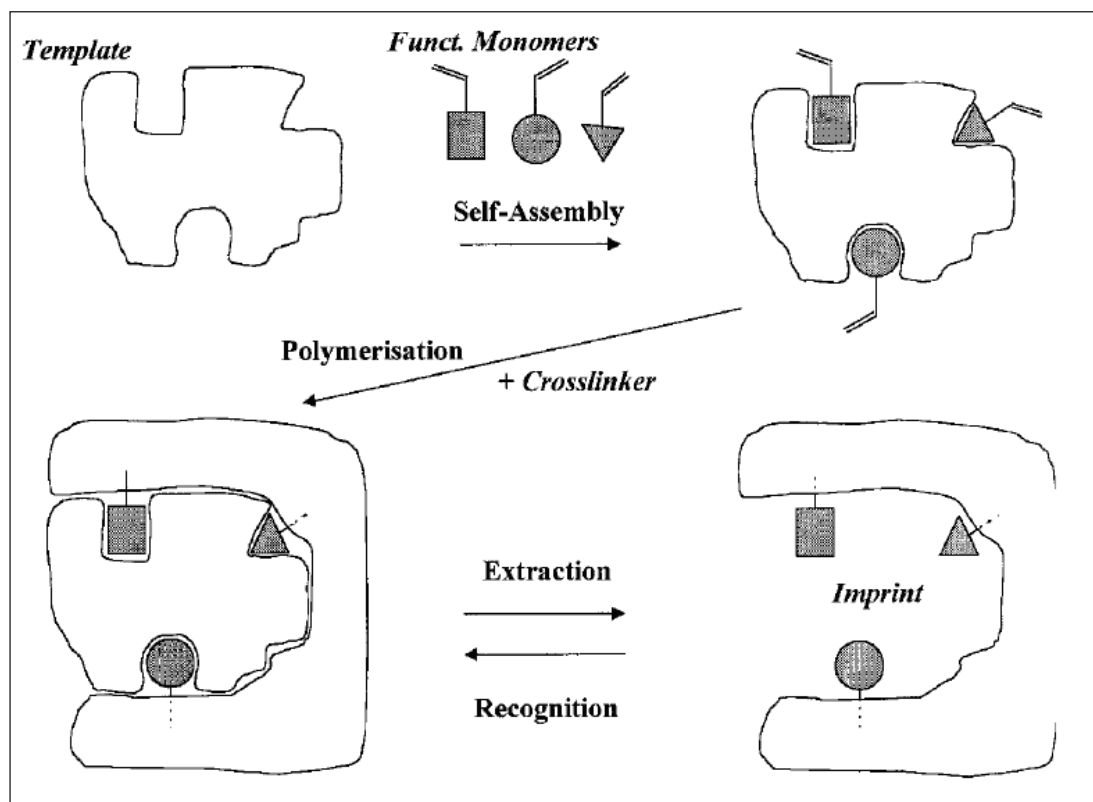


Figure 1 Principle of molecular imprinting.

Source: Oliver Bruggemann, "Molecularly imprinted polymers: A new dimension in analytical bioseparation," *Synthetic Polymers for Biotechnology and Medicine* (2003): 135.

#### 1.4 Preparation strategies

Two kinds of essential molecular imprinting strategies have been established based on covalent bonds or non-covalent interactions between the template and functional monomers. In both cases, the functional monomers, chosen so as to allow interactions with the functional groups of the imprinted molecule, are polymerized in the presence of the imprinted molecule.

##### 1.4.1 Covalent imprinting

In covalent approach, the imprinted molecule is covalently coupled to a polymerizable molecule. The binding of this type of polymer-relies on reversible covalent bonds. After copolymerization with crosslinker, the imprint molecule is chemically cleaved from the highly crosslinked polymer. In the 1970's Wulff et al developed an imprinting method based on the covalent immobilization of

cis-diol-sugar templates via vinylized boronate ester bridges to the functional monomer (Figure 2). The template molecules were extracted from the polymer networks by hydrolysis. The remaining MIP cavities showed high specificity for the template sugars. The disadvantage of this procedure was the time-consuming step of derivatizing the templates prior to the polymerization and the slow process of reaching equilibrium during the application of the MIP for bioseparation. The latter was due to the necessity of the templates to form covalent bonds to the polymer for recognition (Bruggemann 2003: 134-142). Moreover, the requirements of covalent imprinting are different from those for non-covalent imprinting, particularly with respect to ratios of functional monomer, crosslinker, and template. However, since the choice of reversible covalent interactions and the number of potential templates are substantially limited, reversible covalent interactions with polymerizable monomers are fewer in number and often require an acid hydrolysis procedure to cleave the covalent bonds between the template and the functional monomer (Yan and Row 2006: 155-178, Wulff and Biffis 2000: 71-107, Mayes and Whitcombe 2005: 1742-1748).

In case of covalent interactions the choice of the functional monomer, which has to be linked covalently to the template prior to imprinting, depends on the chemistry of the template. Templates containing cis-diol groups are usually esterified with a vinyl-boronic acid component to yield a reversible bis-ester. If this is not possible, alternatives are the generation of Schiff-bases (azomethines). This requires an amino group on the template and a carboxyl acid group on the functional monomer, which are shown in Table 1 (Bruggemann 2003: 134-142).

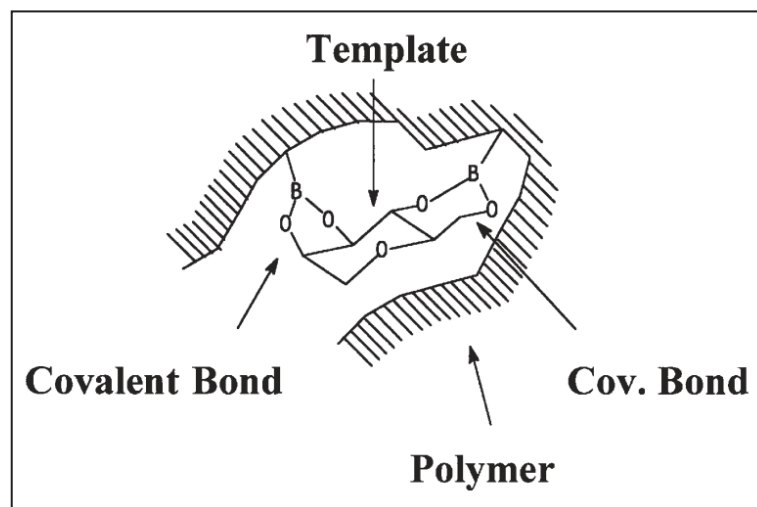


Figure 2 Covalent molecular imprinting.

Source: Oliver Bruggemann, "Molecularly imprinted polymers: A new dimension in analytical bioseparation," Synthetic Polymers for Biotechnology and Medicine (2003): 136.

Table 1 Functional monomer for use in covalent molecular imprinting.

<p>p-Vinylphenylboronic acid (forming boronates with cis-diol-templates)</p>	<p>p-Vinylbenzyl-amine (forming azomethines and amides with carbonyl- and carboxyl-templates)</p>
<p>2-(p-Vinylphenyl)-1,3-propane diol (forming ketales with carbonyl-templates)</p>	<p>p-Vinylbenzyl alcohol (forming ether and ester with alcohol- and acid-templates)</p>
<p>p-Vinylphenyl carbonyl (forming Schiff bases with amine-templates)</p>	<p>p-Vinylbenzoic acid (forming ester and amides with alcohol- and amine-templates respectively)</p>

Source: Oliver Bruggemann, "Molecularly imprinted polymers: A new dimension in analytical bioseparation," Synthetic Polymers for Biotechnology and Medicine (2003): 139.

### 1.4.2 Non-covalent imprinting

Non-covalent approach is the most frequently used method to prepare MIP due to its simplicity. During the non-covalent approach, the special binding sites are formed by the self-assembly between the template and monomer, followed by a crosslinked co-polymerization. The imprint molecules interact, during both the imprinting procedure and the rebinding, with the polymer via non-covalent interactions, e.g. ionic, hydrophobic and hydrogen bonding. The non-covalent imprinting approach seems to hold more potential for the future of molecular imprinting due to the vast number of compounds, including biological compounds, which are capable of non-covalent interactions with functional monomers (Yan and Row 2006: 155-178). Mosbach et al pioneered a non-covalent way to generate MIPs, which just calls for a self-assembly of template and functional monomer (Figure 3). The polymerizable “functional monomers” may associate with the template via a variety of interactions, including H-bridge formation, electrostatic and hydrophobic interaction. The polymerizable groups of the functional monomers are again incorporated in a highly crosslinked polymer network and hence once more a specific imprint (cavity) is created in the polymer. After template extraction under relatively gentle conditions, the non-covalent MIPs have been successfully used in areas such as separation techniques, catalysis and sensor technology. Since only non-covalent interactions are operative during both imprinting and application of the MIPs, the adsorption kinetics are usually much faster than in case of the covalent ones. In non-covalent, the affinity between the template and the functional monomer should be as high as possible. For templates carrying amino groups, acidic monomers such as acrylic or methacrylic acid, have given good results. For templates with carboxylic acid groups, the best choice seems to be a basic functional monomer, for example vinylpyridine, as counterpart. These monomers will lead to ionic interactions, which are stronger than hydrogen bonds or just hydrophobic ones. Figure 4 shows a number of functional monomers which are suitable for non-covalent imprinting. Different types of interaction are possible, including ionic and/or hydrogen bonds, electrostatic, hydrophobic/hydrophobic and/or van der Waals interactions (Bruggemann 2003: 134-141, Sellergren 2000: 113-180, Mayes and Whitcombe 2005: 1751-1760).

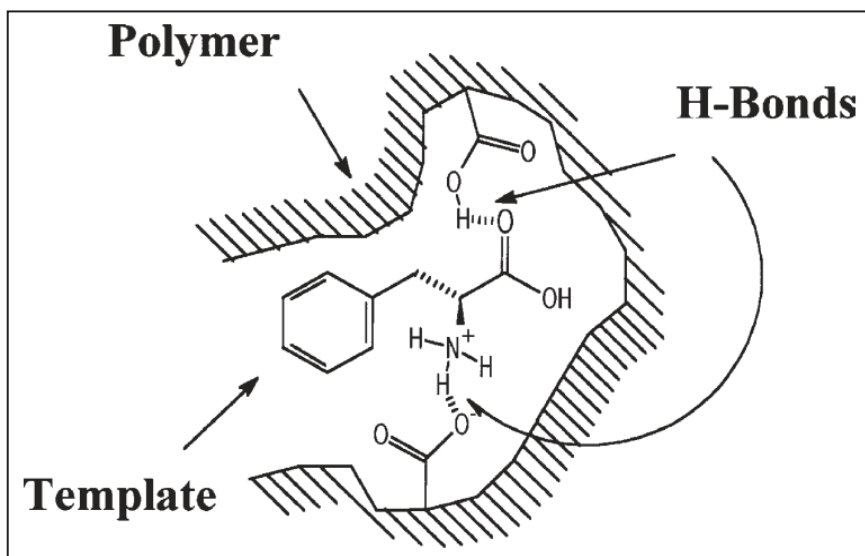


Figure 3 Non-covalent molecular imprinting.

Source: Oliver Bruggemann, “Molecularly imprinted polymers: A new dimension in analytical bioseparation,” Synthetic Polymers for Biotechnology and Medicine (2003): 136.

### 1.5 Factors influencing the specificity and selectivity characteristics of the imprinted polymers.

The challenge of designing and synthesizing a MIPs can be a daunting prospect to the uninitiated practitioner, not least because of the sheer number of experimental variables involved such as the nature and levels of template, functional monomers, crosslinkers, solvents and initiator, the method of initiation and the duration of polymerization.

#### 1.5.1 Template

In all molecular imprinting processes the template is central importance and it directs organization of the functional groups pendent to the functional monomers. In terms of compatibility with free radical polymerization, templates should ideally be chemically inert under the polymerization conditions, thus alternative imprinting strategies may have to be sought if the template can participate in radical reactions or is for any other reason unstable under the polymerization conditions. The followings are legitimate questions to ask of a template:

1. Does the template bear any polymerisable groups?
2. Does the template bear functionality that could potentially inhibit or retard a free radical polymerization? Such as a thiol group or a hydroquinone moiety.
3. Will the template be stable at moderately elevated temperatures? For example, at or around 60°C if AIBN is being used as the chemical initiator (Yan and Row 2006: 160-161).

Table 2 Important print molecules used for generating MIPs applied in separation techniques.

<b>Class of Compounds</b>	<b>Template</b>
Amino acids, peptides, proteins	Cbz-L-Glu-OH (Z)-L-Ala-L-Ala-OMe Boc-L-Trp-OH L-phenylalanine Boc-L-Trp Boc-L-Phe RNase A
Drugs	Oxacillin R-propranolol Theophylline Pentamidine
Pesticides, herbicides	S-(+)-2-phenylpropionic acid Atrazine 2,4-Dichlorophenoxyacetic acid
Nucleotides	NAD <sup>+</sup>
Nucleotide bases	9-Ethyladenin
Carbohydrates	Galactose derivatives Fructose derivatives
Steroids	Cholesterol
Metal ions	Cu <sup>2+</sup>
Dyes	Rhodanile blue

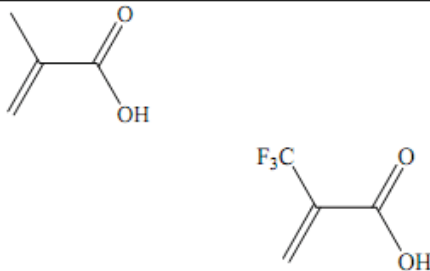
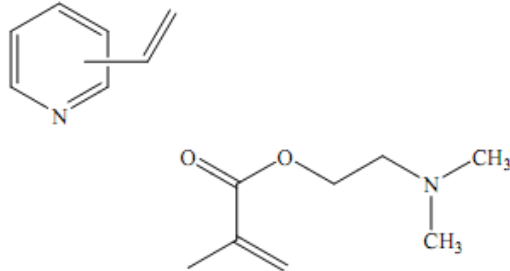
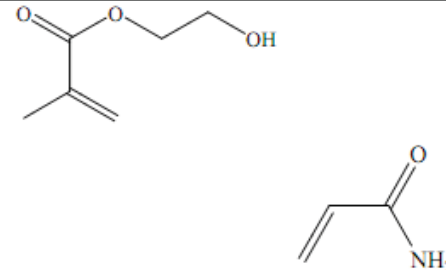
Source: Oliver Bruggemann, "Molecularly imprinted polymers: A new dimension in analytical bioseparation," Synthetic Polymers for Biotechnology and Medicine (2003): 142.

### 1.5.2 Functional monomers

The functional monomer contains at least a vinyl group and another functional group, through which it can interact with the template. Non-covalent imprinting requires the selection of an appropriate functional monomer that will form strong intermolecular interactions with the template. Commonly used functional monomers can be classified into three main categories (Table 3). The acidic functional monomers are useful for templates that can accept a proton; alternatively basic functional monomers will form better interactions with templates that can donate protons. For uncharged templates, a neutral functional monomer may help increase their interaction (Mayes and Whitcombe 2005: 1751-1760). To help in the selection process the strength of association between the template and functional monomer can be studied by spectroscopy, as the spectra changes are related to the change in the interaction between the template and functional monomer. FT-IR, <sup>1</sup>H-NMR or UV/Vis have been used in the past (Karim et al. 2005: 1795– 1808).

Functional monomers are responsible for the binding interactions in the imprinted binding sites and, for non-covalent molecular imprinting protocols, are normally used in excess relative to the number of moles of template to favor the formation of template, functional monomer assemblies (template to functional monomer ratios of 1:4 and upwards are rather common for non-covalent imprinting). It is clearly very important to match the functionality of the template with the functionality of the functional monomer in a complementary fashion (for example H-bond donor with H-bond acceptor) in order to maximize complex formation and thus the imprinting effect. Higher retention and resolution was found by the two co-monomer imprinting polymer than the single monomer imprinting polymer, which indicated an increase in the affinity of the MIPs with the sample as a result of the cooperation effect of the binding sites. However, it is important to bear reactivity ratios of the monomers to ensure those co-polymerizations are feasible. (Yan and Row 2006: 155-178).

Table 3 Commonly used functional monomers for non-covalent imprinting.

Classification	Structure	Functional monomer
Acidic		Methacrylic acid (MAA)  Trifluoromethacrylic acid (TFMAA)
Basic		<i>ortho- or para-</i> Vinyl pyridine  <i>N, N-</i> Dimethylaminoethyl methacrylate
Neutral		2-Hydroxyethyl methacrylate (HEMA)  Acrylamide

Source: A.G. Mayes, M.J. Whitcombe, "Synthetic strategies for the generation of molecularly imprinted organic polymers," *Advanced Drug Delivery Reviews* (2005): 1755– 1756.

### 1.5.3 Solvents

Apart from its influence on the template-monomer strength interactions mentioned previously, the solvent used in the pre-polymerization structure plays an important role in the morphology of the obtained polymer in terms of specific surface area and pore diameter (Martin-Esteban 2001: 795–802). Generally, a low surface area and low porosity leads to low template recognition in the subsequent rebinding experiments owing to slow diffusion of the target molecule through the porous structure. It is quite difficult to predict in advance the right solvent for the successful production of polymer because even when using a solvent capable of stabilizing the template-monomer complex during the pre-polymerization step it is

possible to obtain a polymer with an inadequate morphology, which decreases the template recognition (Martin-Esteban 2001: 795-802). Solvents with a low dielectric constant (poor solvents), such as chloroform and toluene, are thus preferred to good ones since they offer an adequate medium to stabilize hydrogen bonding and/or electrostatic interactions between monomers and templates leading to precipitation of growing chains during the polymerization process (Martin-Esteban 2001: 795-802). When solvents with higher dielectric constants (example acetonitrile) were used, the obtained polymers usually showed a lower affinity to rebind the template. Protic solvents, such as water and methanol, are not recommended since they not only hinder polymerization but also disrupt the template-monomer hydrogen-bonding interactions (Martin-Esteban 2001: 795-802).

### **1.5.3 Solvents**

Apart from its influence on the template-monomer strength interactions mentioned previously, the solvent used in the pre-polymerization structure plays an important role in the morphology of the obtained polymer in terms of specific surface area and pore diameter (Martin-Esteban 2001: 795–802). Generally, a low surface area and low porosity leads to low template recognition in the subsequent rebinding experiments owing to slow diffusion of the target molecule through the porous structure. It is quite difficult to predict in advance the right solvent for the successful production of polymer because even when using a solvent capable of stabilizing the template-monomer complex during the pre-polymerization step it is possible to obtain a polymer with an inadequate morphology, which decreases the template recognition (Martin-Esteban 2001: 795-802). Solvents with a low dielectric constant (poor solvents), such as chloroform and toluene, are thus preferred to good ones since they offer an adequate medium to stabilize hydrogen bonding and/or electrostatic interactions between monomers and templates leading to precipitation of growing chains during the polymerization process (Martin-Esteban 2001: 795-802). When solvents with higher dielectric constants (example acetonitrile) were used, the obtained polymers usually showed a lower affinity to rebind the template. Protic solvents, such as water and methanol, are not recommended since they not only hinder polymerization but also disrupt the template-monomer hydrogen-bonding interactions (Martin-Esteban 2001: 795-802).

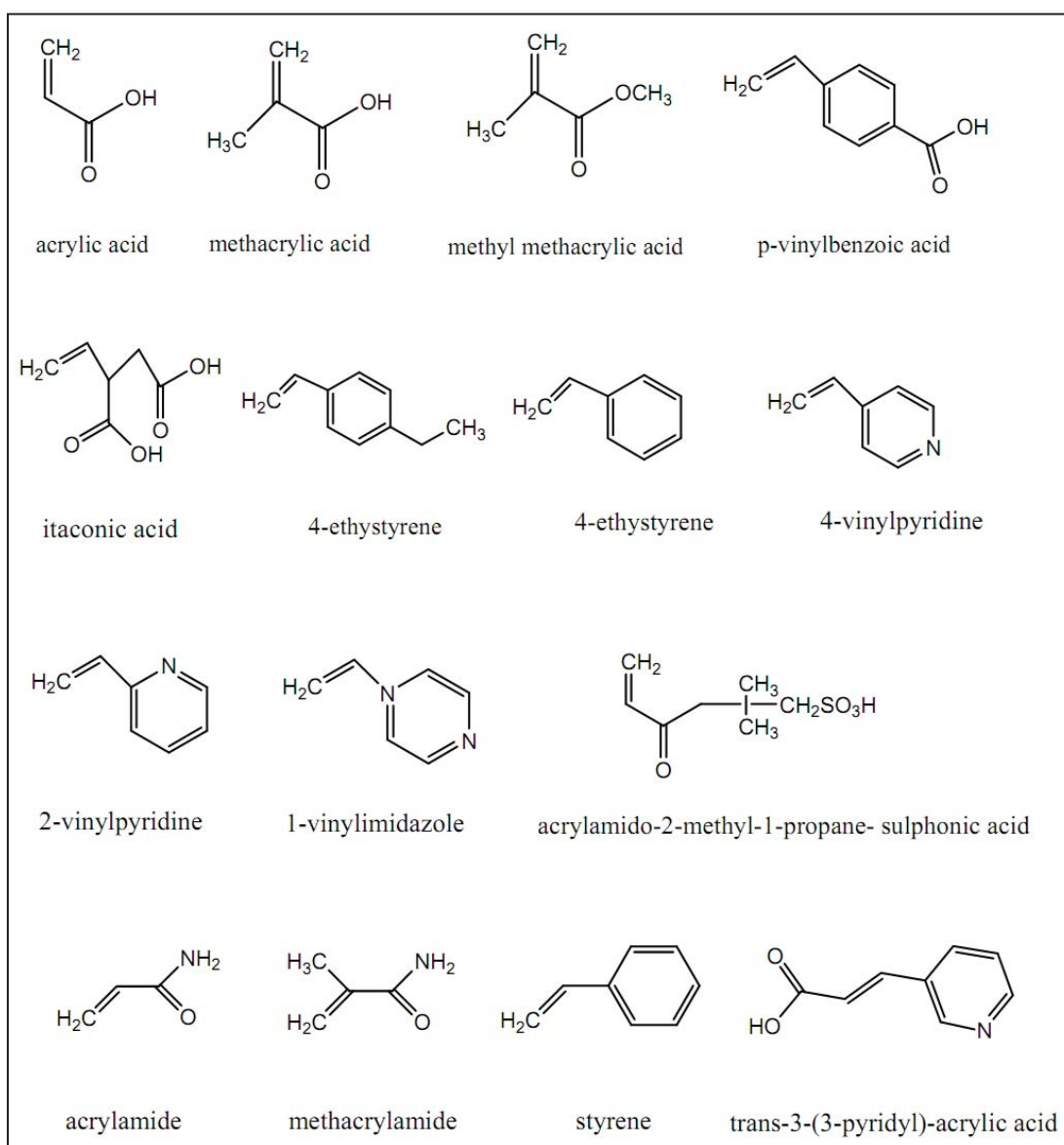


Figure 4 Functional monomers commonly used in non-covalent molecular imprinting procedures.

Source: Hongyuan Yan, Kyung Ho Row, "Characteristic and synthetic approach of Molecularly imprinted polymer," *International Journal of Molecular Sciences* (2006): 162.

### 1.5.4 Crosslinker agents

In order to guarantee the stability of the template-monomer complex during polymerization and to increase polymer porosity, a high degree of cross-linking is necessary. In an imprinted polymer the crosslinker fulfils three major functions. First of all, the crosslinker is important in controlling the morphology of

the polymer matrix, whether it is gel-type, macroporous or a microgel powder. Secondly, it serves to stabilize the imprinted binding site. Finally, it imparts mechanical stability to the polymer matrix. Much has been written about the effect of the cross-linker on the molecular recognition behavior of imprinted polymers, but from a polymerization point of view, high cross-link ratios are generally preferred in order to access permanently porous (macroporous) materials and in order to be able to generate materials with adequate mechanical stability (Yan and Row 2006: 155-178). Polymers with cross-link ratios in excess of 80% are often used. For the same reason that one should match the reactivity ratios of functional monomers in a cocktail polymerization to ensure smooth incorporation of the co-monomers, the reactivity ratio of the crosslinker should ideally also be matched to that of the functional monomers. Quite a number of crosslinkers compatible with molecular imprinting are known, many of which are commercially available and a few of which are capable of simultaneously complexing with the template and thus acting as functional monomers. The chemical structures of several well-known crosslinkers are shown in Figure 5 (Yan and Row 2006: 155-178). For example, ethylene glycol dimethacrylate (EGDMA) is the crosslinker often used in methacrylate-based systems, since it provides mechanical and thermal stability, good wettability and rapid mass transfer. For instance, it has been reported that at least 50% of the total monomer in a MAA-ethylene glycol dimethacrylate (EGDMA) system has to be EGDMA, otherwise no recognition can take place (Sellergren 2000: 113-180)

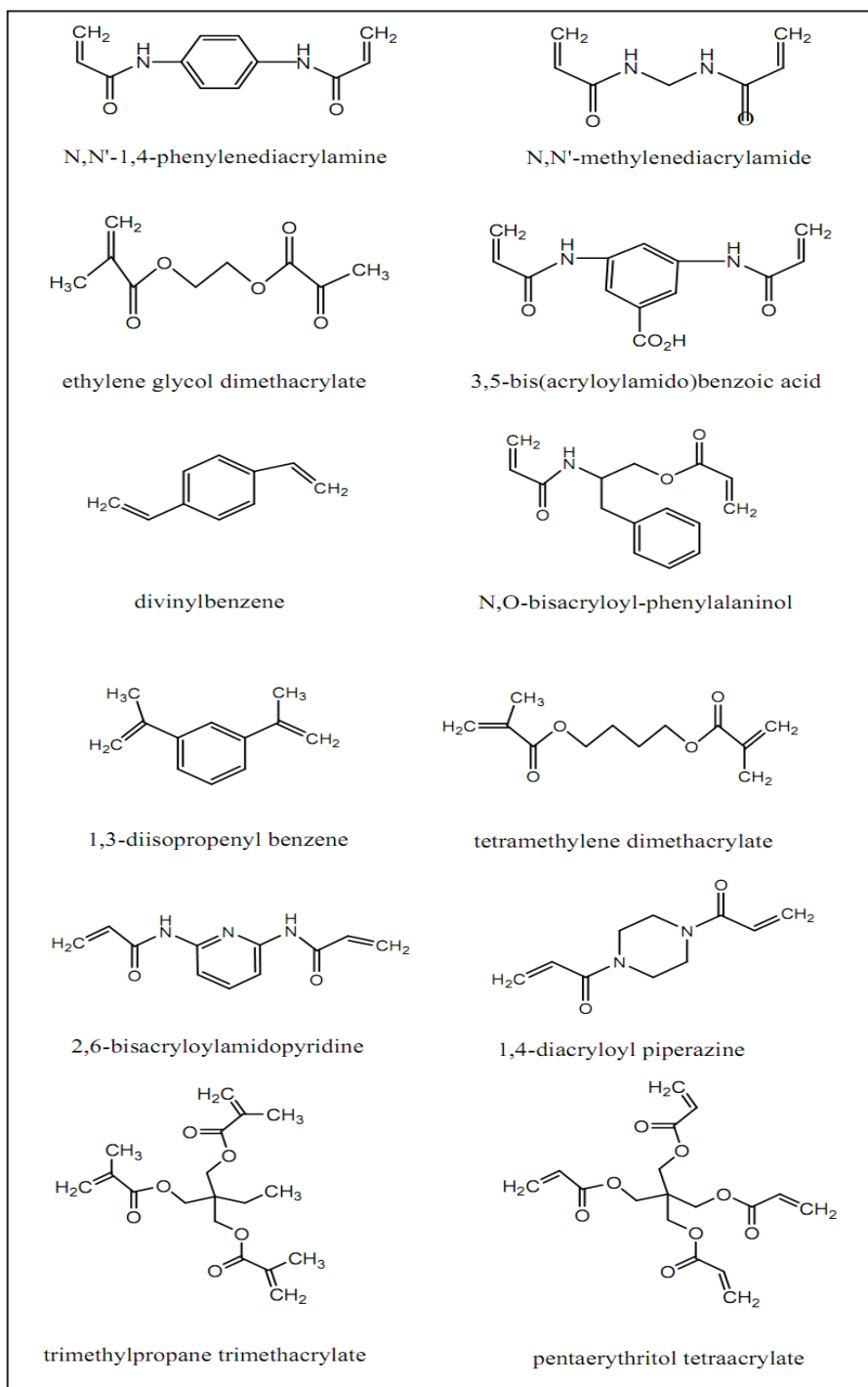


Figure 5 Chemical structure of common crosslinkers used in non-covalent molecular imprinting.

Source: Hongyuan Yan, Kyung Ho Row, "Characteristic and synthetic approach of molecularly imprinted polymer," *International Journal of Molecular Sciences* (2006): 164.

## 1.6 Characterization of molecular imprinted polymers

In order to draw conclusions of how variables related to the preparation of porous solids affect their useful properties, it is necessary to characterize the structure and morphology of the materials. First it should be established that the polymerization has proceeded to full conversion of the monomers and, ideally, the regularity and structure of the primary chains should be studied. It is also important to determine the accessibility and microenvironment of the functional groups and binding sites. In chromatography, these factors are directly related to the sample load capacity and mass transfer kinetics of the stationary phase. In molecular imprinting the number of these binding sites depends on the amount of template that can be recovered by various washing procedures. Sensitive methods for quantifying this amount must be found. Knowledge about dynamic processes, such as polymer chain mobility or side chain mobility and rates of transport of small molecules within the pores, is important to understand the behavior of MIPs. A more far reaching goal is to find methods allowing the binding sites to be characterized at a molecular level. Until now the methods have been used to gain information related to the above properties (Sellergren and Hall 2000: 21-55).

### 1.6.1 Pore system, surface areas, texture

#### 1.6.1.1 Porosimetry (N<sub>2</sub> sorption, Hg penetration)

#### 1.6.1.2 Microscopy (SEM)

#### 1.6.1.3 Swelling and solvent uptake

### 1.6.2 Conformational transitions, thermostability

#### 1.6.2.1 Thermal analysis (TGA, DSC)

### 1.6.3 Polymer yield, composition

#### 1.6.3.1 Elemental analysis

#### 1.6.3.2 CP-MAS-solid state NMR

### 1.6.4 Chemical and structural information

#### 1.6.4.1 Potentiometric titrations

#### 1.6.4.2 FTIR CP-MAS-solid state NMR Fluorescence probes

### *NMR*

The direct evidence for the formation of non-covalent monomer–template interactions, the extent of which is reflected in the total binding term,  $\Delta\Delta G$

bind, was first presented in an NMR study by Sellergren et al. The results suggested the minor presence of template self-association and higher order complexes. Whitcombe et al. also adopted a similar approach, where NMR chemical shift studies allowed the calculation of dissociation constants and a potential means for predicting the binding capacities of MIPs. The NMR characterizations of functional monomer-template interactions have also been applied to the study of the interactions between many other functional monomers and templates. In most of these studies, it was also possible to determine the exact composition of the complex. For example, Nicholls investigated in detail the characterization of complexes between nicotine and methacrylic acid (K.Karim et al. 2005: 1795-1808).

#### *FTIR*

Fourier transform infrared spectroscopy (FTIR) is a technique capable to determine the modification of the structure of a molecule. It has been used particularly with samples in solution or in the solid state. The imprinting process begins with a complexation between a functional monomer and a template generally via hydrogen bonding. The formation of this bond can be readily identifiable using FTIR since the stretching frequency of hydroxyl or amino groups (hydrogen bond donors) and carbonyl groups (hydrogen bond acceptors) are displaced and an observable shift can be identified. However, the presence of solvent can interfere on the determination of specific characteristics of complexation. This explains why this technique is not well applied to the pre-polymerization solution analysis. Brune et al. investigated the interaction by FTIR between phenolic compounds and an analogue of the acrylic ester monomer, ethyl propionate in hexane. Duffy et al. characterized by FTIR pre- and post-polymerization binding properties of an imprinted membrane for thymine using 2, 6-diacetyldiaminopyridine as a functional monomer. Liquid spectroscopy clearly shows the three hydrogen bonds linking the monomer and template molecules in the pre polymerization mixture. The three characteristic bands of the amino groups above  $3000\text{ cm}^{-1}$  remained after the polymerization, indicating that the template-monomer complex was still present in the polymer. However, the binding constant of the imprinted membrane for the thymine was estimated to be ten times lower than that of the soluble monomer. This decrease was attributed to a

shrinkage during cross-linking and loss of freedom of the monomer (K.Karim et al. 2005: 1795-1808 ).

### *UV*

Complexation has also been studied using UV spectroscopic titrations in order to calculate the dissociation constants for the solution adducts and the relative concentration of fully complexed templates in the polymerization mixture. This approach was also used to verify the inert nature of the cross-linking agent ethylene glycol dimethacrylate and for the screening of candidate functional monomers. In another paper, Striegler and Tewes used UV spectroscopy to choose the best ligand for copper capable of providing effective functional monomers for carbohydrate imprinted polymer synthesis. The experimental data firstly estimated the copper-ligand stability in order to select the best ligand, and secondly to evaluate the apparent binding constants between the copper-containing functional monomers and different hexoses in alkaline pH. The complex [(diethylenetriamine) copper(II)] dinitrate appeared to be the most promising monomer for the complexation with sugars, and it was found that the binding involved only hydroxyl groups at C1 and C2 of the carbohydrates. The main advantage of this technique is its simplicity of use and the possibility to control monomers-template complex formation in aqueous media (K. Karim et al. 2005: 1795-1808).

## **1.7 Applications by molecular imprinted polymers**

### **1.7.1 Application of molecular imprinting in drug delivery**

Synthetic molecularly selective receptors such as MIPs have broad application in many area of science (Figure 6) (Sellaergren and Allender 2005: 1733-1741). MIPs can be programmed to recognize a large variety of target structures with antibody-like affinities and selectivities.

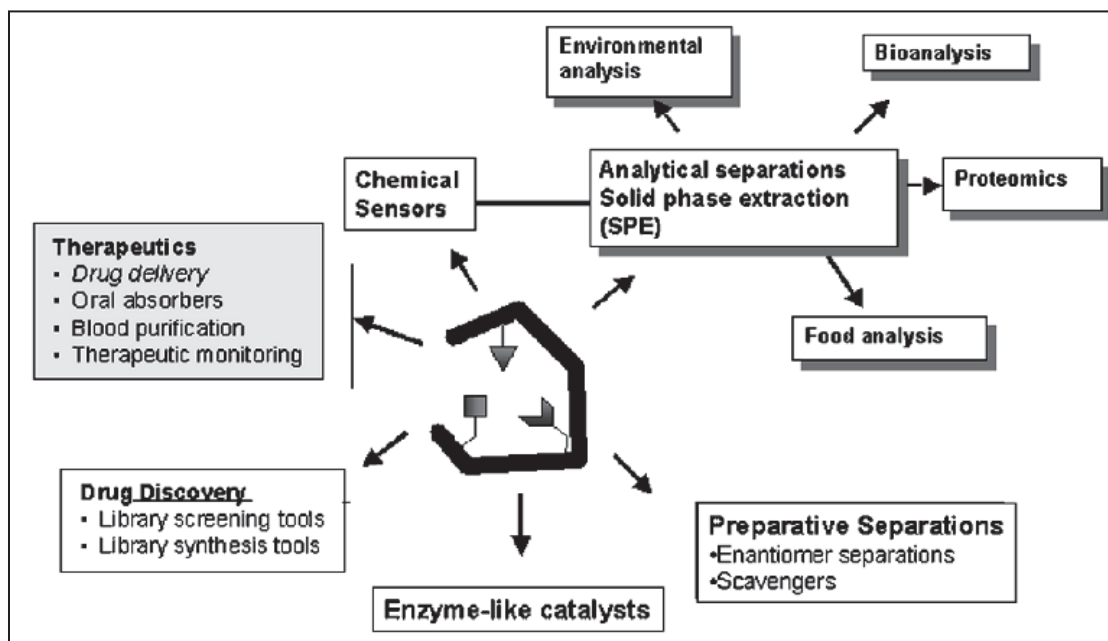


Figure 6 The applications envisaged for MIPs.

Source: Borje Sellergren, "Molecularly imprinted polymers: A bridge to advanced drug delivery," *Advanced Drug Delivery Reviews* (2005): 1734.

### 1.7.2 Molecularly imprinted membrane (MIM)

The main advantages of membrane technology are related to the unique separation principle such as the transport selectivity of the membrane. The separations with membranes do not require additives, and they can be performed isothermally at low temperatures and compared to other thermal separation processes at low energy consumption. Both upscaling and downscaling of membrane processes as well as their integration into other separation or reaction processes are easy (Mathias Ulbricht 2006: 2217–2262). Technology of MIPs can compose with membrane technology to improve membrane selectivity and mostly used for separation or sensor application. Either simultaneous formation of MIP structure and membrane morphology (self-supported MIM) or composing of MIP with support membrane (MIP composite membrane) can prepare MIM. Piletkey and coworkers could prepare MIM by in situ crosslinker polymerization of acrylate monomer forming a film in the presence of adenosine monophosphate (AMP), in diffusion experiments possess selective permeability for this nucleotide. However, this method normally has a poor mechanical stability obtain MIM. For MIPs composite

membrane, it may be prepared in the form of pore filling MIPs, thin layer MIPs or MIP particles composing membrane. In pore filling MIP composite membrane, MIP synthesis mixtures such as methacrylic acid (MAA)/ethylene glycol dimethacrylate (EDMA) have been polymerized in mm-thick glassfilters to fill their pores (Piletsky et al. 1999: 263-278). Jantarat and coworkers have produced self-assembled composite porous cellulose membranes containing MIP particles. It was planned to employ a phase inversion technique with the use of polycaprolactone-triol as plasticiser. Initial design objectives included the requirement that there should be a high accessibility of the template molecule (S-enantiomer of propranolol) to the binding sites on MIP particles and a high permeability of the resultant membrane. MIP nanoparticle-on-microspheres (NOM) selective for S-propranolol were successfully prepared using suspension polymerization. (Jantarat et al. 2008: 212–225). Afterward Jing-Yu Wang and coworker have reported MIP composite membranes for selective binding and permeation of S-Naproxen (S-Nap), which were synthesized using the copolymerization method with 4-vinyl-pyridine (4-VPy) as functional monomers and ethylene glycol dimethacrylate (EDMA) as cross-linkers. There are several works that have been reported for successful Naproxen separation using imprinting technology (Wang et al. 2009: 84-90). Molecularly imprinted nanoparticles were encapsulated into polymer nanofibers with a simple electrospinning method. The composite nanofibers form non-wovenmats that can be used as affinity membrane to greatly simplify solid phase extraction of drug residues in analytical samples. Upward 100% of PPL-imprinted nanoparticles can be easily encapsulated into poly (ethylene terephthalate) (PET) nanofibers, ensuring the composite materials to have a high specific binding capacity. The molecularly imprinted nanoparticles and microspheres were prepared using precipitation polymerization method (Yoshimatsu et al. 2007: 112-121) and successively encapsulated into PET nanofibers by electrospinning (Yoshimatsu et al. 2008: 1208-1215).

## **2. Electrospinning**

Electrospinning is a simple and versatile method for generating ultrathin fibers from a rich variety of materials that include polymers, composites and ceramics. This nonmechanical, electrostatic technique involves the use of a high voltage

electrostatic field to charge the surface of a polymer solution droplet and thus to induce the ejection of a liquid jet through a spinneret (Figure 7). In electrospinning process a high voltage is applied to a polymer solution such that electric field is induced within the solution. When the applied electric field overcomes the surface tension of the droplet, a charged jet of polymer solution is ejected. The route of the charged jet is controlled by the electric field. A solution jet will erupt from the droplet at the tip of the needle resulting in the formation of a Taylor cone. The electrospinning jet will travel forwards the region of lower potential, which in most cases, is a grounded collector. There are many parameters that will influence the morphology of the resultant electrospun fiber, from beaded fibers to fibers with pores on its surface (Ramakrishna 2005: 15-21, 90).

The following parameters and processing variables affect the electrospinning process system parameters such as molecular weight, molecular weight distribution and architecture (branched, linear) of the polymer, and polymer solution properties (viscosity, conductivity, dielectric constant, and surface tension, charge carried by the spinning jet) and process parameters such as electric potential, flow rate and concentration, distance between the capillary and collection screen, ambient parameters (temperature, humidity and air velocity in the chamber) and finally motion of the target screen (Chronakis 2005 : 283–293, Ramakrishna 2005: 90-154).

### **3. Methacrylate-Based Copolymers**

Methacrylic acid and ethylene methacrylic acid ester that were the compounds of interest employed in this study, as the monomers for preparation of MIPs are found to have biocompatibility and non-toxicity. Poly (methacrylic acid) and polyethylene glycol (PEG)-based polymers are also used for producing pharmaceutical products such as pharmaceutical tablets, capsules, confectionary or food with water-based ingestible. Methacrylic acid-methacrylic acid ester copolymer with the trademark is widely used as enteric polymer in controlled drug delivery (Wiley and Sons 1962: 404-419, Jantarat et al. 2008: 212-225).

The Polymethacrylates for pharmaceutical applications are known worldwide in the industry under the trademark “Eudragit”. Eudragit polymers are

copolymers derived from esters of acrylic and methacrylic acid, whose physicochemical properties are determined by functional groups. Methacrylate-based copolymers with a variety of functional properties of Eudragit are presented in Table 4. (Eudragit Acrylic Polymers for Solid Oral Dosage Forms [Online], accessed 5 October 2011. Available from <http://abstracts.aapspharmaceutica.com/ExpoAAPS09/Data/EC/Event/Exhibitors/33/productBrochure1.pdf>)

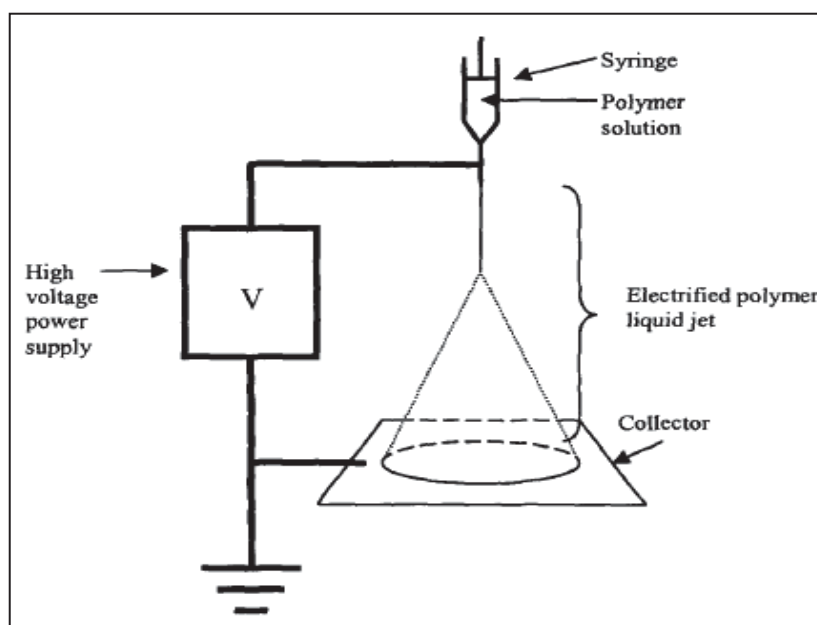


Figure 7 Schematic diagram of the electrospinning process.

Source: Seeram Ramakrishna, Kazutoshi Fujihara, et al., An introduction to electrospinning and nanofibers (Singapore: World Scientific Publishing Co.Pte. Ltd., 2005): 17.

### 3.1 Polymethacrylates for pharmaceutical purposes

In parallel with the above-mentioned Eudragit products, a series of pharmaceutical applications for polymethacrylates opened up, many of which could be served by simple copolymerization. Examples of such products are presented in Table 5.

Table 4 Methacrylate-based copolymers with a variety of functional properties.

Functionality	Trade name Description
Anionic polymer of methacrylic acid and methacrylates with a -COOH group	<p>Eudragit L 100-55 : powder, spray dried L 30 D-55 which can be reconstituted for targeted delivery in the duodenum</p> <p>Eudragit L 30 D-55 : aqueous dispersion, pH dependent polymer soluble above pH 5.5 for targeted delivery in the duodenum</p> <p>Eudragit L 100 : powder, pH dependent polymer soluble above pH 6.0 for targeted delivery in the jejunum</p> <p>Eudragit S 100 : powder, pH dependent polymer soluble above pH 7.0 for targeted delivery in the ileum.</p> <p>Eudragit FS 30 D : aqueous dispersion, pH dependent polymer soluble above pH 7.0, requires no plasticizer</p>
Cationic polymer with a dimethylaminoethyl ammonium group	<p>Eudragit E 100 : granules, pH dependent, soluble in gastric fluid up to 5.0, swellable and permeable above pH 5.0.</p> <p>Eudragit E PO : powder form of E-100</p>
Copolymers of acrylate and methacrylates with quarternary ammonium group.	<p><b>Insoluble, High Permeability</b></p> <p>Eudragit RL 30D : aqueous dispersion, pH independent polymer for sustained release formulations</p> <p>Eudragit RL PO : powder, pH independent polymer for matrix formulations</p> <p>Eudragit RL 100 : granules, pH independent</p> <p><b>Insoluble, Low Permeability</b></p> <p>Eudragit RS 30D : aqueous dispersion, pH independent polymer for sustained release formulations</p> <p>Eudragit RS PO : powder, pH independent polymer for matrix formulations</p> <p>Eudragit RS 100 : granules, pH independent</p>

Source: Eudragit Acrylic Polymers for Solid Oral Dosage Forms [Online], accessed 5 October 2011. Available from <http://abstracts.aapspharmaceutica.com/ExpoAAPS09/Data/EC/Event/Exhibitors/33/productBrochure1.pdf>

Table 5 Use of poly(meth) acrylates in the pharmaceutical industry.

Use	Monomers/product examples	Reference
<b>Cutaneous</b>		
Ointments, gels	(Meth)acrylic acid/CARBOPOL <sup>®</sup> (Goodrich)	Völker (1961)
Mucal ointments	Methacrylic acid	Bremecker (1982)
Wound sprays	Methyl methacrylate, ethoxyethyl methacrylate/ FLINT <sup>®</sup> , NOBECUTAN <sup>®</sup>	
Wound sealants	Cyanoethyl methacrylate	
Transdermal systems	Methyl methacrylate/EUDRAGIT <sup>®</sup> (Röhm)	Stricker (1980)
<b>Oral</b>		
Ion-exchange resins	Methyl methacrylate/AMBERLITE <sup>®</sup> (Rohm & Haas, Philadelphia)	Chauhry (1956) Farhadieh (1971)
Matrix tablets	Methyl methacrylate/GRADUMET <sup>®</sup> (Abbott)	Speiser (1964)
Bead polymers	Methyl methacrylate	Speiser (1964)
Extrusion + injection molding	Methyl methacrylate	Rhodes (1970)
Coprecipitates	Methacrylic acid	
Film coatings		
gastro-soluble	Aminoalkyl methacrylate/EUDRAGIT <sup>®</sup> (Röhm)	Falck (1960)
gastro-resistant/ entero-soluble	(Meth)acrylic acid/EUDRAGIT <sup>®</sup> (Röhm)	Trommsdorff (1952)
permeable	Methyl methacrylate/EUDRAGIT <sup>®</sup> (Röhm)	Lehmann (1967)
Drug capsules	Methyl methacrylate/EUDRAGIT <sup>®</sup> (Röhm)	Lehmann (1971)
<b>Parenteral</b>		
Interferon inductors	(Meth)acrylic acid	De Somer (1968)
Plasma expanders	(Meth)acrylic acid alkylamide	Kopecek (1973)
Vaccines	Methyl methacrylate ("nanocapsules")	Speiser (1973)
Polymer-bound insulin	(Meth)acrylic acid (anhydride)	Krämer (1972)

Source: Rohm Pharma Polymer Introduction: Synthetic polymers for coating pharmaceutical dosage forms [Online], accessed 5 October 2011. Available from [http://80.241.206.189/en/pharmapolymers/service/literature/practical\\_course.Par.0001.TRow.0002.TCell.0003.File.tmp/pc\\_02\\_introduction.pdf](http://80.241.206.189/en/pharmapolymers/service/literature/practical_course.Par.0001.TRow.0002.TCell.0003.File.tmp/pc_02_introduction.pdf)

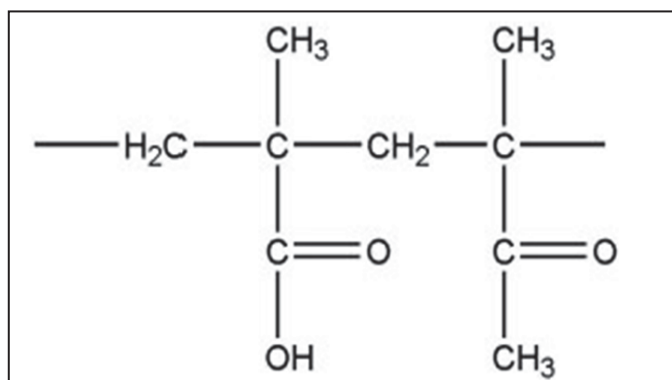


Figure 8 Poly(methacrylic acid-co-methyl methacrylate) (Eudragit L100; Mw 135,000 Da)

Source: Varaporn Pornsopone, Pitt Supaphol, et al., “Electrospinning of Methacrylate-Based Copolymers: Effects of Solution Concentration and Applied Electrical Potential on Morphological Appearance of As-Spun Fibers,” Polymer Engineering and Science (2005): 1074.

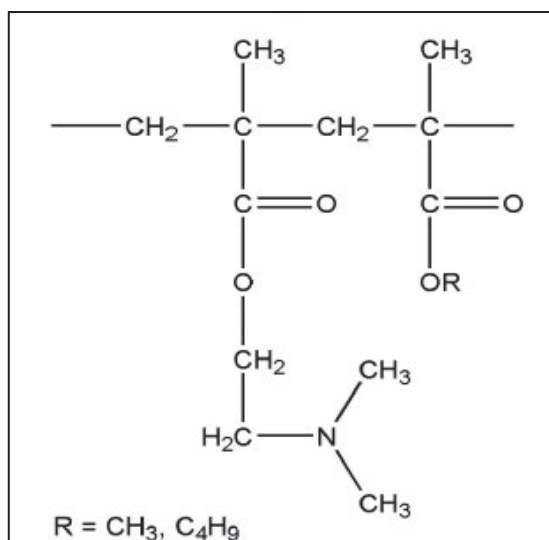


Figure 9 Poly-(butyl methacrylate-co-(2-dimethylaminoethyl) methacrylate-co-methyl methacrylate) (Eudragit EPO; Mw 150,000 Da)

Source: Source: Varaporn Pornsopone, Pitt Supaphol, et al., “Electrospinning of Methacrylate-Based Copolymers: Effects of Solution Concentration and Applied Electrical Potential on Morphological Appearance of As-Spun Fibers,” Polymer Engineering and Science (2005): 1074.

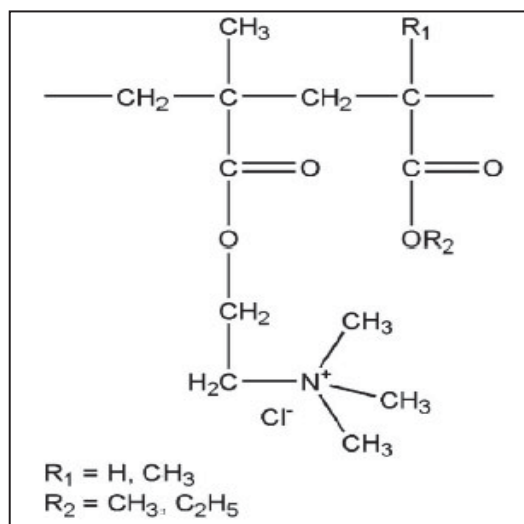


Figure 10 Poly(ethyl acrylate-co-methyl methacrylate-co-trimethyl-ammonioethyl methacrylate chloride) (Eudragit RLPO; Mw 150,000 Da)

Source: Varaporn Pornsopone, Pitt Supaphol, et al., "Electrospinning of methacrylate-based copolymers: Effects of solution concentration and applied electrical potential on morphological appearance of as-spun fibers," Polymer Engineering and Science (2005): 1074.

Aqueous Eudragit dispersions eliminate all problems associated with organic solvents, such as flammability, toxicity and harmful emissions. They are simpler and less expensive to process and therefore more versatile in use.

#### 4. Beta-adrenergic antagonist drug

##### 4.1 Propranolol

Propranolol one of the most widely prescribed  $\beta$ -adrenergic antagonist drug in the long-term treatment of hypertension and cardiovascular diseases is usually taken orally, although an intravenous form is available for acute administration. Propranolol is rapidly absorbed from gastrointestinal tract, but the oral bioavailability is low (~30%) due to significant first pass metabolism. Its molecular structure contains an aromatic naphthyloxy group attached to a side alkyl chain possessing a secondary hydroxyl and amine functional group (Figure 11). It possesses two enantiomers due to the presence of a chiral carbon in the alkyl side chain, adjacent to a hydroxyl group. Propranolol possesses one chiral center and the S-isomer is 100–

130 times as active as its R-isomer (Physicians Desk Reference 2009: 1484, Jantarat et al. 2008: 213).

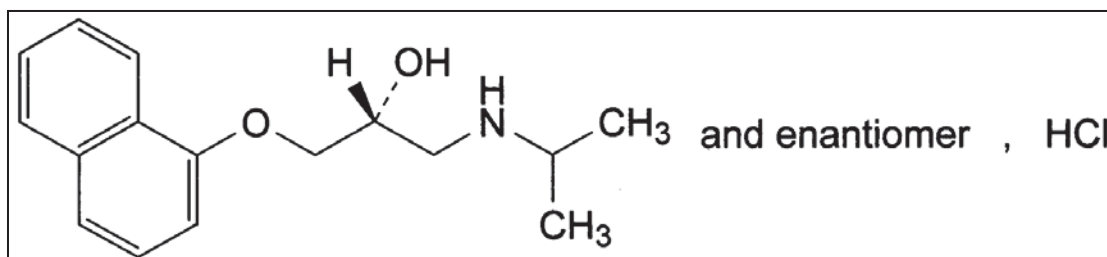


Figure 11 Structure of Propranolol Hydrochloride

Source: British Pharmacopoeial Commission, The British Pharmacopoeia, London: The Pharmaceutical Press 2010: 1786.

*Chemical Formula* : C<sub>16</sub>H<sub>21</sub>NO<sub>2</sub>

*Chemical Name*

(2RS)-1-[(1-Methylethyl)amino]-3-(naphthalen-1-yloxy) propan-2-ol

*Molecular weight* (Pharmaceutical codex 1994: 1025)

Propranolol 259.3

Propranolol hydrochloride 295.8

*Physical properties* (Pharmaceutical codex 1994: 1026)

Propranolol exists in the form of crystals.

Propranolol hydrochloride is a white or almost white powder; odourless, with a bitter taste. It absorbs less than 1% of water at 25°C at relative humidity up to 80%

*Melting point* (Pharmaceutical codex 1994: 1026)

Propranolol melt in the range of 94°C to 96°C

Propranolol hydrochloride melt in the range of 163°C to 166°C

*Dissociation constant*

pKa 9.5 (24°C) (Pharmaceutical codex 1994: 1026)

*Solubility*

Propranolol hydrochloride is soluble in water and in ethanol (96%). (British Pharmacopoeial Commission 2010: 1786).

Propranolol hydrochloride is soluble 1 in 20 of water and 1 in 20 of ethanol; slightly soluble in chloroform and practically insoluble in ether (Pharmaceutical codex 1994: 1026).

#### *Stability*

Propranolol hydrochloride is affected by light. In aqueous solutions, it decomposes with oxidation of the isopropylamine sidechain, accompanied by reduction in the pH and discoloration of the solution. Solutions are most stable at pH 3.0 and decompose rapidly under alkaline conditions (Pharmaceutical codex 1994: 1026).

#### *Propranolol formulations*

Propranolol is currently marketed throughout the world in a variety of forms: Prolonged-release Propranolol Capsules, Propranolol Injection capsules, Propranolol Tablets

## **4.2 Atenolol**

*Chemical Formula* :  $C_{14}H_{22}N_2O_3$

*Chemical Name*

2-[4-[(2RS)-2-Hydroxy-3-[(1-methylethyl)amino]propoxy]phenyl]acetamide.

*Molecular weight* (BP 2010)

266.3

*Physical properties* (Pharmaceutical codex 1994: 747)

Atenolol is white or almost white powder; odourless or almost odourless.

*Melting point*

Atenolol melts in the range of 152 °C to 155 °C (BP 2010).

Atenolol has been reported to melt in the ranges 146°C to 148°C, 150°C to 152°C, and 152°C to 155°C (Pharmaceutical codex 1994: 747).

*Dissociation constant*

pKa 9.6 (24°C) (Pharmaceutical codex 1994: 747)

*Solubility*

Atenolol is Sparingly soluble in water, soluble in anhydrous ethanol, slightly soluble in methylene chloride. (British Pharmacopoeial Commission 2010:

185-187).

#### *Stability*

Atenolol as powder and in tablets was reported to remain stable and unchanged in appearance after storage at 50% to 60% relative humidity and 45 to 50 for seven days (Pharmaceutical codex 1994: 747).

#### *Atenolol formulations*

Atenolol is currently marketed throughout the world in a variety of forms: Atenolol Injection, Atenolol Oral Solution, Atenolol Tablets (BP2010).

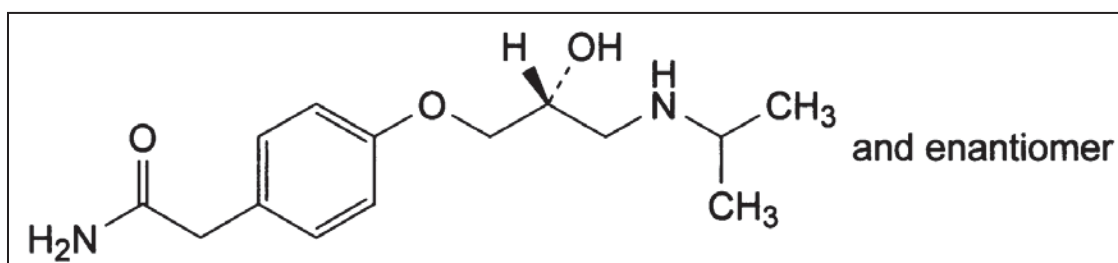


Figure 12 Structure of Atenolol

Source: British Pharmacopoeial Commission, The British Pharmacopoeia, London: The Pharmaceutical Press, 2010: 185.

### **4.3 Metoprolol Tartrate**

*Chemical Formula* :  $(C_{15}H_{25}NO_3)_2 \cdot C_4H_6O_6$

*Chemical Name*

Bis[(2RS)-1-[4-(2-methoxyethyl)phenoxy]-3-[(1-methylethyl)amino]ropan-2-ol] (2R,3R)-2,3-dihydroxybutanedioate.

*Molecular weight* (British Pharmacopoeial Commission 2010: 1421)

685

*Physical properties* (British Pharmacopoeial Commission 2010: 1421)

Metoprolol Tartrate is a white or almost white, crystalline powder or colourless crystals.

*Dissociation constant*

pKa 9.5

*Solubility*

Metoprolol Tartrate is very soluble in water, freely soluble in alcohol. (British Pharmacopoeial Commission 2010: 1421).

*Metoprolol Tartrate formulations*

Metoprolol Tartrate is currently marketed throughout the world in a variety of forms: Metoprolol Injection, Metoprolol Tartrate Tablets, Prolonged-release Metoprolol Tartrate Tablet (BP2010).

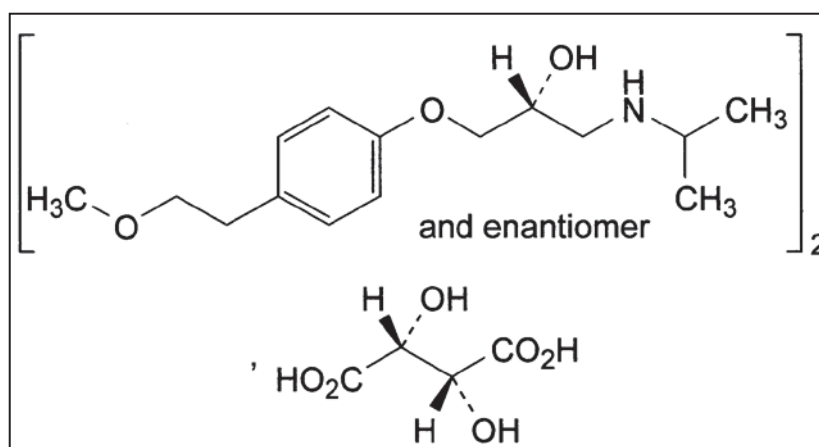


Figure 13 Structure of Metoprolol Tartrate

Source: British Pharmacopoeial Commission, The British Pharmacopoeia, London: The Pharmaceutical Press, 2010: 1421.

#### 4.4 Timolol Maleate

*Chemical Formula* :  $C_{13}H_{24}N_4O_3S, C_4H_4O_4$

*Chemical Name*

(2S)-1-[(1,1-dimethylethyl)amino]-3-[[4-(morpholin-4-yl)-1,2,5-thiadiazol-3-yl]oxy]propan-2-ol (Z)-butenedioate.

*Molecular weight* (British Pharmacopoeial Commission 2010: 2100)  
432.5

*Physical properties* (British Pharmacopoeial Commission 2010: 2100)

Timolol Maleate is a white or almost white, crystalline powder or colourless crystals, soluble in water and in ethanol (96 %).

*Melting point* (British Pharmacopoeial Commission 2010: 2100)

Timolol Maleate melts at about 199 °C, with decomposition.

*Dissociation constant*

pKa 8.8 (Pharmaceutical codex 1994: 1075)

*Solubility*

Timolol Maleate is soluble 1 in 15 of water, 1 in 21 of ethanol and in methanol; it is sparingly soluble in chloroform (1 in 40) and propylene glycol; it is practically insoluble or insoluble in ether and in cyclohexane (British Pharmacopoeial Commission 2010: 2100).

*Stability*

Timolol Maleate is reported to be extremely stable at room temperature both in the solid state and in aqueous solutions. (Pharmaceutical codex 1994: 1075).

*Timolol Maleate formulations*

Timolol Maleate is currently marketed throughout the world in a variety of forms: Timolol Eye Drops, Timolol Tablets (British Pharmacopoeial Commission 2010: 2100).

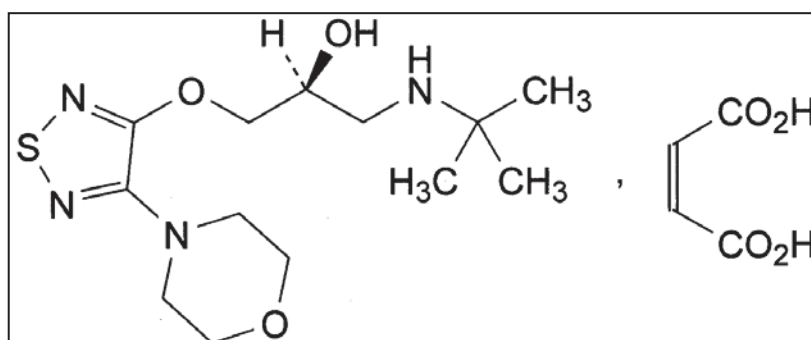


Figure 14 Structure of Timolol Maleate

Source: British Pharmacopoeial Commission, The British Pharmacopoeia, (London: The Pharmaceutical Press, 2010): 2100.

## CHAPTER 3

### MATERIALS AND METHODS

#### 1. Materials

1. Acetic acid (Lab Scan, Dublin, Ireland)
2. Acetonitrile (Lab Scan, Dublin, Ireland)
3. Atenolol (ATE) (Berlin Pharmaceutical Ind.co., Ltd, Thailand)
4. Benzoyl peroxide 75% (BP) (Sigma-Aldrich, co., St. Louis, MO, USA)
5. di-basic Sodium phosphate ( $\text{Na}_2\text{HPO}_4$ ) (Baker analyzed, Phillipburg, Malaysia)
6. Dichloromethane (Asian scientific, co.,Ltd, Thailand)
7. N,N-Dimethylformamide ( $\text{DMF} \geq 99.8\%$ ) (Brightchem Sdn Bhd, Malaysia)
8. Divinylbenzene 80% (DVB) (Sigma-Aldrich, co., St. Louis, MO, USA)
9. Ethanol absolute (Mallinckrodt chemical, Malaysia)
10. Isopropyl alcohol (IPA) (Lab Scan, Dublin, Ireland)
11. Methanol HPLC grade (Lab Scan, Dublin, Ireland)
12. Methyl methacrylate 99% (MMA) (Sigma-Aldrich, co., St. Louis, MO, USA)
13. Metoprolol tartrate (MET) (V&S chemi group co., Ltd, Thailand)
14. Mono-basic Sodium phosphate ( $\text{NaH}_2\text{PO}_4$ ) (Ajax Finechem, Australia)
15. N,N-Dimethylacetamide ( $\text{DMAc} \geq 99.5\%$ ) (Sigma-Aldrich, co., St. Louis, MO, USA)
16. Orthophosphoric acid 85% (Merch, Darmstadt, Germany)
17. Poly-(butyl methacrylate-co-(2-dimethylaminoethyl) methacrylate-co-methyl methacrylate) (Eudragit EPO; Rohm GmbH, co., Darmstadt, Germany)
18. Poly(ethyl acrylate-co-methyl methacrylate-co-trimethylammonioethyl methacrylate chloride) (Eudragit RL100; Rohm GmbH, co., Darmstadt, Germany)

19. Poly(ethyl acrylate-co-methyl methacrylate-co-trimethylammonioethyl methacrylate chloride) (Eudragit RS-100; Rohm GmbH, co., Darmstadt, Germany)
20. Poly(methacrylic acid-co-methyl methacrylate) (Eudragit L100; Rohm GmbH, co., Darmstadt, Germany)
21. Poly(methacrylic acid-co-methyl methacrylate) (Eudragit S100; Rohm GmbH, co., Darmstadt, Germany)
22. Poly(ethyl acrylate-co-methyl methacrylate-co-trimethylammonioethyl methacrylate chloride) (Eudragit RLPO; Rohm GmbH, co., Darmstadt, Germany)
23. Polyvinyl alcohol (PVA; MW 85,000–124,000, 87–89% hydrolyzed, Sigma-Aldrich, co., St. Louis, MO, USA)
24. Propranolol hydrochloride (PPL) (In-kind gifts from Assistant Professor Padungkwan Chitropas, Department of Pharmaceutical Technology, Faculty of Pharmacy, Khon Kaen university, Thailand)
25. Sodium hydroxide (Lab Scan, Dublin, Ireland.)
26. Timolol maleate (TIM) (Ven Petro-chem&pharma, India)
27. Triethylamine (Fluka, Buchs, Belgium.)

## 2. Equipments

1. Analytical balance (Satorius CP224S, Sartorius CP3202S; Scientific promotion Co., Ltd.)
2. Ball mill (Retsch PM100, Germany)
3. Brookfield DV-III programmable viscometer (Brookfield Engineering Lab., USA)
4. ECtestr11+ conductivity meter (Eutech.instrument, Malaysia)
5. Eppendorf Safe-Lock tubes (1.5 ml)
6. Filtration membranes Nylon 0.45  $\mu\text{m}$
7. Glass Syringe 5 mL
8. High performance liquid chromatography (HPLC) with diode array detector (Agilent Technologies GmbH, Waldbronn, Germany)
  - a. Autosampler (G1313A, Agilent Technologies GmbH, Waldbronn; Germany)

- b. Degasser (G1322A, Agilent Technologies GmbH, Waldbronn; Germany)
- c. Liquid chromatography pumps (G1311A, Agilent Technologies GmbH, Waldbronn; Germany)
- d. ChromSword software (Agilent Technologies GmbH, Waldbronn; Germany)
- e. Diode array detector (G1315B, Agilent Technologies GmbH, Waldbronn; Germany)
- f. HPLC column: C18, 5 $\mu$ m, 4.6x 250 mm (Thermo; USA)
2. High voltage supply (Gamma high voltage, Ormond Beach, FL).
3. Magnetic stirrer and magnetic bar
4. Measuring pipettes (1, 2, 5, 10 mL)
5. Micropipette 20-100  $\mu$ L, 100-1000  $\mu$ L, 1-5 mL (Biohit; Gibthai Co., Ltd; Thailand)
6. Micropipette tip
7. Oil bath (IKA-Werke GmbH & Co.; USA)
8. Orbital shaking incubator model SI4
9. pH meter (HORIBA compact pH meter B-212, Sartorius Professional Meter PP-15 )
10. Pipette aid (Powerpette Plus)
11. Scanning electron microscope (SEM; JEOL, JSM-6400)
12. Stainless pliers
13. Stainless steel needle No.20
14. Stirring motor IKA RW 20 Digital
15. UV/Visible spectrophotometer (NanoVue plus, GE Healthcare Life Sciences; USA)

### 3. Methods

#### 3.1 Synthesis of the PPL-selective imprinted polymer beads

PPL-imprinted polymer beads were synthesized by oil in water (o/w) emulsion polymerization using the formulations described in Table 1. The PPL in free base form was dissolved in the oil phase containing MMA as a functional monomer, DVB as crosslinker and BP as an initiator. Oil phase was gradually added into the aqueous phase (500 ml) of a 0.5 % w/v PVA solution, at 85 °C under a fixed stirring (400 rpm). The solution was maintained this condition until the polymerization was finished (4 h). Thereafter, the beads were washed several times with deionized water and methanol. The template was extracted from the polymer microspheres by sequential washing with 1:9:9 (v/v/v) acetic acid, dichloromethane and methanol mixture until no template could be detected from the washing solvent by UV spectrophotometer at 290 nm. Non molecular imprinted polymers (NIPs) were prepared by the same method as molecularly imprinted polymers (MIPs) except the addition of template during polymerization and finally dried at 60°C for 6 h in hot air oven. The percentage yield of NIP and MIP beads were calculated by equation.

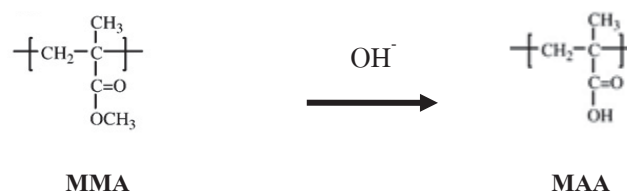
$$\text{Yield (\%)} = \frac{\text{Total weight of polymer beads (Experimental value)}}{\text{Total amount of monomer added (Theoretical value)}} \times 100$$

The morphology and particle size of dried beads were determined by scanning electron microscopic (SEM). Before viewing, the samples were fixed on stubs and sputter-coated with gold in a vacuum evaporator. The particle size of dried beads was determined by using image analysis software (JMicroVision V.1.2.7, Switzerland).

##### 3.1.1 Alkali hydrolytic reaction of polymer beads

The methyl ester group was transformed into carboxylic group by alkaline hydrolysis according to scheme 1. One gram of each polymer beads was hydrolyzed in a mixture of 4 g of NaOH and 1.8 ml of deionized water in 80 g of isopropyl alcohol at 85°C for 12 h. The MIPs and NIPs were filtered, washed with excess deionized water until neutral pH, and finally dried at 60°C for 6 h in hot air

oven. The final beads were kept in a tightly closed container until further investigation.



*Scheme 1* Alkali hydrolysis

Table 6 Formulations of PPL-imprinted and non-PPL imprinted polymer beads

Formula	PPL Template (g)	MMA (ml)	DVB (g)	BP (g)
NIP1	0	75	2	3
NIP2	0	75	2.5	3
NIP3	0	75	3	3
MIP1	0.4	75	2	3
MIP2	0.4	75	2.5	3
MIP3	0.4	75	3	3
MIP4	0.6	75	2	3
MIP5	0.6	75	2.5	3
MIP6	0.6	75	3	3
MIP7	0.8	75	2	3
MIP8	0.8	75	2.5	3
MIP9	0.8	75	3	3

*Abbreviations:* NIP, non molecular imprinted polymers; MIP, molecularly imprinted polymers; MMA, methyl methacrylate; DVB, divinylbenzene; BP, benzoyl peroxide

### 3.1.2 Characterization of chemical structure MIP and NIP beads

The chemical structure of MIP and NIP beads were examined by Fourier transform infrared spectroscopy (FTIR). The beads were crushed into KBr pellets. The infrared (IR) spectra of the obtained pellets were recorded over the range 500–4,000  $\text{cm}^{-1}$  by FTIR (Nicolet FTIR spectrometer 4700, USA).

### 3.1.3 Drug reloading of PPL-selective MIPs

All formulations of PPL-selective imprinted polymer beads as described in Table 1 were reloaded with PPL (PPL 1g/20ml of water) in order to

evaluate the binding of drug from the aqueous solution. In this process, the weight ratios of PPL HCl : MIP9 (1:0.5, 1:1, 1:2) or PPL HCl : NIP3 (1:0.5, 1:1, 1:2) as a control were varied. The mixture was agitated at 200 rpm for 48 h at 30°C. The incubated dispersions were sampled every 2 h by centrifugation at 3000 rpm for 5 min. The concentration of PPL in the supernatant was determined using UV spectrophotometer at 290 nm. The amount of each bound drug was calculated from the difference in concentrations before and after incubation. All experiments were run in triplicate (n=3). In this research, the MIP8 and NIP2 formula in Table 1 were chosen in order to study the effect of % reloading. Comparing the binding ability, other  $\beta$ -blockers (ATE, MET, TIM) were similarly prepared using the weight ratio of  $\beta$ -blockers (ATE, MET, TIM): MIPs or NIPs as 1:1. The mixture of the  $\beta$ -blockers solution (PPL, ATE, MET, TIM) was incubated with MIP and NIP in the weight ratios of (1:1). The concentration of each  $\beta$ -blocker in the supernatant was determined using HPLC method. (see section 3.4)

## **3.2 Electrospun fiber**

### **3.2.1 Preparation of polymer solutions**

The homogeneous clear solutions were prepared by dissolving methacrylate-based copolymers in each three solvents (ethanol, DMA/ethanol (80/20) and DMF/ethanol (67/33)) at room temperature. Methacrylate-based copolymers used in this work i.e. Eudragit L100, Eudragit S100, Eudragit EPO, Eudragit RL100, Eudragit RLPO and Eudragit RS100 were prepared as the solutions at the concentrations varied from 20% to 60% (w/v). Before electrospinning, shear viscosity and conductivity of all the solutions were measured by using a Brookfield DV-III programmable viscometer and a ECtestr11+ conductivity at 25°C, respectively.

### **3.2.2 Preparation and characterization of fiber**

Electrospun copolymer fibers were prepared by the following procedures. Firstly, a solution of methacrylate-based copolymers was filled in a 5-mL glass syringe with a blunt-ended aluminium needle as a nozzle. The distance from a tip to aluminium collector was fixed at 15 cm. The feeding rate of each methacrylate-based copolymers solution was 0.5 mL h<sup>-1</sup> by means of a KD scientific syringe pump. The methacrylate-based copolymers solution was electrospun at a positive voltage of 15 kV from a high voltage supply onto aluminium plate on a drum which acted as a

ground electrode. Finally, the morphology of the methacrylate-based copolymer fibers were evaluated by scanning electron microscopic (SEM). The average diameter of the methacrylate-based copolymer fibers was determined by using image analysis software (JMicroVision V.1.2.7, Switzerland).

### **3.3 Preparation of electrospun copolymer fiber containing MIPs and NIPs.**

The Eudragit RS100 solution at a concentration of 40% (w/v) was chosen for the preparation of Eudragit RS100 fiber containing MIP8 and NIP2. The particle of beads were reduced the size by ball mill (speed 400 rpm) kept in a tightly closed container and used for alkali hydrolysis. The MIP8 or NIP2 beads content (10-50% w/w) was added in the polymer solution to obtain Eudragit RS100 fiber. The electrospinning of Eudragit RS100 fiber containing polymer beads were carried out at room temperature at a high voltage of 15 kV. A grounded aluminum foil was used as the counter electrode and mounted at a distance of 15 cm from the spinneret.

#### **3.3.1 Evaluation of the $\beta$ -blockers binding affinity of NIPs and MIPs composite Eudragit RS100 fiber**

The electrospun fibers containing polymer beads were cut into circular plates with a diameter of 1.5 cm and then pulled away from the aluminum plate substrate. The mixture of the  $\beta$ -blockers solution (PPL, ATE, MET, TIM) was incubated with electrospun fiber containing MIPs and NIPs in the weight ratios of (1:1). The mixture was agitated at 200 rpm for 2 h at 30°C. The incubated dispersions were withdrawn every 3, 5, 10, 20, 40, 60 and 120 min. The amount of each bound drug was calculated from the difference in concentrations before and after incubation. All experiments were run in triplicate (n=3). The concentration of each  $\beta$ -blockers in the supernatant was determined using HPLC method.

#### **3.3.2 Characterization of NIPs and MIPs composite Eudragit RS100 fiber**

The chemical structure of NIPs and MIPs composite Eudragit RS100 fiber were examined by FTIR. The beads were previously dried and crushed into KBr pellets. The IR spectra of the obtained pellets were recorded over the range 500–4,000  $\text{cm}^{-1}$  by a Fourier transform infrared spectrophotometer.

The morphological structure of NIPs and MIPs composite Eudragit RS100 fiber were examined using SEM.

### 3.4 HPLC analysis

The HPLC system consisted of a pump, HPLC column C18, 4.6 mm x 250 mm, a diode array detector and an integrator. The flow rate of mobile phase was 0.8 ml/min. The injected volume was 20  $\mu$ l. The mobile phase for all drugs was composed of acetonitrile and phosphate buffer (pH 7.4), with 0.2% (w/v) of triethylamine, the pH was adjusted to 3 by using 85% orthophosphoric acid. The detection wavelength was set at 225, 227, 290, 294 nm for ATE, MET, PPL and TIM, respectively.

#### 3.4.1 Standard curve for evaluating the binding affinity of $\beta$ -blockers into the imprinted polymers.

##### *Standard solutions of propranolol*

The stock solution of propranolol in a concentration of 10 mM was prepared, and then the stock solution was diluted with mobile phase to 0.2, 0.4, 0.6, 0.8 mM.

##### *Standard solutions of atenolol, metoprolol, timolol*

The stock solution concentration was 10 mM of atenolol, metoprolol and timolol. The stock solution was diluted with mobile phase to 0.5, 1.0, 1.5 mM.

### 3.5 Statistical analysis

All experimental measurements were triplicately performed. Resulted values were expressed as mean value  $\pm$  standard deviation (SD). The different percentage loading between NIPs and MIPs were analyzed using the independent samples t-test. Statistical significance of differences in percentage loading of all polymer bead formulations were examined using one-way-analysis of variance (ANOVA) followed by least significant difference post hoc test. The significant level was set at  $p < 0.05$ .

## CHAPTER 4

### RESULTS AND DISCUSSION

#### 1. MIP beads synthesis and characterization

In molecular imprinting processes, template and crosslinker are the important factors affecting the binding affinity and specificity of imprinted polymer. Previous studies have demonstrated that imprinted microspheres selective for propranolol (PPL) could be synthesized by precipitation polymerization method. Yoshimatsu et al. studied an effect of crosslinkers ratio (DVB and TRIM) on character of microspheres such as binding affinity, specificity and size. The result indicated that use of DVB cross-linker resulted in higher binding affinity and specificity for PPL than that of prepared by using TRIM. Here, providing additional  $\pi$ - $\pi$  interaction with the aromatic moiety of (S)-propranolol in acetonitrile during the imprinting reaction by DVB was expected as the reason (Yoshimatsu et al. 2007:112-121). Therefore, the crosslinker (DVB) was chosen to use in this work.

As shown in Table 6, the formulations prepared by oil in water (o/w) emulsion polymerization method using methyl methacrylate (MMA) as monomer, BP as an initiator, and different amounts of DVB and PPL as crosslinker and an imprinted template, respectively. Non molecular imprinted polymer (NIP) prepared by the same way as MIP except the addition of a template during polymerization was used as a control. The percentage yield of NIP and MIP beads was shown in Table 7. The percentage yield of MIP beads slightly increased with increasing the amount of DVB (2-3 g), whereas, % yield of MIP beads decreased with increasing the amount of PPL. The morphology and particle size of dried beads were determined by scanning electron microscopic (SEM) shown in Table 8. The SEM images of NIP appeared to be spherical and smooth surface without evidence of collapsed particles, whereas MIP showed less sphere with small pore on the surface. The particle size of the beads was about 50-100  $\mu\text{m}$  depended on amount of DVB and PPL. The particle size of NIP decreased with increasing the amount of DVB. Increment of crosslinker amount

resulted in stronger binding interaction between crosslinker and monomer during polymerization process which later rendered a decrement of beads size. As shown in Table 8, with increasing the amount of PPL, smaller particle was formed in all system suggesting that the template compound had an important influence on the particle growth during the precipitation polymerization. Previous study reported that in the absence of template, MAA can form hydrogen-bonded dimers in the non-imprinted system. In the imprinted system, there is an additional molecular interaction between MAA and propranolol, which might affect the growth of the cross-linked polymer nuclei to result in smaller polymer beads (Yoshimatsu et al. 2007:112-121).

Table 7 Percentage yield of PPL-imprinted and non-PPL imprinted polymer beads formulations.

<b>Formula</b>	<b>Yield (%)</b>
<b>NIP 1</b>	53.2
<b>NIP 2</b>	48.3
<b>NIP 3</b>	42.6
<b>MIP 1</b>	31.4
<b>MIP 2</b>	26.5
<b>MIP 3</b>	44.4
<b>MIP 4</b>	18.6
<b>MIP 5</b>	18.2
<b>MIP 6</b>	25.0
<b>MIP 7</b>	8.4
<b>MIP 8</b>	6.4
<b>MIP 9</b>	12.5

The FT-IR spectra of NIP2 and MIP8 microspheres were shown in Figure 15. The NIPs spectra exhibited a sharp intense peak at  $1732\text{ cm}^{-1}$ , attributing to the presence of C=O stretching vibrations. The broad peak ranging from 1300 to  $1000\text{ cm}^{-1}$  was due to C–O (ester bond) stretching vibrations. The broad peak from 3100 to

2900  $\text{cm}^{-1}$  was due to the presence of C-H stretching vibrations. The FT-IR spectra of MIP8 microspheres (Figure 15b) exhibited the same pattern of the peaks as that of the NIP2 microspheres except for the peaks exhibited at 799  $\text{cm}^{-1}$  which assigned to the substituted naphthalene of PPL. Since an alteration of the FT-IR spectra in the area corresponding to carbonyl group and C-O of ester bond was not observed but an alteration was found in the area that assigning to naphthalene of PPL, therefore, this indicated that PPL was embedded into MIP beads without bonding.

Polymer beads were hydrolyzed because of the preliminary test shown that PPL could not be bound in the drug solution during drug loading process. Therefore, the methyl groups of MIP and NIP were then removed by alkali hydrolysis reaction to generate the carboxylic acid functional groups. To evaluate the success of alkali hydrolytic reaction of polymer beads, the IR spectra of the obtained polymer beads were determined. The non hydrolyzed MIP8 and MIP8 microspheres were shown in Figure 16. The FT-IR spectra of hydrolyzed MIP8 microspheres (Figure 16b) gave all the peaks that were shown for non hydrolyzed MIP8 microspheres except that broad and strong peak of O-H stretching of carboxyl group between 3000 and 3500  $\text{cm}^{-1}$  is observed in the spectrum of hydrolyzed MIP8 microspheres.

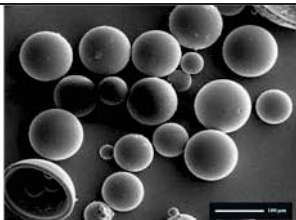
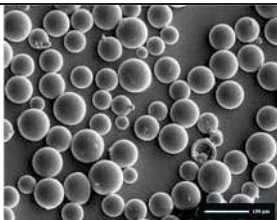
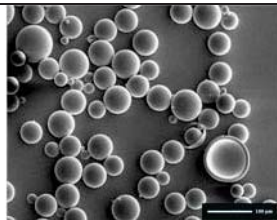
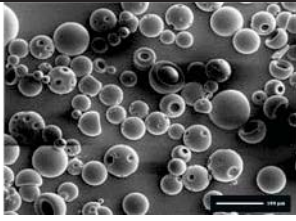
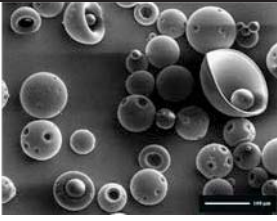
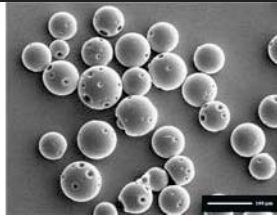
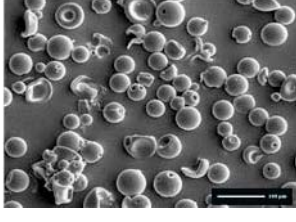
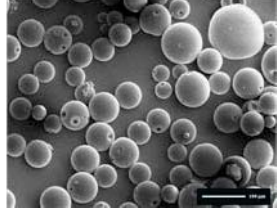
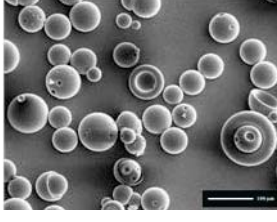
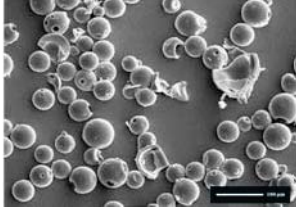
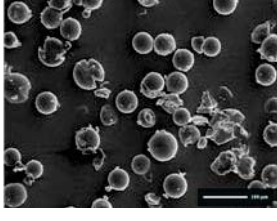
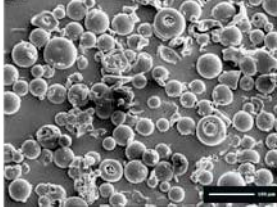
## **2. Optimization of NIP and MIP microspheres**

In order to investigate the optimal polymerization conditions for PLL loading, NIP and MIP microspheres were formulated in different amounts of PPL template or DVB (Table 6). After polymerization step, the polymer beads were washed with a mixture of acetic acid, methanol and dichloromethane in the ratio of 1:9:9 (v/v/v). Dichloromethane was added for swell beads, acetic acid and methanol were added for removing the un-reacted monomers and template molecules. Then, the methyl groups of polymer beads were removed by alkali hydrolysis reaction to generate the carboxylic acid functional groups. Therefore, the polymer beads were reloaded with PPL in order to evaluate the binding of PLL from the aqueous solution. In this reloading process, the weight ratios of PPL: MIP9 (1:0.5, 1:1, 1:2) or PPL: NIP3 (1:0.5, 1:1, 1:2) as a control were varied. The results were shown in Figure 17-19. The percentage reloading of PPL was increased by an increasing polymer beads.

Percentage drug reloading at 48 h of the formulation NIP3, was 20%, 60% and 100 % for increasing the ratio of the beads 1:0.5, 1:1 and 1:2, respectively (Figure 17a). Whereas, the percentage drug reloading at 48 h of the formulation MIP9 was faster increased than that of NIP3, the percentage drug reloading was 40%, 80% and 100 % for increasing the ratio of the beads 1:0.5, 1:1 and 1:2, respectively (Figure 17b). At 1:1 ratio, the PPL could be reloaded in the MIP9 at a higher extent and rate than in NIP3. Therefore the ratio of drug to polymer bead of 1:1 was chosen for further experiment.

Figure 18 showed the effect of amount of PPL template on the percentage of PPL reloading at the ratio of drug to polymer beads of 1:1 in the polymer beads (NIP3 = PPL 0 g, MIP3 = PPL 0.4 g, MIP6 = PPL 0.6 g and MIP9 = PPL 0.8 g). The result showed that increasing of the amount of PPL template, the percentage reloading of PPL was increased. Therefore, the formulation MIP9 (PPL 0.8 g) was chosen for further experiment.

Table 8 SEM images of polymer beads obtaining PPL as a template, MMA as a functional monomer, DVB as crosslinker and BP as an initiator (at magnification of 100X)

PPL (g) Template	MMA(ml):DVB(g):BP(g)		
	75:2:3	75:2.5:3	75:3:3
0	 99.7± 13.6 μm	 62.6±10.6 μm	 59.1±8.3 μm
0.4	 69.9±12.6 μm	 81.8±14.8 μm	 81.1±10.7 μm
0.6	 50.4±9.1 μm	 70.2±13.4 μm	 68.5±15.0 μm
0.8	 53.8±9.0 μm	 54.1±6.3 μm	 50.5±11.9 μm

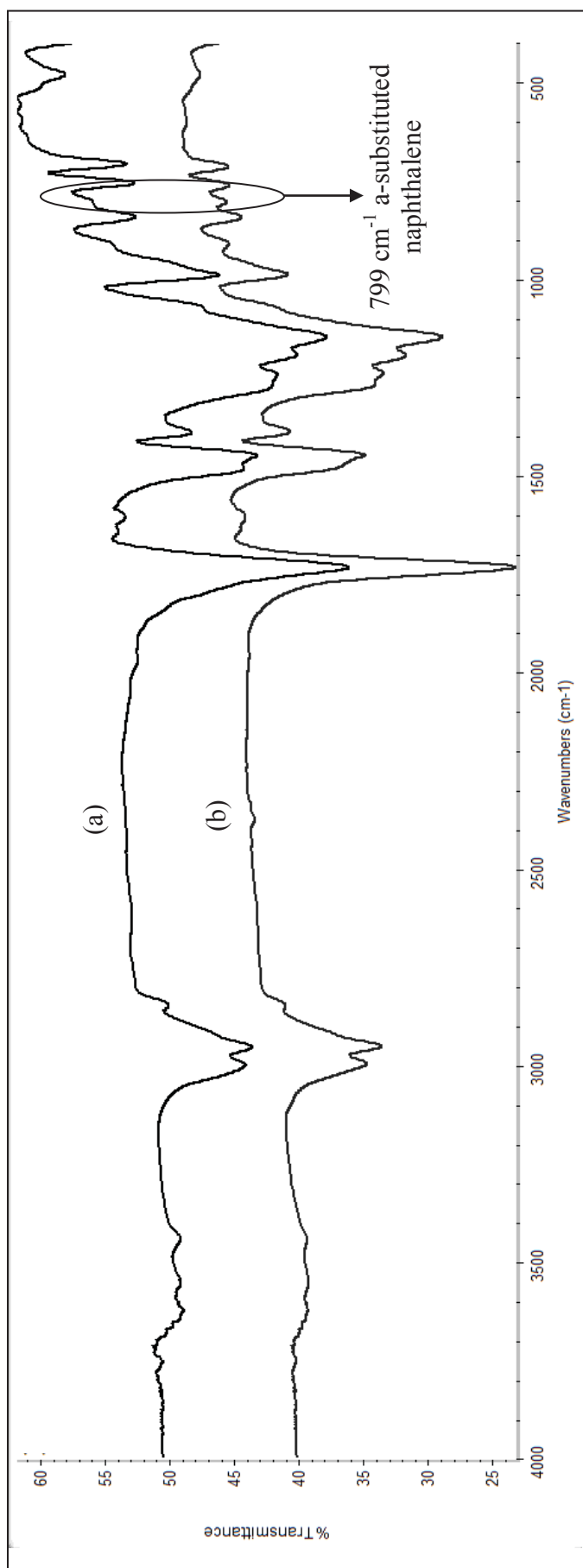


Figure 15 FT-IR spectra of (a) NIP2 and (b) MIP8 beads.

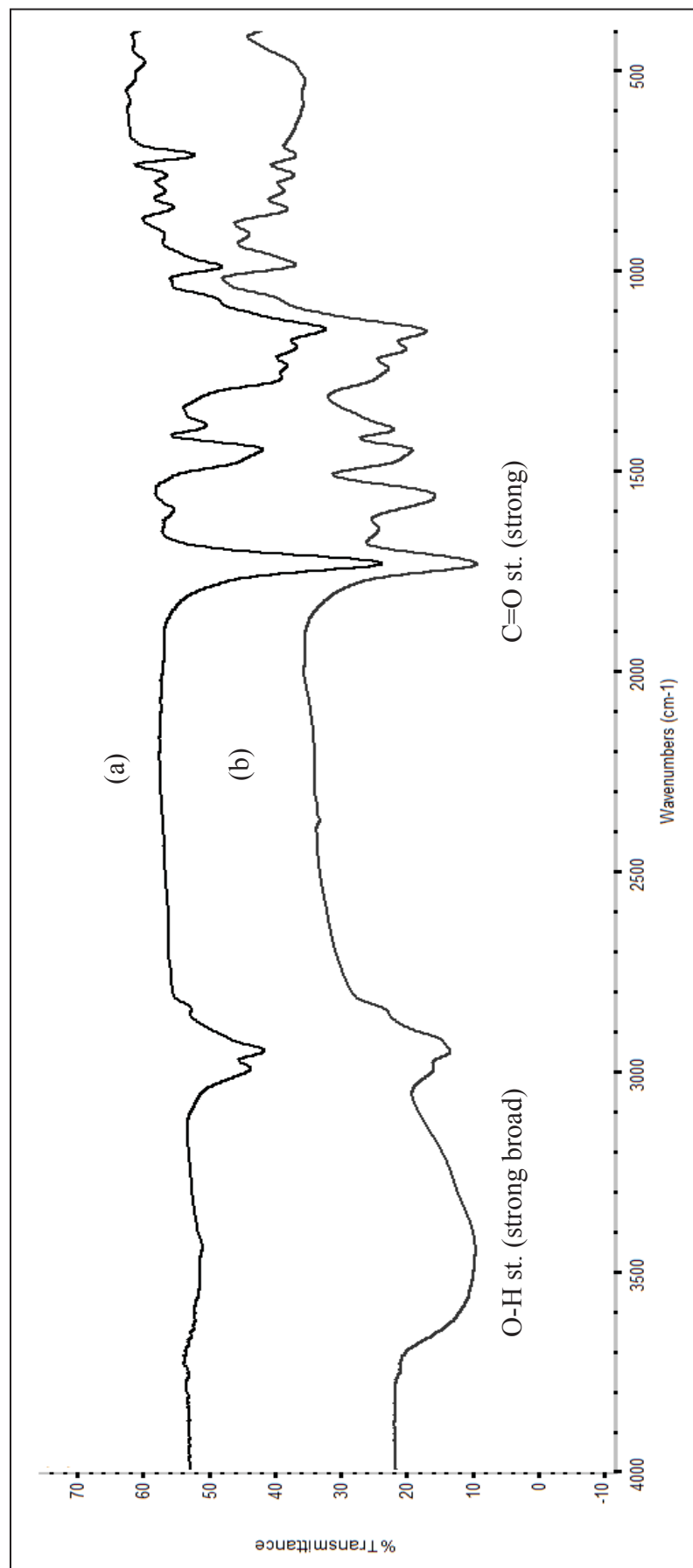


Figure 16 FT-IR spectra of (a) non hydrolyzed and (b) hydrolyzed MIP8 beads.

Figure 19 showed the effect of amount of crosslinker (DVB) on the percentage of PPL reloading at the ratio of drug to polymer beads of 1:1. Figure 19b showed the percentage of PPL reloading in the polymer beads formulation MIP7 (DVB 2 g), MIP8 (DVB 2.5 g) and MIP9 (DVB 3 g) at the ratio of drug to polymer beads of 1:1. The results showed that the amount of the DVB crosslinker affected on the percentage of PPL reloading in the beads. The percentage of PPL reloading increased to reach the maximum when the DVB increased from 2 g to 2.5 g, then decreased by further increment of the DVB (3 g). This might be due to the condensation of the polymer beads that led to a lowering of the drug penetration into the beads. The percentage of PPL reloading in the polymer beads formulation NIP1 (DVB 2 g), NIP2 (DVB 2.5 g) and NIP3 (DVB 3 g) at the ratio of drug to polymer beads of 1:1 (Figure 19a) exhibited the same pattern of the percentage of PPL reloading as that of the percentage of PPL reloading in the polymer beads formulation MIP7-9. However, the PPL could be loaded in all of the MIP at a higher extent and rate than that the NIP. Therefore this formulation MIP8 (DVB 2.5 g) was chosen for further experiment.

### **3. Evaluation of the $\beta$ -blockers binding affinity of NIP and MIP**

In this study, the MIP8 and NIP2 formula were chosen for study the effect of % reloading. Comparing the binding ability, other  $\beta$ -blockers (ATE, MET, TIM) were similarly prepared using the weight ratio of  $\beta$ -blockers (ATE, MET, TIM): MIP8 or NIP2 as 1:1. The mixture of the  $\beta$ -blockers solution (PPL, ATE, MET, TIM) was incubated with MIP8 and NIP2 at the weight ratios of (1:1). The concentration of each  $\beta$ -blocker in the supernatant was determined using HPLC method. Percentage reloading of  $\beta$ -blockers in NIP2 and MIP8 was shown in Figure 20. Comparing the binding ability to other  $\beta$ -blockers (ATE, MET and TIM), PPL showed the highest percent drug reloading in MIP8 (> 80%). In addition, the % drug reloading of other  $\beta$ -blockers in MIP8 was similar to NIP (40-60%). Thus, these MIP8 were molecularly selective for PPL.

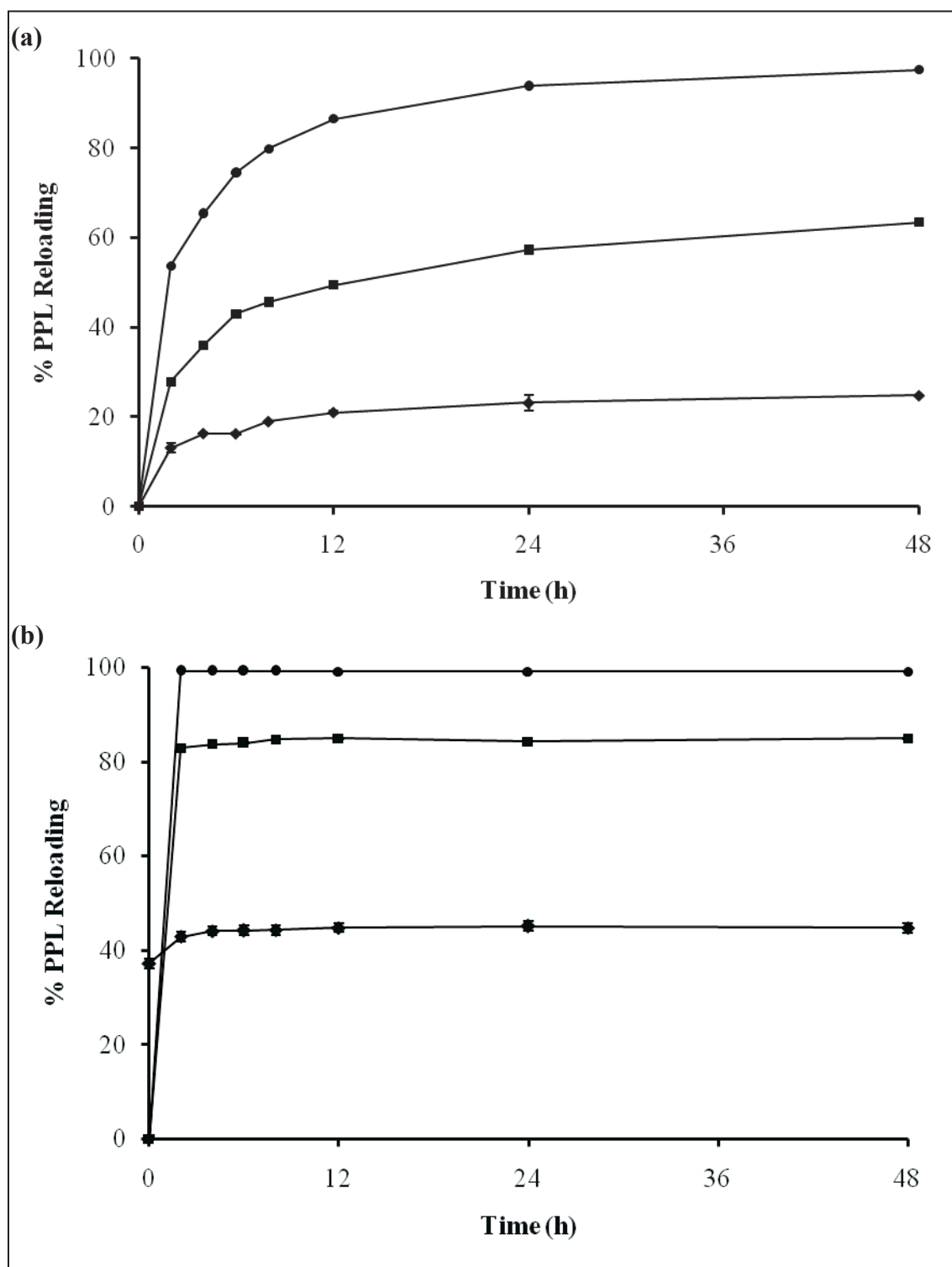


Figure 17 The percentage PPL reloading in (a) NIP3 and (b) MIP9 at the drug to polymer bead ratio of (◆) 1:0.5, (■) 1:1, (●) 1:2.

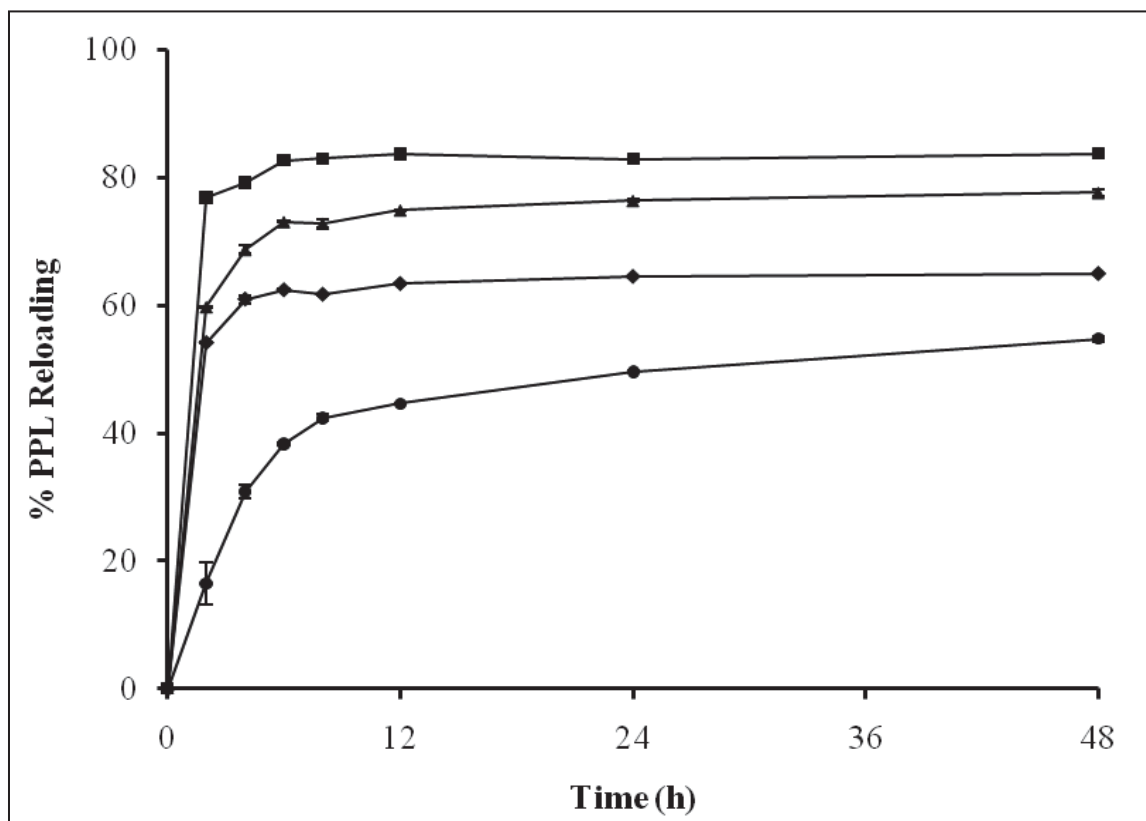


Figure 18 The percentage PPL reloading in polymer beads at the drug to polymer bead ratio of (1:1) at various amount of PPL: (●) NIP3 (PPL0 g), (◆) MIP3 (PPL0.4 g), (▲) MIP6 (PPL0.6 g), and (■) MIP9 (PPL0.8 g).

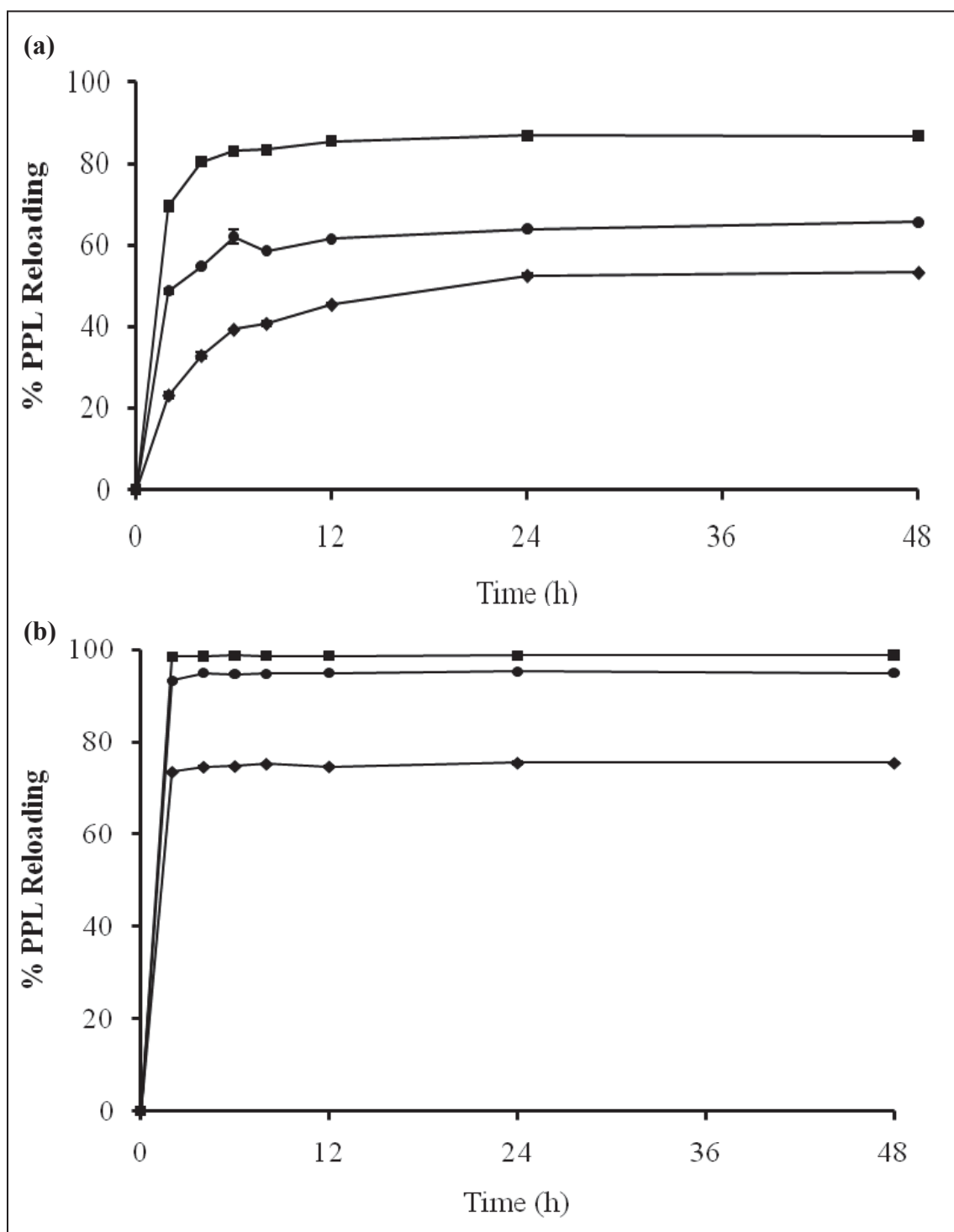


Figure 19 The percentage PPL reloading in (a) NIP; (●) NIP1 (DVB 2 g), (■) NIP2 (DVB 2.5 g), (◆) NIP3 (DVB 3 g) and (b) MIP; (●) MIP7 (DVB 2 g), (■) MIP8 (DVB 2.5 g), (◆) MIP9 (DVB 3 g) at the drug to polymer bead ratio of 1:1.

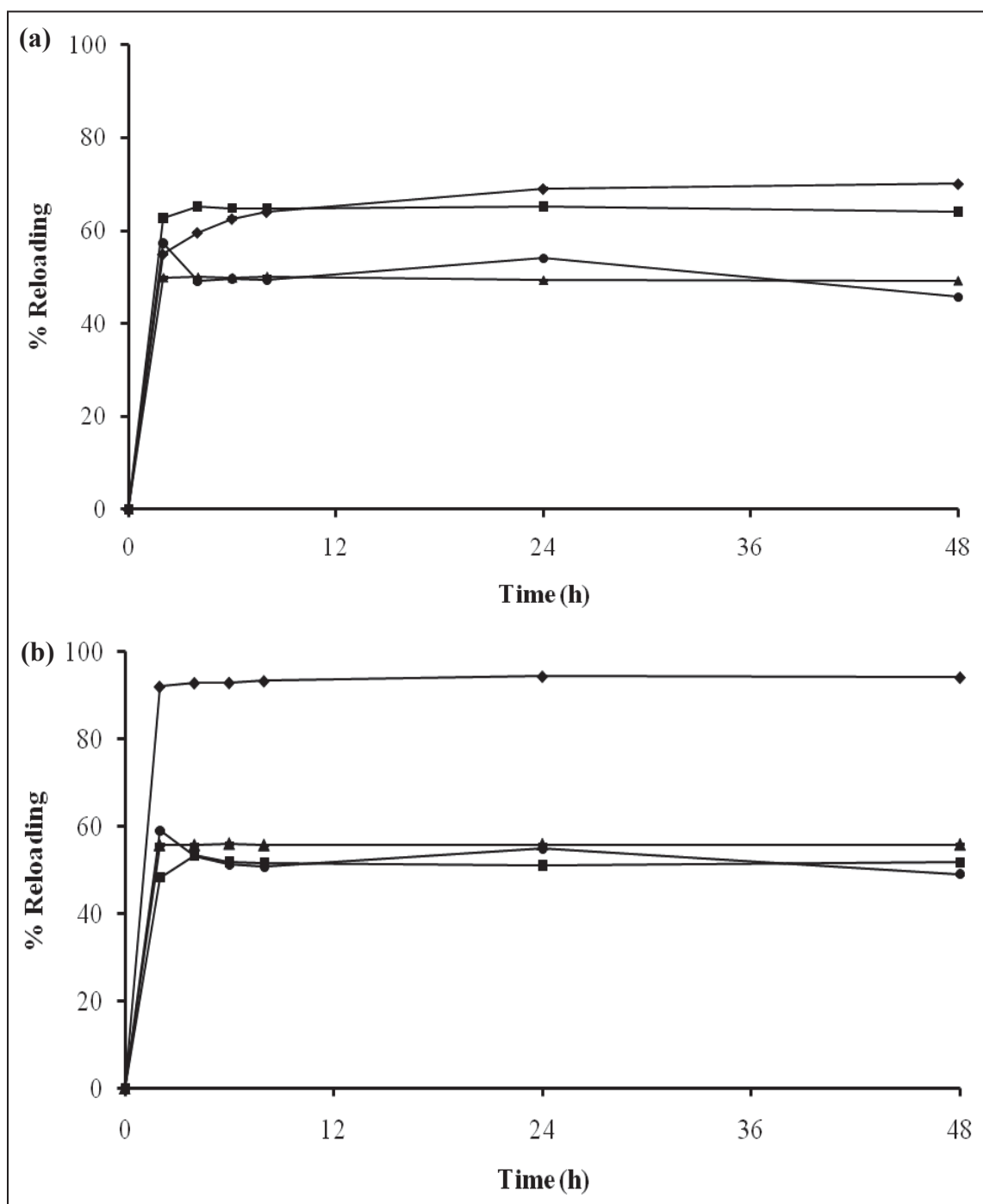


Figure 20 The percentage reloading of  $\beta$ -blocker at ratio of drug to polymer beads (1:1) (a) NIPs and (b) MIPs, (●) ATE, (■) MET, (▲) TIM, (◆) PL.

#### 4. Electrospun fiber

Methacrylate-based copolymers (Eudragit; E) were used as a polymer base for production of MIP membrane. These copolymers are different in their chemical characteristics and they are able to dissolve in aqueous medium at different pH. In this study, six commercially available methacrylate-based copolymers (E-L100, E-S100, E-EPO, E-RLPO, E-RL100 and E-RS100) were chosen and fabricated into fibers using the electrospinning technique. The polymer concentration and solvent systems (EtOH, DMA/EtOH and DMF/EtOH) used in this study were shown in Table 9. Table 10-15 showed the SEM images of electrospun products from all of methacrylate-based copolymer solutions.

E-L100, the SEM image of fibers prepared by 20%-25%w/v E-L100 solution in DMA/EtOH exhibited bead-on-string structure while 20%w/v E-L100 solution in DMF/EtOH demonstrated smooth fiber with a fiber diameter size of  $562.9 \pm 84.7$  nm (Table 10).

E-S100, the SEM image of fibers prepared by 25% E-S100 solution in DMA/EtOH exhibited smooth fiber with a fiber diameter size of  $422.8 \pm 35.6$  nm (Table 11).

E-EPO, the SEM images of the fiber spun from 25% E-EPO solution in ethanol and 35% E-EPO solution in DMA/EtOH exhibited bead-on-string structure. While the fiber spun from the solution contained the polymer higher concentration of 30 and 35% in ethanol demonstrated smooth fiber with a fiber diameter size of  $782.3 \pm 179.4$  nm and  $1322.8 \pm 358.8$  nm, respectively, whereas 35% E-S100 solution in DMF/EtOH exhibited smooth fiber with a small diameter of  $793.2 \pm 140.8$  nm (Table 12).

E-RLPO, the SEM images of the fiber spun from E-RLPO solution in ethanol exhibited flat shape. The fiber diameter size increased with increasing the amount of E-RLPO. The fiber diameter sizes of 25%, 30% and 35% E-RLPO solution in ethanol were  $496.2 \pm 161.1$  nm,  $1150.6 \pm 577.3$  nm and  $1588.1 \pm 250.7$  nm, respectively. 25% and 35% E-RLPO solution in DMA/EtOH exhibited bead-on-string structure while 35% E-RLPO solution in DMF/EtOH demonstrated smooth fiber with diameter size of  $793.2 \pm 140.8$  nm (Table 13).

Table 14 showed SEM images of E-RL100. The fiber diameter size increased with decreasing the amount of E-RL100. The diameter sizes of the fiber spun from 30%, 35% and 40% E-RLPO in DMF/EtOH were  $524.3 \pm 185.6$  nm,  $459.9 \pm 319.3$  nm and  $287.6 \pm 61.7$  nm, respectively.

E-RS100, the SEM image of the fiber spun from 40 to 60%w/v E-RS100 solution in both DMA/EtOH and DMF/EtOH showed smooth fibers, that in DMF/EtOH exhibited larger size than that of in DMA/EtOH (Table 15). Low concentrations of polymers (< 40 %) did not have enough chain entanglement to withstand both the electrostatic and Coulombic repulsion forces. Increasing the polymer concentration to 40% w/v, E-RS100 in DMA/EtOH resulted in a combination of smooth and beaded fibers. Further increase in the polymer concentration from 40 to 60%w/v E-RS100 in DMF/EtOH resulted in the formation of smooth fibers. However, increasing polymer concentration also resulted in increase diameter of as-spun fibers.

Table 9 The polymer concentration and solvents used to prepare of fibers

Solvent	Concentration of Eudragit (%w/v)					
	E-L100	E-S100	E-EPO	E-RLPO	E-RL100	E-RS100
EtOH	-	-	25, 30, 35	25, 30, 35	-	x
DMA/EtOH	20, 25	20, 25	35	25, 35	x	30, 40, 50, 60
DMF/EtOH	20	25	35	35	30,35, 40	30, 40, 50, 60

Note: x, the polymer solution could not be spun as fiber: -, not tested

Table 10 SEM images at magnification of 1500X and diameter of methacrylate-based copolymers (E- L100) fiber mats obtained from 20 and 25% E-L100 solutions in DMA/EtOH (80/20) and DMF/EtOH (33/67).

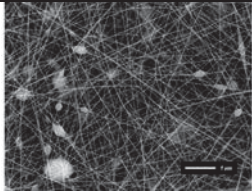
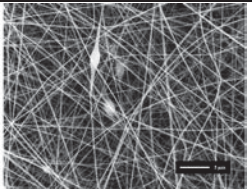
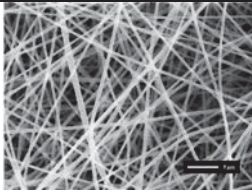
solvent	<b>L100</b>	
	20%	25%
DMA/EtOH	 211.3±24.9 nm	 246.5±24.7 nm
DMF/EtOH	 562.9±84.7 nm	-

Table 11 SEM images at magnification of 1500X and diameter of methacrylate-based copolymers (E-S100) fiber mats obtained from 20% and 25% E-S100 solution in DMA/EtOH (80/20) and DMF/EtOH (33/67).

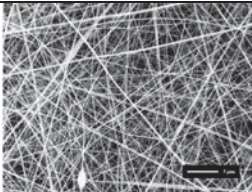
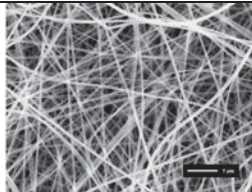
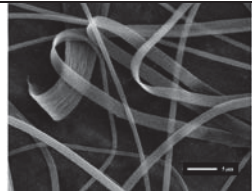
solvent	<b>S100</b>	
	20%	25%
DMA/EtOH	 324.3±71.5 nm	 422.8±35.6 nm
DMF/EtOH	-	 1568.8±1279.9nm

Table 12 SEM images at magnification of 1500X and diameter of methacrylate-based copolymers (E-EPO) fiber mats obtained from 25, 30 and 35% EPO solutions in EtOH, DMA/EtOH (80/20) and DMF/EtOH (33/67).

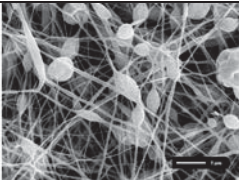
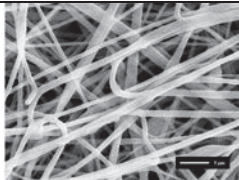
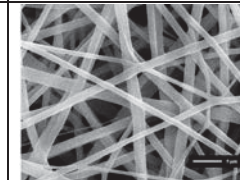
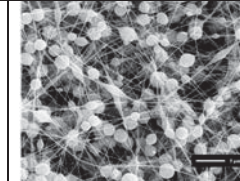
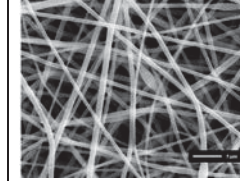
solvent	EPO		
	25%	30%	35%
EtOH	 384.7±77.5 nm	 782.3±179.4 nm	 1322.8±358.8 nm
DMA/EtOH	-	-	 243.0±54.4 nm
DMF/EtOH	-	-	 793.2±140.8 nm

Table 13 SEM images at magnification of 1500X and diameter of methacrylate-based copolymers (E-RLPO) fiber mats obtained from 25, 30, 35% RLPO solutions in EtOH, DMA/EtOH (80/20) and DMF/EtOH (33/67).

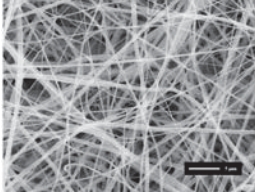
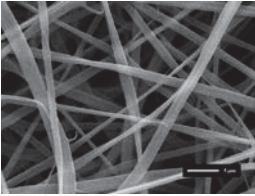
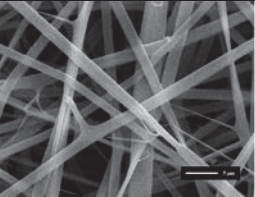
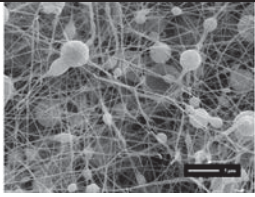
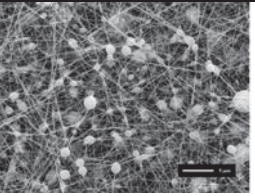
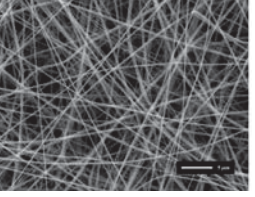
solvent	RLPO		
	25%	30%	35%
EtOH	 496.2±161.1 nm	 1150.6±577.3 nm	 1588.1±250.7 nm
DMA/EtOH	 463.0±195.2 nm	-	 204.3±18.5 nm
DMF/EtOH	-	-	 417.0±109.4 nm

Table 14 SEM images at magnification of 1500X and diameter of methacrylate-based copolymers (E-RL100) fiber mats obtained from 30, 35, 40% RL100 solutions in DMF/EtOH (33/67).

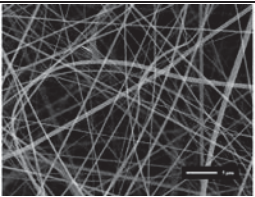
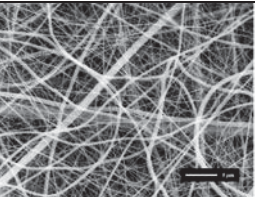
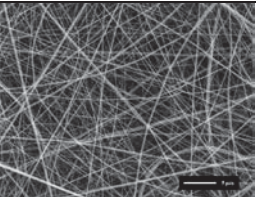
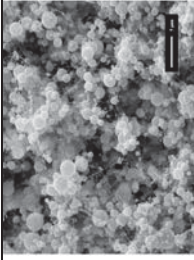
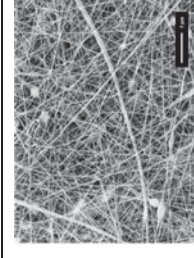
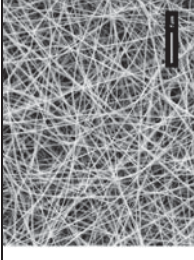
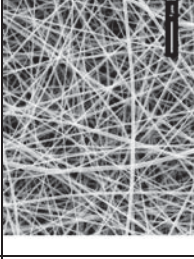
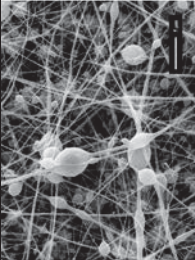
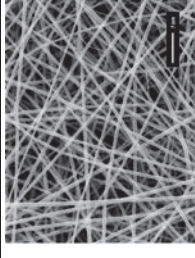
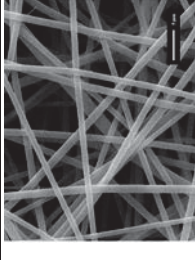
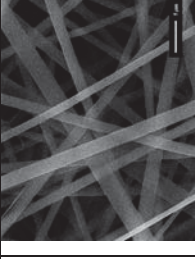
solvent	RL100		
	30%	35%	40%
DMF/EtOH	 524.3±185.6 nm	 459.9±319.3nm	 287.6±61.7 nm

Table 15 SEM images at magnification of 1500X and diameter of methacrylate-based copolymers (E-RS100) fiber mats obtained from 30, 40, 50 and 60% E-RS100 solution in DMA/EtOH (80/20) and DMF/EtOH (33/67).

solvent	RS100			
	30%	40%	50%	60%
DMA/EtOH	 86.0±14.6 nm	 310.5±156.9 nm	 309.5±41.1 nm	 416.9±156.7 nm
	 307.0±93.7 nm	 545.3±50.7 nm	 1119.4±141.6 nm	 1687.4±554.5 nm

## 5. Preparation of electrospun copolymer fiber containing MIPs and NIPs

40%w/v E-RS100 in DMF/EtOH (33/67) was chosen for the preparation of fibers containing NIP2 and MIP8. This polymer was chosen due to its properties which are water insoluble and pH independent solubility. The particle of the MIP8 was reduced size by ball mill and sieved through the 400 mesh. The irregular, rough morphology with diameters of  $20.4 \pm 6.5 \mu\text{m}$  was obtained (Figure 21). In this study, amounts of MIP8 were varied in the range of 10 to 50 % w/w, added into the 40%w/v E-RS100 solution, and then spun as fibers. The E-RS100 solution containing MIP8 (> 50%w/w) could not be electrospun because of an excess amount of MIP resulting in the clogging of E-RS100 solution at capillary tip during the electrospinning process. In this process, 10-50% w/w MIP8 was initially added into the 40%w/v E-RS100 polymer solution and then spun as fiber by electrospinning process. Thereafter, the obtained fibers were dissolved in ethanol to liberate the embedded MIP beads. Then the MIP was weighed, and the % bead content was calculated as the following equation.

$$\% \text{ bead content} = \frac{\text{Total amount of obtained beads}}{\text{Total amount of initial beads}} \times 100$$

The beads content was increased by an increasing of initial added the polymer beads (Table 16). Therefore, The 50% w/w MIP was initially added into 40%w/v E-RS100 in DMF/EtOH (33/67) solution to obtain fiber containing beads. Figure 22 showed the SEM images of fiber with 50% w/w MIP8 (Fig.22c and d) and without 50% w/w MIP8 (Fig. 22a and b).

Table 16 The bead content after electrospinning process of an initially added 10-50% w/w of MIP8 beads in 40% w/v E-RS100 solutions.

Initial polymer beads (%w/w)	Bead content (%)
10	67.00
20	72.73
30	84.22
40	87.21
50	89.55

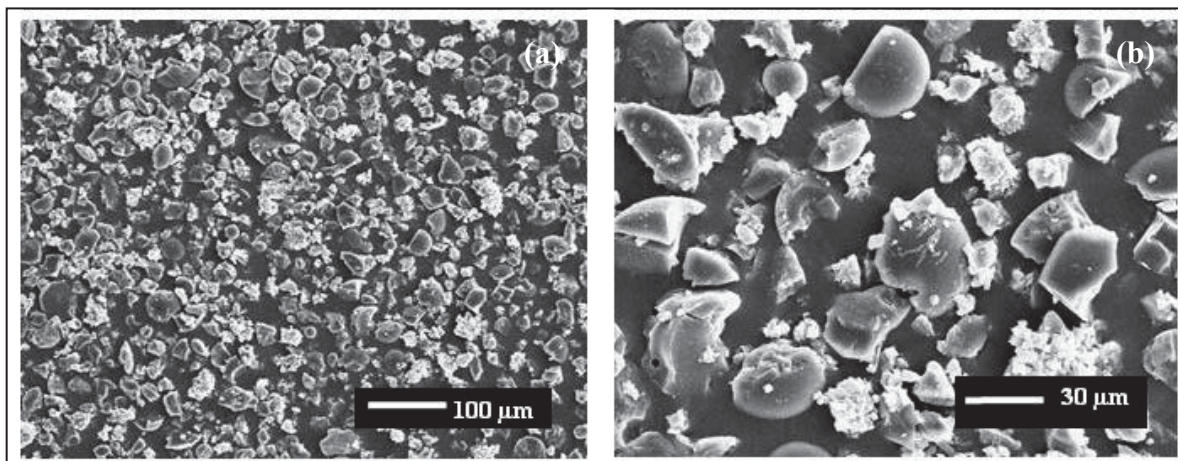


Figure 21 SEM images of the MIP8 after reduced the particle size by ball mill and sieving through the 400 mesh (a) at magnification of 100X and (b) at magnification of 350X.

##### 5. The $\beta$ -blockers binding affinity of the membrane fiber containing MIP

The selectivity for PPL of the membrane fiber containing polymer beads was investigated by determining its binding ability comparing to other  $\beta$ -blockers (ATE, MET, TIM). Testing solution containing 0.01M of each drug (PLL, ATE, MET, TIM) was prepared. Percentage reloading of  $\beta$ -blocker at ratio of drug to polymer beads of 1:1 for NIP2 composite E-RS100 fiber and MIP8 composite E-RS100 fiber was shown in Figure 23. The results revealed that PPL could be bound with higher extent and rate to the MIP8 composite E-RS100 fiber than NIP2 composite E-RS100 fiber. Moreover, PPL had higher affinity to the MIP8 than that of the other  $\beta$ -blockers. This indicated that MIP8 composite E-RS100 fiber had higher selectivity to PPL than the other  $\beta$ -blockers. Whereas the % drug reloading of NIP2 composite E-RS100 fiber was nearly to 0% which indicated that NIP2 had no selectivity to all of the tested drugs. Thus, this MIP8 composite E-RS100 fiber was molecularly selective for PPL. NIP2 and MIP8 in the form of polymer beads were found slightly higher selective to PPL. In contrast, after the polymer beads were embedded into the E-RS100 fiber, the selectivity of NIP2 and MIP8 to the PPL was clearly observed.

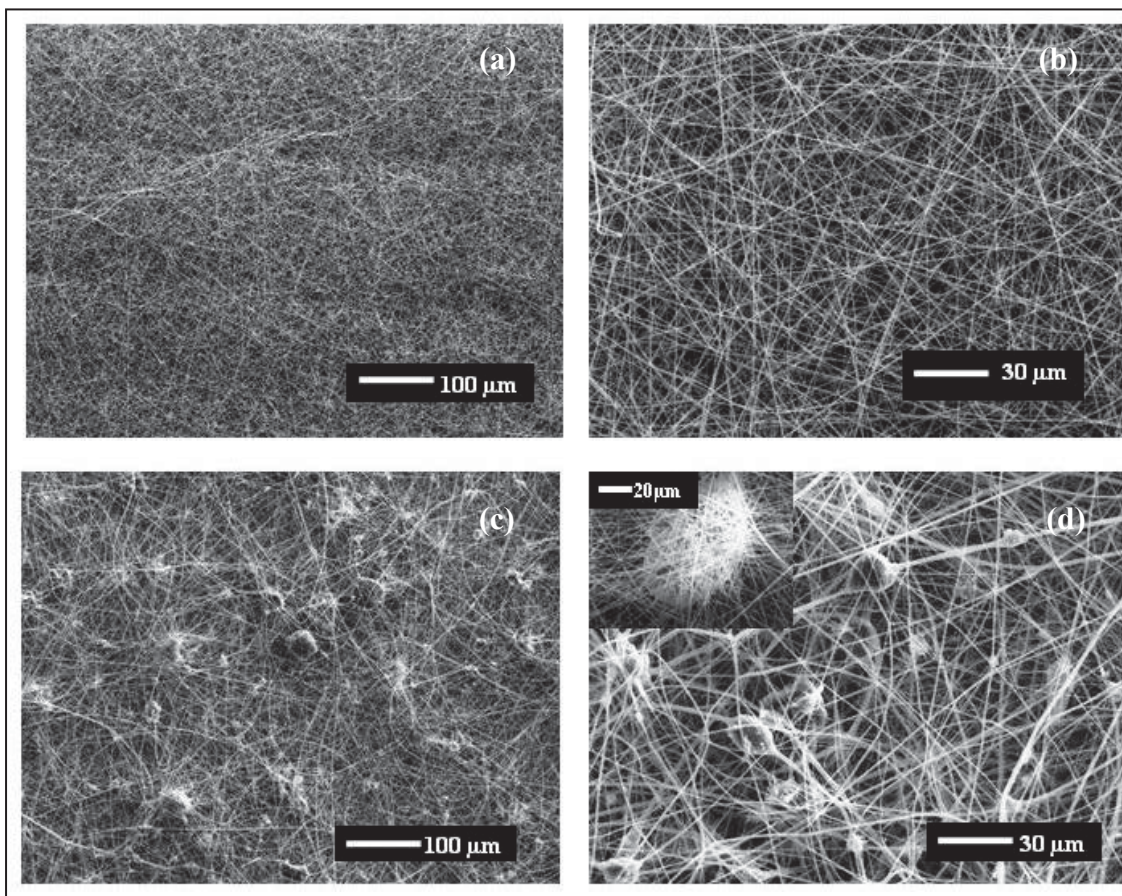


Figure 22 SEM images of the (a, b) E-RS100 fibers; (c, d) E-RS100 fibers containing 50 % MIP8 (a, c at magnification of 100X and b, d at magnification of 350X).

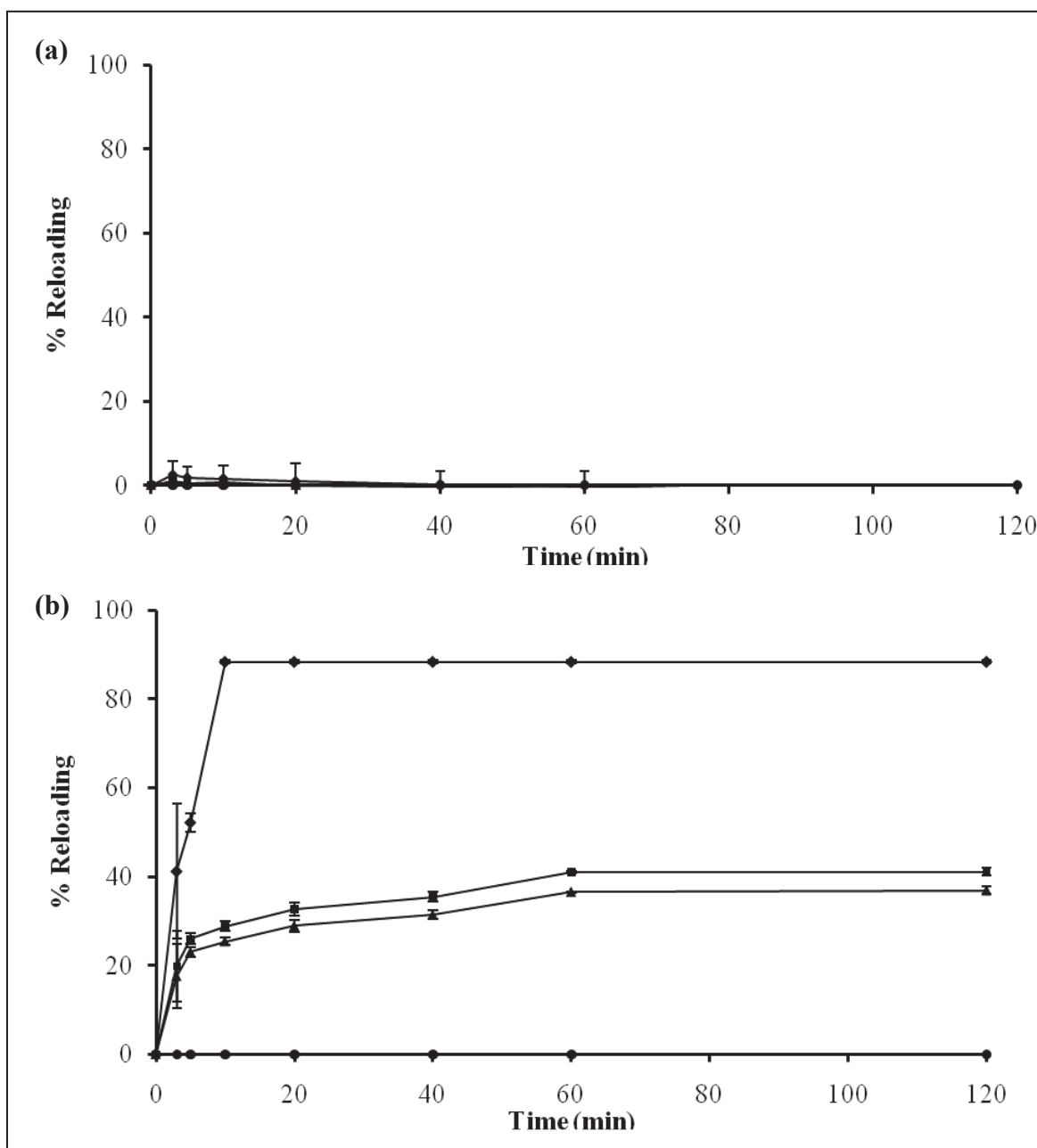


Figure 23 The percentage reloading of  $\beta$ -blocker at ratio of drug to polymer beads (1:1) (a) NIPs composite E-RS100 fiber and (b) MIPs composite E-RS100 fiber, (●) ATE, (■) MET, (▲) TIM, (◆) PPL.

## CHAPTER 5

### CONCLUSIONS

Molecularly imprinted polymers (MIPs) are the synthetic polymers which contain the specific molecular cavities that are complementary in shape and functional groups with imprinted template molecule. The aim of this study was to synthesize the MIP beads capable of selective binding to propranolol (PPL) via oil in water (o/w) polymerization using methyl methacrylate (MMA) monomer and divinylbenzene (DVB) cross-linker. PPL was added during polymerization as an imprinted template molecule. Non molecularly imprinted polymer (NIP) beads were prepared by the same way as MIP except the addition of a template during polymerization which was used as a control in order to determine the selectivity of the resultant MIP beads. The selectivity for PPL of MIP beads or milled MIP beads incorporated with Eudragit fiber membranes prepared by electrospinning technique was investigated by comparing the binding ability to other  $\beta$ -blockers (atenolol, metoprolol and timolol). The results of this study could be concluded as follow:

#### 1. Synthesis of the PPL-selective imprinted polymer beads

The molecularly imprinted microspheres selective for PPL were successfully synthesized using MMA as monomer, BP as an initiator, and different amounts of DVB and PPL as cross-linker and an imprinted template, respectively, which was prepared by o/w emulsion polymerization method. The particle size and percentage yield of NIP and MIP beads depended on amounts of DVB and PPL. The particle size of NIP decreased with increasing the amount of DVB, whereas increasing the amount of PPL, smaller particle was formed in all systems. The particle size of the beads was about 50-100  $\mu\text{m}$ . The percentage yield of MIP beads slightly increased with increasing the amount of DVB (2-3 g), whereas, the percentage yield of MIP beads decreased with increasing the amount of PPL. The percentage reloading of PPL was increased by an increasing the ratio of PPL to polymer beads. Comparing the binding ability to other  $\beta$ -blockers (ATE, MET and TIM), PPL showed the highest

percentage reloading in MIP8 (> 80%). The reloading of other  $\beta$ -blockers in MIP8 was similar to NIP2, which was about 40-60%.

## **2. Electrospun fiber**

In this study, six commercially available methacrylate-based copolymers (E-L100, E-S100, E-EPO, E-RLPO, E-RL100 and E-RS100) were chosen and fabricated into fibers using the electrospinning technique, and optimization of the parameters in the electrospinning process including methacrylate-based copolymers concentration and ratio of mixed solvents. 40%w/v E-RS100 in DMF/EtOH (33/67) was chosen for the preparation of fibers containing NIP2 and MIP8.

## **3. Preparation of electrospun copolymer fiber containing MIPs and NIPs**

In this study, amounts of MIP8 were varied in the range of 10 to 50 % w/w and added into the 40%w/v E-RS100 solution and then spun as fibers. The selectivity for PPL of the membrane fiber containing polymer beads was investigated by determining its binding ability in comparison to other  $\beta$ -blockers (ATE, MET, TIM). PPL could be bound with higher extent and rate to the MIP8 composite E-RS100 fiber than NIP2 composite E-RS100 fiber. Moreover, PPL had higher affinity to the MIP8 than the other  $\beta$ -blockers. This result indicated that MIP8 composite E-RS100 fiber had higher selectivity to PPL than the other  $\beta$ -blockers.

The results revealed that PPL could be selectively bound with higher extent and rate to the MIP composite E-RS100 fibers than NIP composite E-RS100. Therefore, this membrane can be further developed for various applications in pharmaceutical and other affinity separation fields.

## BIBLIOGRAPHY

- Ma, Z., M. Kotaki, and S. Ramakrishna. "Surface modified nonwoven polysulphone (PSU) fiber mesh by electrospinning: A novel affinity membrane." Journal of Membrane Science 272 (2006): 179–187.
- Huanga, Z.M. et al. "A review on polymer nanofibers by electrospinning and their applications in nanocomposites." Composites Science and Technology 63 (2003): 2223–2253.
- Chronakis, I.S. "Novel nanocomposites and nanoceramics based on polymer nanofibers using electrospinning process—A review." Journal of Materials Processing Technology 167 (2005): 283–293.
- Mayes, A.G., and M.J. Whitcombe. "Synthetic strategies for the generation of molecularly imprinted organic polymers." Advanced Drug Delivery Reviews 57 (2005): 1742–1778.
- Andersson, H.S., and I.A. Nicholls. "A historical perspective of the development of molecular imprinting." Molecularly Imprinted Polymers : Man-made Mimics of Antibodies and their Applications in Analytical Chemistry 23 (2000): 1-70.
- Sellergren, B., and C.J. Allender. "Molecularly imprinted polymers: A bridge to advanced drug delivery" Advanced Drug Delivery Reviews 57 (2005): 1733–174.
- Yan, H., and K.H. Row. "Characteristic and Synthetic Approach of Molecularly Imprinted Polymer." International Journal of Molecular Sciences 7 (2006):155-178.

- Ramstrom, O., L. Ye and K. Mosbach. "Artificial antibodies to corticosteroids prepared by molecular imprinting." Chemistry and Biology 3 (1996): 471-477.
- Yoshimatsu, K. et al. "Selective molecular adsorption using electrospun nanofiber affinity membranes." Biosensors and Bioelectronics 23 (2008): 1208–1215.
- Nostrum, C.F. "Molecular imprinting: A new tool for drug innovation." Drug Discovery Today: Technologies 2 (2005): 119-124.
- Bruggemann, O. "Molecularly Imprinted Polymers: A New Dimension in Analytical Bioseparation." Synthetic Polymers for Biotechnology and Medicine (2003): 134-142.
- Wulff, G. and A. Biffis. "Molecular imprinting with covalent or stoichiometric non-covalent interactions." Molecularly Imprinted Polymers : Man-made Mimics of Antibodies and their Applications in Analytical Chemistry 23 (2000): 1-111.
- Esteban, A.M. "Molecularly imprinted polymers: new molecular recognition materials for selective solid-phase extraction of organic compounds." Fresenius J Anal Chem 370 (2001): 795–802.
- Sellergren, B., "The non-covalent approach to molecular imprinting." Molecularly Imprinted Polymers : Man-made Mimics of Antibodies and their Applications in Analytical Chemistry 23 (2000): 113-180.
- Sellergren, B. and A.J. Hall. "Fundamental aspects on the synthesis and characterisation of imprinted network polymers." Molecularly Imprinted Polymers : Man-made Mimics of Antibodies and their Applications in Analytical Chemistry 23 (2000): 39-41.
- Karim, K. and F. Breton. "How to find effective functional monomers for effective molecularly imprinted polymers." Advanced Drug Delivery Reviews 57 (2005): 1795– 1808.

- Ulbricht, M. "Advanced functional polymer membranes." Polymer 47 (2006): 2217–2262.
- Piletsky, S.A. et al. "Receptor and transport properties of imprinted polymer membranes-a review." Journal of Membrane Science 157 (1999): 263–278.
- Wang, J.Y. et al. "Binding constant and transport property of S-Naproxen molecularly imprinted composite membrane." Journal of Membrane Science 331 (2009): 84–90.
- Jantarat, C. et al. "S-Propranolol imprinted polymer nanoparticle-on-microsphere composite porous cellulose membrane for the enantioselectively controlled delivery of racemic propranolol." International Journal of Pharmaceutics 349 (2008): 212–225.
- Yoshimatsu, K. et al. "Uniform molecularly imprinted microspheres and nanoparticles prepared by precipitation polymerization: The control of particle size suitable for different analytical applications." Analytica Chimica Acta 584 (2007): 112–121.
- Keiichi Yoshimatsu, Lei Ye et al., "Selective molecular adsorption using electrospun nanofiber affinity membranes." Biosensors and Bioelectronics 23 (2008): 1208–1215
- Chronakis, I.S. "Novel nanocomposites and nanoceramics based on polymer nanofibers using electrospinning process—A review." Journal of Materials Processing Technology 167 (2005): 283–293.
- Ramakrishna, S. et al. "Introduction." An Introduction to Electrospinning and Nanofibers, 1-21. Singapore: World Scientific Publishing Co.,2005.
- Evonik Rohm GmbH Pharma, Polymers Eudragit Acrylic Polymers for Solid Oral Dosage Forms [Online]. Accessed 5 October 2011. Available from <http://abstracts.aapspharmaceutica.com/ExpoAAPS09/Data/EC/Event/Exhibitors/33/productBrochure1.pdf>

- Rohm Pharma Polymer, Introduction: Synthetic Polymers for Coating Pharmaceutical Dosage Forms [Online]. Accessed 5 October 2011. Available from [http://80.241.206.189/en/pharmapolymers/service/literature/practical\\_course.Par.0001.TRow.0002.TCell.0003.File.tmp/pc\\_02\\_introduction.pdf](http://80.241.206.189/en/pharmapolymers/service/literature/practical_course.Par.0001.TRow.0002.TCell.0003.File.tmp/pc_02_introduction.pdf)
- Billmeyer, F.W. "Properties of commercial polymer." Textbook of Polymer Science, 404-419. Japan: Toppan Company, 1962.
- Pornsopone, V. et al., "Electrospinning of Methacrylate-Based Copolymers: Effects of Solution Concentration and Applied Electrical Potential on Morphological Appearance of As-Spun Fibers." Polymer Engineering and Science (2005): 1073-1080.
- British Pharmacopoeial Commission., The British Pharmacopoeia 2010, 185-187, 1421-1422, 1786-1787, 2100-2101. London: The Pharmaceutical Press, 2010.
- Lund, W. The Pharmaceutical Codex 1994, 747-748, 1074-1075. London: The Pharmaceutical Press, 1994.

## **APPENDIX**

## **APPENDIX A**

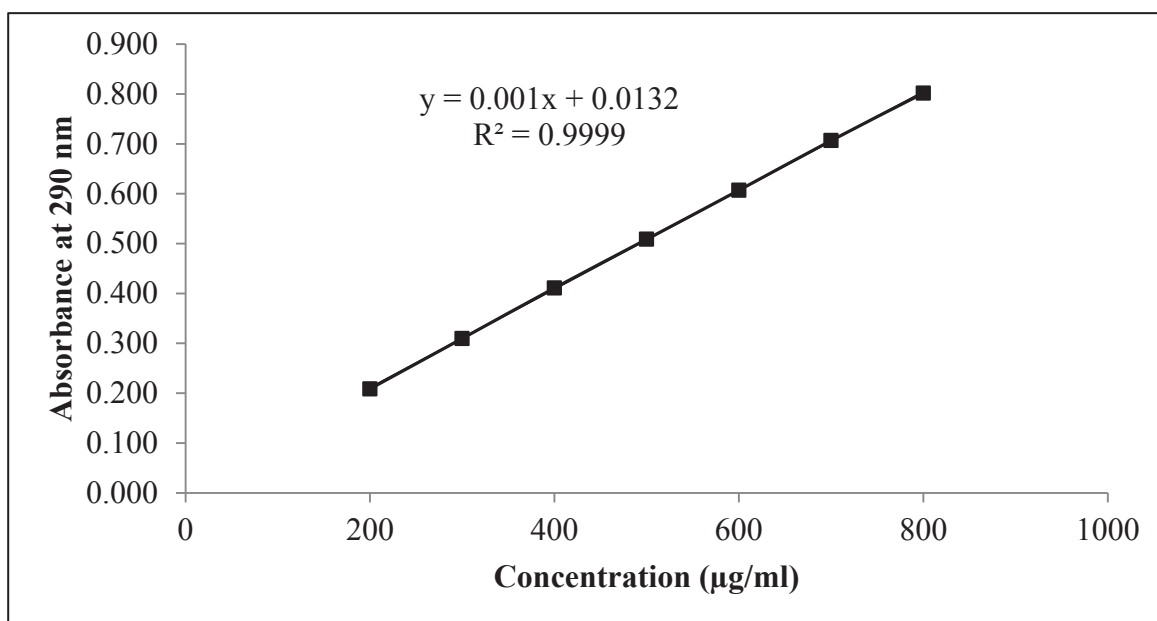


Figure 24 The calibration curve of PPL for percentage drug reloading assay

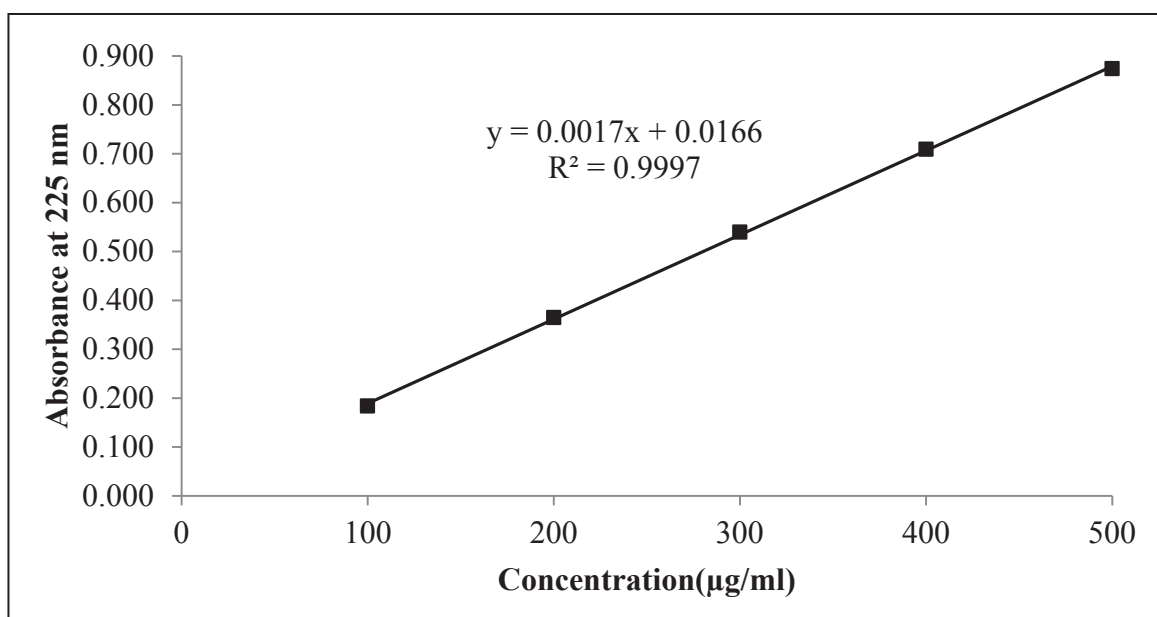


Figure 25 The calibration curve of ATE for percentage drug reloading assay

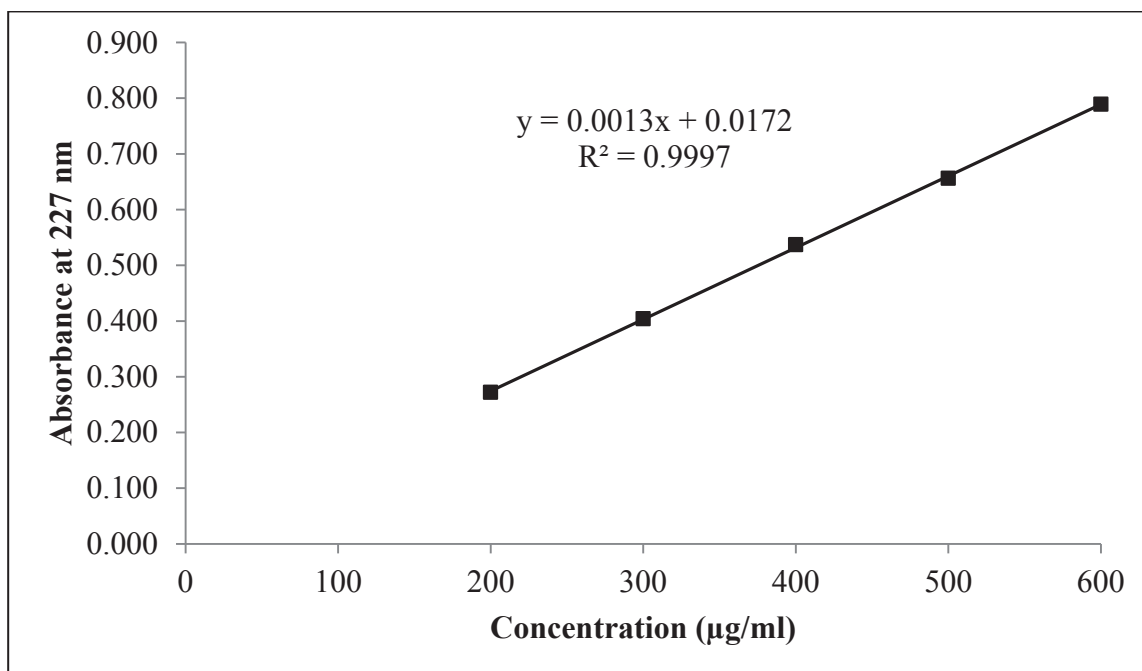


Figure 26 The calibration curve of MET for percentage drug reloading assay

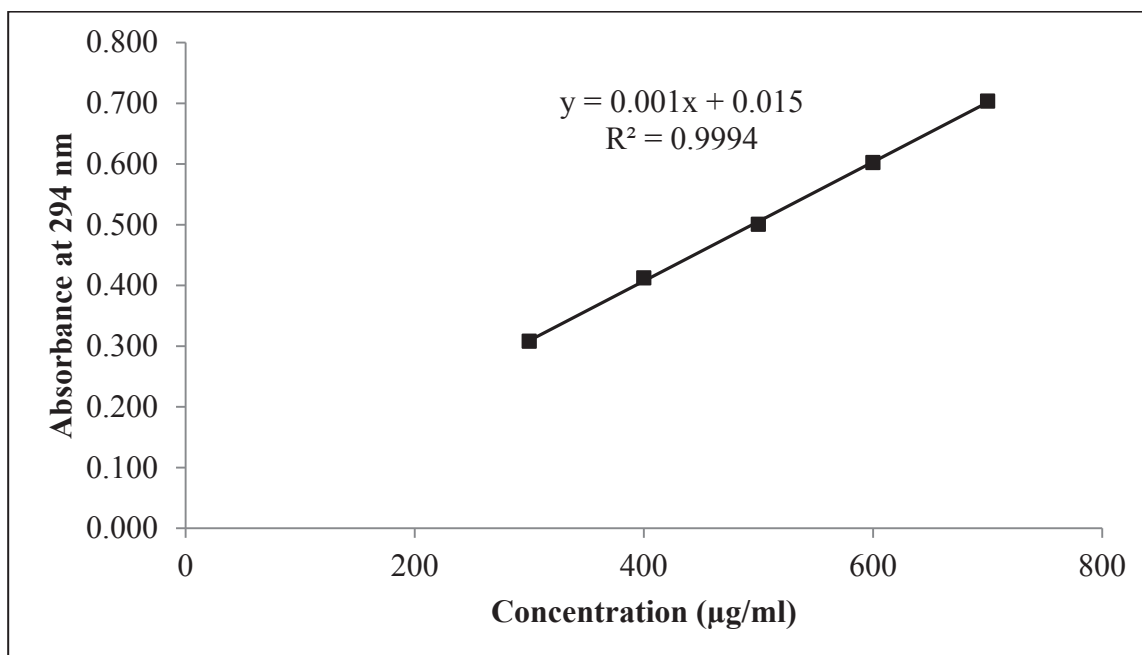


Figure 27 The calibration curve of TIM for percentage drug reloading assay

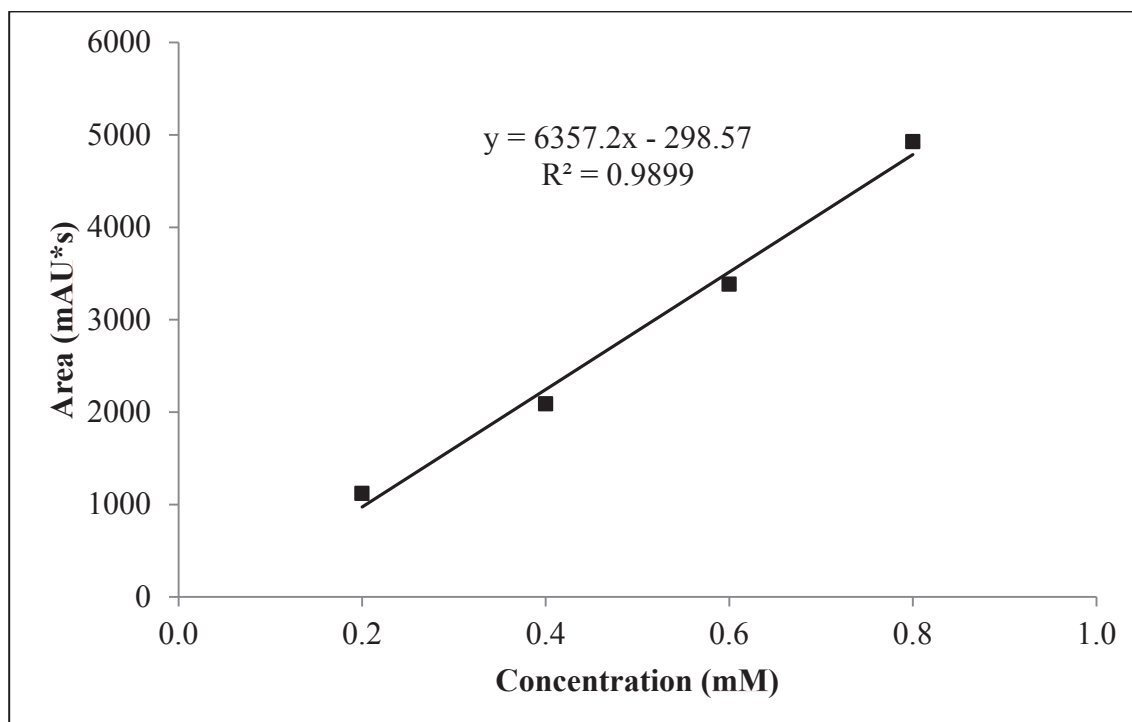


Figure 28 The calibration curve of PPL for percentage drug reloading assay

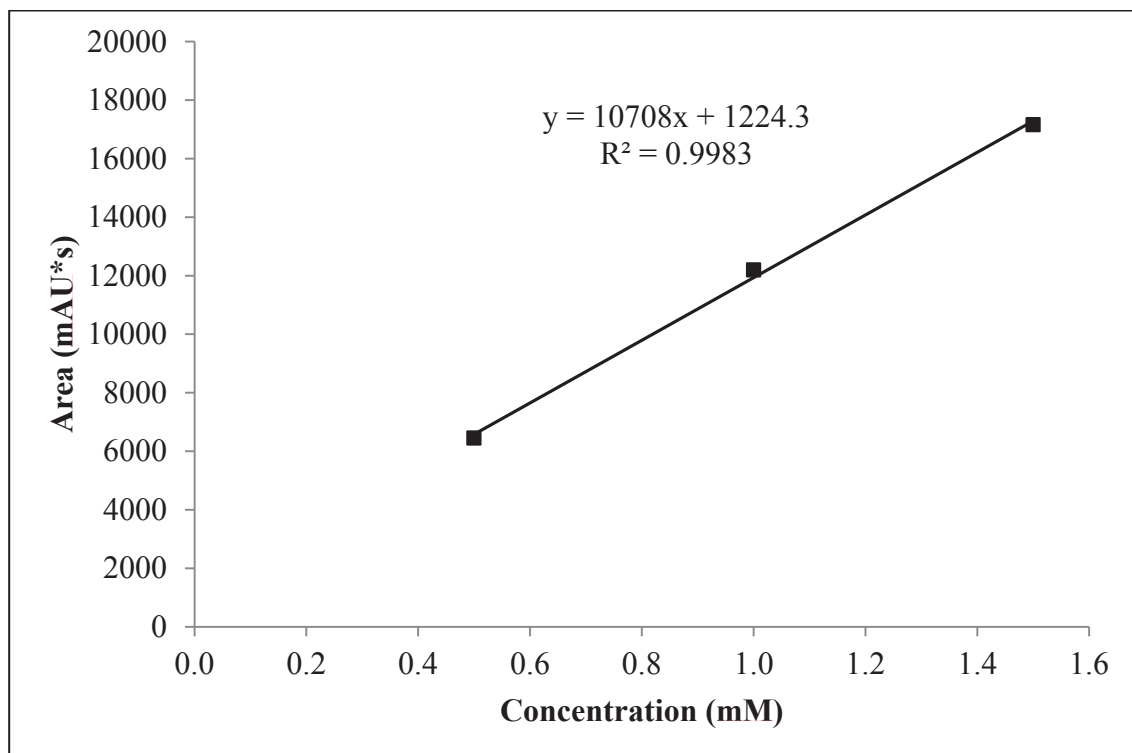


Figure 29 The calibration curve of ATE for percentage drug reloading assay

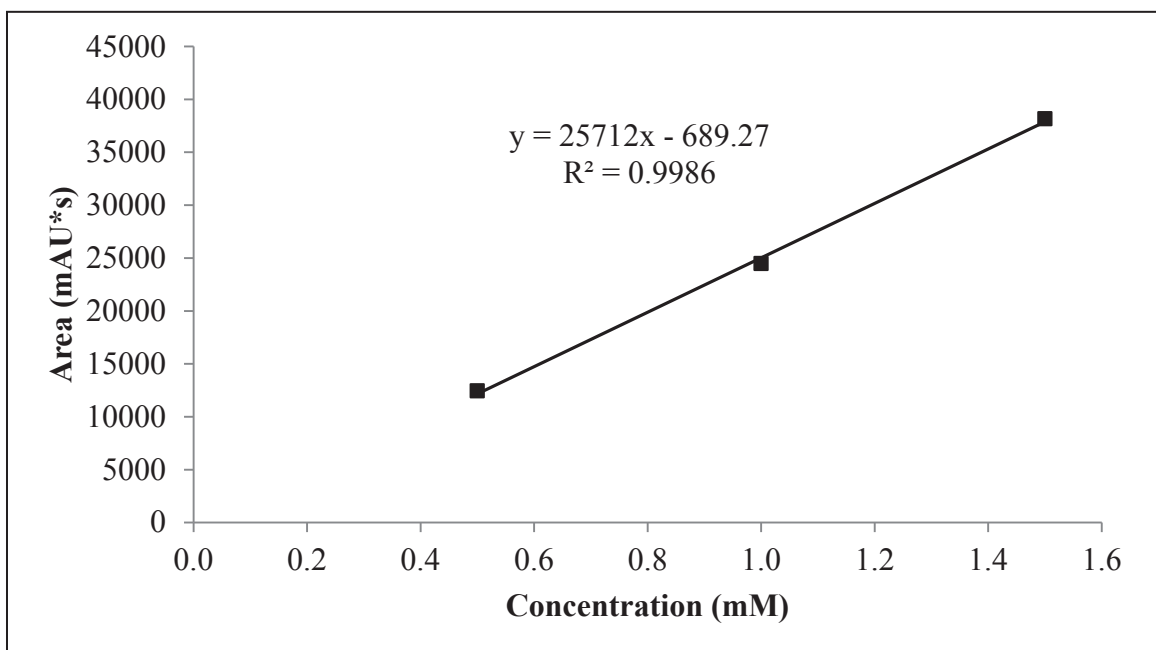


Figure 30 The calibration curve of MET for percentage drug reloading assay

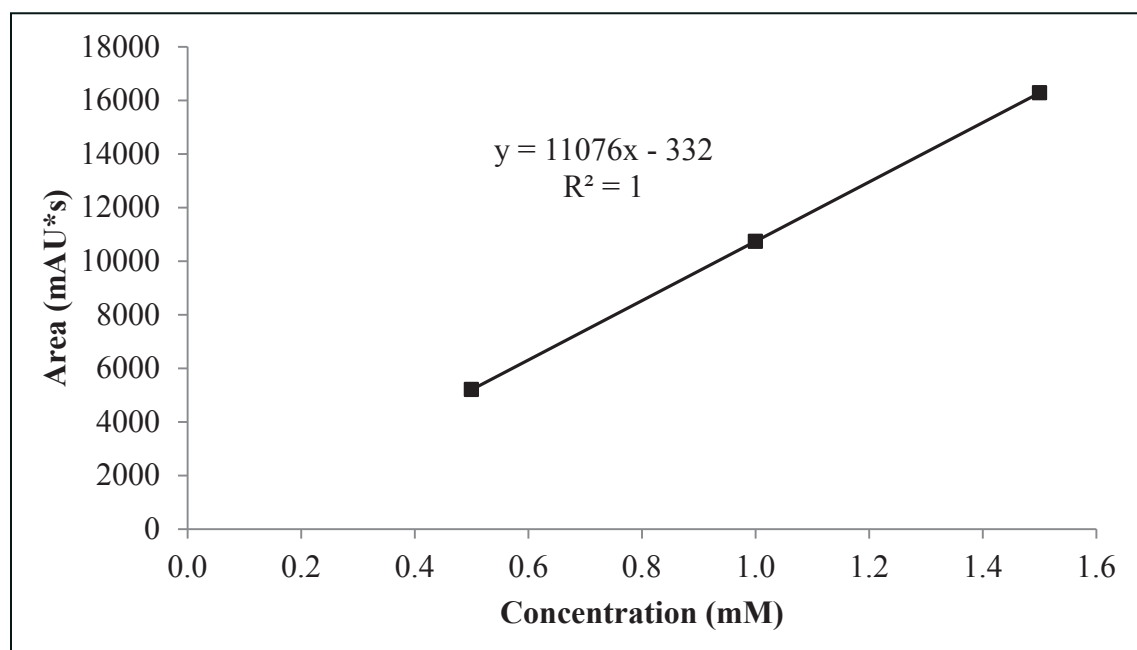


Figure 31 The calibration curve of TIM for percentage drug reloading assay

## **APPENDIX B**

**Table 17** Conductivity and viscosity of 20 and 25 % w/v Eudragit® L100 and S100 solution in DMA/EtOH and DMF/EtOH.

Types of Eudragit®	solvents	Conductivity( $\mu$ S/cm)		Viscosity(cP)	
		20(%w/v)	25(%w/v)	20(%w/v)	25(%w/v)
L100	DMA/EtOH	28.3 $\pm$ 2.4	27.3 $\pm$ 1.6	144.1 $\pm$ 0.4	152.2 $\pm$ 3.4
	DMF/EtOH	46.6 $\pm$ 4.2	-	143.4 $\pm$ 6.6	-
S100	DMA/EtOH	36.1 $\pm$ 2.2	35.1 $\pm$ 0.5	115.5 $\pm$ 4.3	380.4 $\pm$ 5.0
	DMF/EtOH	-	43.4 $\pm$ 2.3	-	539.3 $\pm$ 42.9

**Table 18** Conductivity and viscosity of 25 and 30 % w/v Eudragit® EPO solution in EtOH, DMA/EtOH and DMF/EtOH

Types of Eudragit®	solvents	Conductivity( $\mu$ S/cm)			Viscosity(cP)		
		25(%w/v)	30(%w/v)	35(%w/v)	25(%w/v)	30(%w/v)	35(%w/v)
EPO	EtOH	6.1 $\pm$ 0.5	5.2 $\pm$ 0.4	5.2 $\pm$ 0.3	36.6 $\pm$ 2.5	86.6 $\pm$ 0.5	85.9 $\pm$ 0.6
	DMA/EtOH	-	-	18.5 $\pm$ 1.6	-	-	62.7 $\pm$ 2.5
	DMF/EtOH	-	-	8.3 $\pm$ 0.7	-	-	53.0 $\pm$ 3.1

**Table 19** Conductivity and viscosity of 25-40 % w/v Eudragit® RLPO and RL100 solution in EtOH, DMA/EtOH and DMF/EtOH

Types of Eudragit®	solvents	Conductivity( $\mu$ S/cm)				Viscosity(cP)			
		25(%w/v)	30(%w/v)	35(%w/v)	40(%w/v)	25(%w/v)	30(%w/v)	35(%w/v)	40(%w/v)
RLPO	EtOH	262.3 $\pm$ 14.5	254.0 $\pm$ 9.8	264.0 $\pm$ 32.4	-	69.1 $\pm$ 2.1	116.7 $\pm$ 0.6	202.2 $\pm$ 0.7	-
	DMA/EtOH	412.3 $\pm$ 14.2	-	342.3 $\pm$ 29.7	-	34.5 $\pm$ 1.8	-	79.2 $\pm$ 0.3	-
	DMF/EtOH	-	-	456.3 $\pm$ 28.0	-	-	-	75.3 $\pm$ 0.4	-
RL100	DMF/EtOH	-	467.0 $\pm$ 19.0	458.3 $\pm$ 4.7	469.7 $\pm$ 9.0	-	42.3 $\pm$ 2.5	45.0 $\pm$ 0.3	70.1 $\pm$ 0.8

**Table 20** Conductivity and viscosity of 30-60% w/v Eudragit®RS100 solution in DMA/EtOH and DMF/EtOH

Types of Eudragit®	solvents	Conductivity( $\mu\text{S}/\text{cm}$ )						Viscosity(cP)		
		30(%w/v)	40(%w/v)	50(%w/v)	60(%w/v)	30(%w/v)	40(%w/v)	50(%w/v)	60(%w/v)	
RS100	DMA/EtOH	254.0 $\pm$ 20.0	210.3 $\pm$ 7.6	168.2 $\pm$ 8.9	214.8 $\pm$ 25.0	39.5 $\pm$ 0.9	98.0 $\pm$ 2.2	203.0 $\pm$ 2.0	645.6 $\pm$ 2.2	
	DMF/EtOH	278.7 $\pm$ 17.2	263.3 $\pm$ 20.7	223.7 $\pm$ 15.0	186.1 $\pm$ 10.7	38.7 $\pm$ 0.7	95.4 $\pm$ 1.2	262.7 $\pm$ 7.6	571.6 $\pm$ 0.7	

## **APPENDIX C**

Table 21 The percentage PPL reloading in NIP3 at the drug to polymer bead ratio of 1:0.5.

Time (h)	% PPL reloading				
	1	2	3	Mean	SD
0	0.79	-0.48	-0.30	0.00	0.69
2	13.15	12.06	14.06	13.09	1.00
4	16.42	16.24	16.24	16.30	0.10
6	16.06	16.06	16.60	16.24	0.31
8	19.15	18.97	18.78	18.97	0.18
12	20.60	21.33	21.15	21.03	0.38
24	21.15	23.87	24.42	23.15	1.75
48	24.96	24.60	24.78	24.78	0.18

Table 22 The percentage PPL reloading in MIP9 at the drug to polymer bead ratio of 1:0.5.

Time (h)	% PPL reloading				
	1	2	3	Mean	SD
0	37.99	37.20	37.31	37.25	0.43
2	42.42	42.65	43.10	42.88	0.35
4	44.01	44.01	44.24	44.13	0.13
6	44.01	44.01	44.35	44.18	0.20
8	44.35	44.35	44.24	44.30	0.07
12	45.04	44.81	44.81	44.81	0.13
24	45.15	44.92	45.26	45.09	0.17
48	44.92	44.81	44.70	44.75	0.11

Table 23 The percentage PPL reloading in NIP3 at the drug to polymer bead ratio of 1:1.

Time (h)	% PPL reloading				
	1	2	3	Mean	SD
0	0.37	0.00	-0.37	0.00	0.37
2	28.37	27.63	27.63	27.88	0.43
4	35.74	35.92	36.29	35.99	0.28
6	42.93	42.93	43.11	42.99	0.11
8	44.77	45.69	46.43	45.63	0.83
12	49.37	49.74	49.19	49.44	0.28
24	57.48	57.30	57.11	57.30	0.18
48	63.38	63.38	63.56	63.44	0.11

Table 24 The percentage PPL reloading in MIP9 at the drug to polymer bead ratio of 1:1.

Time (h)	% PPL reloading				
	1	2	3	Mean	SD
0	0.79	-0.48	-0.30	0.00	0.69
2	81.96	82.98	83.66	82.87	0.86
4	83.79	83.74	83.65	83.73	0.07
6	83.83	84.06	83.92	83.94	0.11
8	84.79	84.79	84.74	84.77	0.03
12	85.01	85.01	84.83	84.95	0.10
24	84.24	84.33	84.24	84.27	0.05
48	84.88	84.92	84.92	84.91	0.03

Table 25 The percentage PPL reloading in NIP3 at the drug to polymer bead ratio of 1:2.

Time (h)	% PPL reloading				
	1	2	3	Mean	SD
0	-0.24	0.12	0.12	0.00	0.21
2	53.69	53.58	53.92	53.73	0.17
4	65.53	65.30	65.42	65.42	0.11
6	74.66	74.43	74.43	74.51	0.13
8	79.79	79.86	79.72	79.79	0.07
12	86.28	86.55	86.62	86.49	0.18
24	93.74	93.92	93.94	93.86	0.11
48	97.41	97.50	97.37	97.43	0.07

Table 26 The percentage PPL reloading in MIP9 at the drug to polymer bead ratio of 1:2.

Time (h)	% PPL reloading				
	1	2	3	Mean	SD
0	-0.24	0.12	0.12	0.00	0.21
2	99.22	99.22	99.22	99.22	0.00
4	99.19	99.20	99.20	99.20	0.00
6	99.19	99.20	99.19	99.20	0.01
8	99.19	99.19	99.18	99.19	0.01
12	99.14	99.14	99.14	99.14	0.00
24	99.20	99.15	99.15	99.16	0.03
48	99.13	99.11	99.14	99.13	0.01

Table 27 The percentage PPL reloading in polymer beads at the drug to polymer bead ratio of (1:1) at various amount of PPL: NIP3 (PPL0 g).

Time (h)	% PPL reloading				
	1	2	3	Mean	SD
0	-0.48	0.24	0.24	0.00	0.42
2	12.65	18.22	18.58	16.48	3.33
4	30.63	32.07	29.91	30.87	1.10
6	38.54	38.00	38.36	38.30	0.27
8	42.86	41.78	42.50	42.38	0.55
12	44.83	44.47	44.47	44.59	0.21
24	49.69	49.69	49.51	49.63	0.10
48	55.26	54.72	54.36	54.78	0.45

Table 28 The percentage PPL reloading in polymer beads at the drug to polymer bead ratio of (1:1) at various amount of PPL: MIP3 (PPL0.4 g).

Time (h)	% PPL reloading				
	1	2	3	Mean	SD
0	-0.48	0.24	0.24	0.00	0.42
2	54.08	54.17	54.26	54.17	0.09
4	60.55	60.64	61.72	60.97	0.65
6	62.26	62.44	62.53	62.41	0.14
8	61.81	61.63	61.72	61.72	0.09
12	63.52	63.43	63.25	63.40	0.14
24	64.50	64.50	64.50	64.50	0.00
48	64.95	64.86	65.04	64.95	0.09

Table 29 The percentage PPL reloading in polymer beads at the drug to polymer bead ratio of (1:1) at various amount of PPL: MIP6 (PPL0.6 g).

Time (h)	% PPL reloading				
	1	2	3	Mean	SD
0	-0.48	0.24	0.24	0.00	0.42
2	59.92	59.65	59.65	59.74	0.16
4	69.27	68.01	68.91	68.73	0.65
6	73.14	73.05	73.14	73.11	0.05
8	73.14	73.32	72.06	72.84	0.68
12	74.84	75.02	74.93	74.93	0.09
24	76.28	76.37	76.64	76.43	0.19
48	77.90	77.99	77.09	77.66	0.50

Table 30 The percentage PPL reloading in polymer beads at the drug to polymer bead ratio of (1:1) at various amount of PPL: MIP9 (PPL0.8 g).

Time (h)	% PPL reloading				
	1	2	3	Mean	SD
0	-0.48	0.24	0.24	0.00	0.42
2	76.64	76.91	77.00	76.85	0.19
4	79.25	78.98	79.43	79.22	0.23
6	82.58	82.94	82.58	82.70	0.21
8	83.03	83.03	82.94	83.00	0.05
12	83.12	83.92	83.92	83.65	0.47
24	83.06	82.94	82.68	82.89	0.20
48	83.75	83.75	83.82	83.78	0.04

Table 31 The percentage PPL reloading in NIP; NIP1 (DVB 2 g) at the drug to polymer bead ratio of 1:1.

Time (h)	% PPL reloading				
	1	2	3	Mean	SD
0	0.70	-1.05	0.35	0.00	0.92
2	48.69	48.17	49.30	48.72	0.57
4	54.71	55.14	54.62	54.82	0.28
6	63.26	63.09	59.95	62.10	1.86
8	58.63	58.54	58.54	58.57	0.05
12	61.68	61.42	61.50	61.53	0.13
24	64.03	63.94	63.94	63.97	0.05
48	65.60	65.60	65.77	65.66	0.10

Table 32 The percentage PPL reloading in NIP; NIP2 (DVB 2.5 g) at the drug to polymer bead ratio of 1:1.

Time (h)	% PPL reloading				
	1	2	3	Mean	SD
0	0.70	-1.05	0.35	0.00	0.92
2	69.69	69.34	69.78	69.61	0.23
4	80.24	80.67	80.50	80.47	0.22
6	83.03	83.11	83.20	83.11	0.09
8	83.98	84.07	82.15	83.40	1.08
12	85.38	85.47	85.55	85.47	0.09
24	86.85	86.82	86.85	86.84	0.01
48	86.72	86.69	86.76	86.72	0.03

Table 33 The percentage PPL reloading in NIP; NIP3 (DVB 3 g) at the drug to polymer bead ratio of 1:1.

Time (h)	% PPL reloading				
	1	2	3	Mean	SD
0	0.70	-1.05	0.35	0.00	0.92
2	23.18	22.31	23.88	23.12	0.79
4	32.42	32.42	33.81	32.88	0.80
6	39.39	39.04	39.56	39.33	0.27
8	40.26	41.48	40.61	40.78	0.63
12	45.49	45.66	45.31	45.49	0.17
24	52.63	52.11	52.98	52.57	0.44
48	53.33	53.50	53.15	53.33	0.17

Table 34 The percentage PPL reloading in MIP; MIP7 (DVB 2 g) at the drug to polymer bead ratio of 1:1.

Time (h)	% PPL reloading				
	1	2	3	Mean	SD
0	0.70	-1.05	0.35	0.00	0.92
2	93.25	93.23	93.25	93.24	0.01
4	94.84	94.91	94.93	94.89	0.05
6	94.73	94.69	94.69	94.70	0.03
8	94.71	94.78	94.82	94.77	0.05
12	94.93	94.97	94.97	94.96	0.03
24	95.19	95.23	95.28	95.23	0.04
48	94.95	94.95	94.88	94.93	0.04

Table 35 The percentage PPL reloading in MIP; MIP8 (DVB 2.5 g) at the drug to polymer bead ratio of 1:1.

Time (h)	% PPL reloading				
	1	2	3	Mean	SD
0	0.70	-1.05	0.35	0.00	0.92
2	98.44	98.43	98.45	98.44	0.01
4	98.58	98.58	98.58	98.58	0.00
6	98.69	98.69	98.68	98.69	0.01
8	98.60	98.60	98.61	98.60	0.01
12	98.63	98.64	98.65	98.64	0.01
24	98.70	98.71	98.72	98.71	0.01
48	98.77	98.80	98.81	98.79	0.02

Table 36 The percentage PPL reloading in MIP; MIP9 (DVB 3 g) at the drug to polymer bead ratio of 1:1.

Time (h)	% PPL reloading				
	1	2	3	Mean	SD
0	0.70	-1.05	0.35	0.00	0.92
2	73.44	73.53	73.53	73.50	0.05
4	74.66	74.75	74.40	74.60	0.18
6	74.75	74.92	74.57	74.75	0.17
8	75.18	75.18	75.36	75.24	0.10
12	74.57	74.75	74.66	74.66	0.09
24	75.18	75.27	75.97	75.47	0.43
48	75.27	75.44	75.62	75.44	0.17

Table 37 The percentage reloading of  $\beta$ -blocker at ratio of drug to polymer beads (1:1) NIPs, ATE.

Time (h)	% PPL reloading				
	1	2	3	Mean	SD
0	-0.04	0.21	-0.17	0.00	0.19
2	57.31	57.31	57.21	57.28	0.06
4	49.45	48.74	49.15	49.11	0.36
6	49.45	49.56	49.86	49.62	0.21
8	49.66	49.35	49.25	49.42	0.21
24	53.94	54.15	54.15	54.08	0.12
48	45.78	45.78	45.47	45.68	0.18

Table 38 The percentage reloading of  $\beta$ -blocker at ratio of drug to polymer beads (1:1) NIPs, MET.

Time (h)	% PPL reloading				
	1	2	3	Mean	SD
0	-0.13	0.38	-0.26	0.00	0.34
2	62.65	62.77	62.77	62.73	0.07
4	65.14	65.27	65.14	65.18	0.07
6	64.95	64.82	64.69	64.82	0.13
8	64.88	64.75	64.75	64.80	0.07
24	65.14	65.07	65.33	65.18	0.13
48	63.03	64.50	64.56	64.03	0.87

Table 39 The percentage reloading of  $\beta$ -blocker at ratio of drug to polymer beads (1:1) NIPs, TIM.

Time (h)	% PPL reloading				
	1	2	3	Mean	SD
0	-0.57	0.29	0.29	0.00	0.49
2	49.63	49.97	49.97	49.86	0.20
4	49.97	50.06	49.89	49.97	0.09
6	49.80	49.97	49.71	49.83	0.13
8	50.14	49.97	50.23	50.11	0.13
24	49.29	49.37	49.29	49.31	0.05
48	49.20	49.20	49.20	49.20	0.00

Table 40 The percentage reloading of  $\beta$ -blocker at ratio of drug to polymer beads (1:1) NIPs, PPL.

Time (h)	% PPL reloading				
	1	2	3	Mean	SD
0	0.54	-0.36	-0.18	0.00	0.48
2	55.13	54.86	54.86	54.95	0.16
4	59.81	59.54	59.45	59.60	0.19
6	62.23	62.77	62.68	62.56	0.29
8	63.76	64.12	64.21	64.03	0.24
24	68.98	68.89	69.16	69.01	0.14
48	70.06	69.97	70.15	70.06	0.09

Table 41 The percentage reloading of  $\beta$ -blocker at ratio of drug to polymer beads (1:1) MIPs, ATE.

Time (h)	% PPL reloading				
	1	2	3	Mean	SD
0	-0.59	0.17	0.42	0.00	0.53
2	58.94	59.04	59.24	59.07	0.15
4	53.58	53.18	52.97	53.24	0.31
6	51.36	51.26	51.46	51.36	0.10
8	50.75	50.95	50.45	50.72	0.25
24	54.89	55.20	54.79	54.96	0.21
48	49.24	49.24	48.73	49.07	0.29

Table 42 The percentage reloading of  $\beta$ -blocker at ratio of drug to polymer beads (1:1) MIPs, MET.

Time (h)	% PPL reloading				
	1	2	3	Mean	SD
0	-0.13	0.38	-0.26	0.00	0.34
2	48.42	48.16	48.29	48.29	0.13
4	53.53	53.27	53.27	53.36	0.15
6	51.74	52.25	51.74	51.91	0.30
8	51.74	51.87	51.48	51.69	0.20
24	50.97	51.10	51.10	51.06	0.07
48	51.48	51.99	51.87	51.78	0.27

Table 43 The percentage reloading of  $\beta$ -blocker at ratio of drug to polymer beads (1:1) MIPs, TIM.

Time (h)	% PPL reloading				
	1	2	3	Mean	SD
0	-0.57	0.29	0.29	0.00	0.49
2	55.88	55.80	55.54	55.74	0.18
4	55.71	55.97	55.45	55.71	0.26
6	55.80	56.05	56.23	56.03	0.22
8	55.71	55.80	55.63	55.71	0.09
24	55.63	55.97	56.05	55.88	0.23
48	55.88	55.88	55.80	55.85	0.05

Table 44 The percentage reloading of  $\beta$ -blocker at ratio of drug to polymer beads (1:1) MIPs, PPL.

Time (h)	% PPL reloading				
	1	2	3	Mean	SD
0	0.54	-0.36	-0.18	0.00	0.48
2	92.11	92.07	91.98	92.05	0.07
4	92.88	92.94	92.85	92.89	0.05
6	92.99	92.92	92.92	92.94	0.04
8	93.35	93.30	93.32	93.32	0.02
24	94.36	94.43	94.36	94.38	0.04
48	94.16	94.16	94.16	94.16	0.00

Table 45 The percentage reloading of  $\beta$ -blocker at ratio of drug to polymer beads  
(1:1) NIPs composite E-RS100 fiber, ATE.

Time (min)	% PPL reloading				
	1	2	3	Mean	SD
0	0.00	0.00	0.00	0.00	0.00
3	0.00	0.00	0.00	0.00	0.00
5	0.00	0.00	0.00	0.00	0.00
10	0.00	0.00	0.00	0.00	0.00
20	0.00	0.00	0.00	0.00	0.00
40	0.00	0.00	0.00	0.00	0.00
60	0.00	0.00	0.00	0.00	0.00
120	0.00	0.00	0.00	0.00	0.00

Table 46 The percentage reloading of  $\beta$ -blocker at ratio of drug to polymer beads  
(1:1) NIPs composite E-RS100 fiber, MET.

Time (min)	% PPL reloading				
	1	2	3	Mean	SD
0	0.00	0.00	0.00	0.00	0.00
3	-0.92	2.22	1.80	1.03	1.70
5	-1.00	1.42	1.22	0.55	1.35
10	-1.17	1.82	1.27	0.64	1.59
20	-2.46	1.20	1.09	-0.06	2.08
40	-1.72	0.23	0.40	-0.37	1.18
60	-2.78	-0.12	0.16	-0.91	1.63
120	-2.96	-4.12	-2.93	-3.34	0.67

Table 47 The percentage reloading of  $\beta$ -blocker at ratio of drug to polymer beads  
(1:1) NIPs composite E-RS100 fiber, TIM.

Time (min)	% PPL reloading				
	1	2	3	Mean	SD
0	0.00	0.00	0.00	0.00	0.00
3	-0.75	2.09	1.74	1.03	1.55
5	-0.89	1.28	1.17	0.52	1.22
10	-0.98	1.70	1.22	0.65	1.43
20	-2.24	1.12	1.12	0.00	1.94
40	-1.56	0.16	0.43	-0.32	1.08
60	-2.60	-0.10	0.10	-0.87	1.50
120	-2.63	-3.96	-2.75	-3.12	0.73

Table 48 The percentage reloading of  $\beta$ -blocker at ratio of drug to polymer beads  
(1:1) NIPs composite E-RS100 fiber, PPL.

Time (min)	% PPL reloading				
	1	2	3	Mean	SD
0	0.00	0.00	0.00	0.00	0.00
3	-1.28	4.44	4.43	2.53	3.30
5	-1.11	3.08	3.53	1.83	2.56
10	-2.01	3.90	3.00	1.63	3.19
20	-3.77	2.90	3.80	0.98	4.13
40	-3.47	2.55	1.61	0.23	3.24
60	-4.71	1.78	1.88	-0.35	3.78
120	-4.37	-2.21	-1.19	-2.59	1.63

Table 49 The percentage reloading of  $\beta$ -blocker at ratio of drug to polymer beads  
(1:1) MIPs composite E-RS100 fiber, ATE.

Time (min)	% PPL reloading				
	1	2	3	Mean	SD
0	0.00	0.00	0.00	0.00	0.00
3	0.00	0.00	0.00	0.00	0.00
5	0.00	0.00	0.00	0.00	0.00
10	0.00	0.00	0.00	0.00	0.00
20	0.00	0.00	0.00	0.00	0.00
40	0.00	0.00	0.00	0.00	0.00
60	0.00	0.00	0.00	0.00	0.00
120	0.00	0.00	0.00	0.00	0.00

Table 50 The percentage reloading of  $\beta$ -blocker at ratio of drug to polymer beads  
(1:1) MIPs composite E-RS100 fiber, MET.

Time (min)	% PPL reloading				
	1	2	3	Mean	SD
0	0.00	0.00	0.00	0.00	0.00
3	10.88	25.91	22.77	19.85	7.93
5	27.01	26.47	24.66	26.04	1.23
10	27.68	29.51	29.40	28.86	1.03
20	32.44	34.31	31.33	32.69	1.51
40	34.41	36.59	35.42	35.47	1.09
60	40.92	41.19	40.96	41.02	0.14
120	40.18	41.95	41.20	41.11	0.89

Table 51 The percentage reloading of  $\beta$ -blocker at ratio of drug to polymer beads  
(1:1) MIPs composite E-RS100 fiber, TIM.

Time (min)	% PPL reloading				
	1	2	3	Mean	SD
0	0.00	0.00	0.00	0.00	0.00
3	9.42	23.15	20.25	17.60	7.24
5	23.96	23.39	21.72	23.02	1.16
10	24.34	25.98	25.98	25.43	0.95
20	28.71	30.37	27.64	28.90	1.38
40	30.40	32.43	31.48	31.44	1.02
60	36.45	36.66	36.67	36.60	0.12
120	36.00	37.66	37.08	36.91	0.85

Table 52 The percentage reloading of  $\beta$ -blocker at ratio of drug to polymer beads  
(1:1) MIPs composite E-RS100 fiber, PPL.

Time (min)	% PPL reloading				
	1	2	3	Mean	SD
0	0.00	0.00	0.00	0.00	0.00
3	24.07	53.11	46.31	41.16	15.19
5	53.24	53.39	49.83	52.15	2.01
10	87.89	88.59	88.55	88.34	0.39
20	87.89	88.59	88.55	88.34	0.39
40	87.89	88.59	88.55	88.34	0.39
60	87.89	88.59	88.55	88.34	0.39
120	87.89	88.59	88.55	88.34	0.39

## **APPENDIX D**

Table 53 List of abbreviations

Symbol	Definition
°C	degree Celsius
%	percentage
MW	molecular weight
$pK_a$	minus logarithm base 10 of $K_a$ , $-\log$
$K_a$	
w/w	weight by weight
v/v	volume by volume
g	gram
nm	nanometer
$\mu\text{m}$	micrometer
min	minute
h	hours
PBS	phosphate-buffered saline
pH	The negative logarithm of the hydrogen ion concentration
qs. to	add to
$R^2$	coefficient of determination
SD	standard deviation
Ave	Average
et al.	and others
etc.	for example, such as
o/w	oil in water
PPL	propranolol
MET	metoprolol
TIM	timolol
ATE	atenolol

Table 53 (continue)

Symbol	Definition
NIP	non molecular imprinted polymers
MIP	molecularly imprinted polymers
MMA	methyl methacrylate
DVB	divinylbenzene
BP	benzoyl peroxide
M	molar
mg	milligram
$\mu\text{g}$	microgram
mL	milliliter
$\mu\text{L}$	microliter
HPLC	High Performance Liquid Chromatography

## BIOGRAPHY

<b>Name</b>	Winita Chaijaroenluk, Miss
<b>Date of Birth</b>	June 01, 1985
<b>Place of Birth</b>	Phichit, Thailand
<b>Workplace</b>	-
<b>Institution Attended</b>	
2004-2008	Silpakorn University: Bachelor of Pharmacy
2009-2011	Silpakorn University: Master of Pharmacy (Pharmaceutical Sciences)

### Presentation

- Winita Chaijaroenluk, Praneet Opanasopit, Theerasak Rojanarata, Tanasait Ngawhirunpat, Prasert Akkaramongkolporn “Development of Propranolol-Selective Imprinted Polymer Beads.” The 3<sup>rd</sup> Annual Northeast Pharmacy Research Conference 2011, 12-13 February 2011; Faculty of Pharmaceutical Sciences, Ubon Ratchathani University, Thailand.